12-17-2015

Development of Glycan Based Diagnostics to Detect Pathogens

xiaohu Zhang

DEVELOPMENT OF GLYCAN BASED DIAGNOSTICS TO DETECT PATHOGENS

by

Xiaohu Zhang

Under the Direction of Dr. Suri Iyer

ABSTRACT

Numerous toxins and pathogens gain entry into mammalian cells using cell surface glycans. The Iyer group at Georgia State University is working on the development of glycoconjugates for the accurate detection of infectious agents. In this thesis, I have focused on the development of glycans to detect influenza virus and norovirus.

In the first section, I have focused on influenza viruses. A panel of synthetic glycans was synthesized as receptor mimics for the specific capture of influenza viruses. The synthetic glycans were printed onto commercial glass slides using a free amine at the end of a spacer to generate a small focused microarray. This glycan printed microarray was evaluated for its ability to capture three strains of influenza viruses. The analytical limit of detection is ~10 pfu/ml, (plaque forming units/milliliter) which is clinical relevant as 10^2 viral particles are typically required to cause infection. We also tested the drug susceptibility of current antivirals, Zanamivir and Ostelamivir using the microarray and determined the feasibility of this system to determine antiviral resistance for different strains.

In addition to optical detection, I developed an electrochemical assay to rapidly detect influenza viruses. Here, we utilized an unique property of influenza viral surface enzyme, Neuraminidase (NA), which cleaves terminal N-Acetyl Neuraminic acid (sialic acid) from cell surfaces and proteins. We designed an electrochemical assay that uses glucose bearing sialic acid substrates. Glucose is released when exposed to viral NA or intact viruses. The released glucose can be detected using repurposed glucose meters. Thus, personal glucose meters that were designed to assist diabetics and prediabetics monitor blood glucose can potentially be used to detect pathogens. Using this approach, we have detected 19 unique strains of influenza viruses.

We also demonstrated drug susceptibility using this assay. The limit of detection of this assay is 10^2 pfu/sample, which is clinically relevant. The results were validated plaque assays and polymerase chain reaction (PCR).

In the second part of this thesis, I focused on norovirus detection. I developed a focused glycan microarray that comprised of a library of histo blood group antigens (HBGAs). The HBGAs were attached to a carrier protein and printed onto activated glass slides. A panel of norovirus virus like particles (VLPs) and strains that included different genogroups was exposed to the microarray. We found that different VLPs and strains give rise to unique binding patterns. When the binding pattern of VLPs for a particular strain were compared to the corresponding intact virus, the binding patterns didn't match well, presumably because the virus does not recognize the same antibody as the VLPs. Unfortunately, antibodies for the virus cannot be generated because the virus cannot be grown in a laboratory setting. Indeed, all norovirus samples are obtained from human challenge studies. I also used surface plasmon resonance (SPR) studies in an effort to determine the binding affinities. Divalent biotinylated H type glycans were synthesized and their binding affinities with different VLPs and viral strains were determined. Initial studies suggest that the binding affinities are strain specific. These results demonstrate that glycans can be used to capture and isolate norovirus, although more research is required to develop glycan based norovirus detection kits.

INDEX WORDS: Influenza Virus, Norovirus, Drug Susceptibility, Virus Detection, Glycans, Electrochemical Assay.

DEVELOPMENT OF GLYCAN BASED DIAGNOSTICS TO DETECT PATHOGENS

by

Xiaohu Zhang

A Dissertation Submitted in Partial Fulfillment of the Requirements for the Degree of

Doctor of Philosophy

in the College of Arts and Sciences

Georgia State University

2015

DEVELOPMENT OF GLYCAN BASED DIAGNOSTICS TO DETECT PATHOGENS

by

Xiaohu Zhang

Committee Chair: Suri Iyer

Committee: Binghe Wang

Jun Yin

Electronic Version Approved:

Office of Graduate Studies

College of Arts and Sciences

Georgia State University

December 2015

DEDICATION

I would like to dedicate this dissertation to my parents (Cheng Zhang and Fengling Yang) and my wife (Dr. Danzhu Wang). They supported me in this long journey. They are and will always stand by me through difficult times, and encourage me to overcome any difficulty that I faced in my life. I thank them for everything they have done to me and will be grateful forever.

ACKNOWLEDGEMENTS

I would like to thank my advisor, Dr. Iyer for his invaluable guidance and support. I learned a lot of things from him, not only about the research, but also how to manage my life. I appreciate everything he has done for me. I would say that I had a wonderful experience working in his laboratory as a Ph.D. student; he is an excellent advisor, a patient teacher, a brilliant researcher, and a good friend.

I would like to thank my committee members Dr. Binghe Wang and Dr. JunYin. Their advice and guidance were extremely helpful.

I would like to thank the Dr. Suri Iyer's Group, Dr. Dinh, Dr. Abasaheb Dhawane, Dr. Bharat Gurale, Dr. Yang Yang, Dr. Yun He, Joyce Sweeney, Amrita Das, and Xikai Cui for their help in research.

I would like to thank Summer for her unconditional love. She is a kind and lovely dog.

TABLES OF CONTENTS

LIST OF FIGURES

LIST OF SCHEMES

LIST OF TABLES

1. Glycan Based Influenza Virus Detection

* Most of the work described in this chapter has been published in two publications:

Zhang, X.[‡]; Dinh, H.[‡]; Sweeney, J.; Yang, Y.; He, Y.; Dhawane, A.; Iyer, S. S., Glycan based detection and drug susceptibility of influenza virus. *Anal. Chem.,* **2014**, *86* (16), 8238-8244. ([‡] *contributed equally to the paper*)

Zhang, X.; Dhawane, A. N.; Sweeney, J.; He, Y.; Vasireddi, M.; Iyer, S. S., Electrochemical assay to detect influenza viruses and measure drug susceptibility. *Angew. Chem. Int. Ed. Engl.,* **2015**, *54* (20), 5929-5932.

1.1 Influenza Virus Introduction

Influenza virus is a deadly respiratory virus that is typically spread through contact, sneezing and coughing. Seasonal influenza associated illnesses causes 200,000 hospitalizations and over 30,000 deaths in the United States every year.[1] Emerging strains can be extremely virulent, for example, recent emergence of avian H5N1 influenza virus in remote location was very concerning as it had a high death rate.[2] Most recently, the 2009 H1N1 strain spread rapidly, but did not have a high death rate. [3]

Influenza virus belongs to the family of orthomyxo-viridae viruses. There are three serologically distinct types, type A, type B and type C. Type A and type B infects mammals where type C viruses does not infect humans.[4] Based on the antigenic properties of the virus surface protein, further classification is designated as H_xN_y, where x and y stand for different types of surface protein, Hemagglutinin (HA) and Neuraminidase (NA), respectively. In addition to H and N, nomenclature includes the year and the location where the virus subtype was isolated. For example, A/California/04/2009 (H1N1), represents a H1N1 strain, Type A, isolated in California in 2009 with a lineage number 4. HA and NA are essential for the influenza virus life cycle, which is described below.

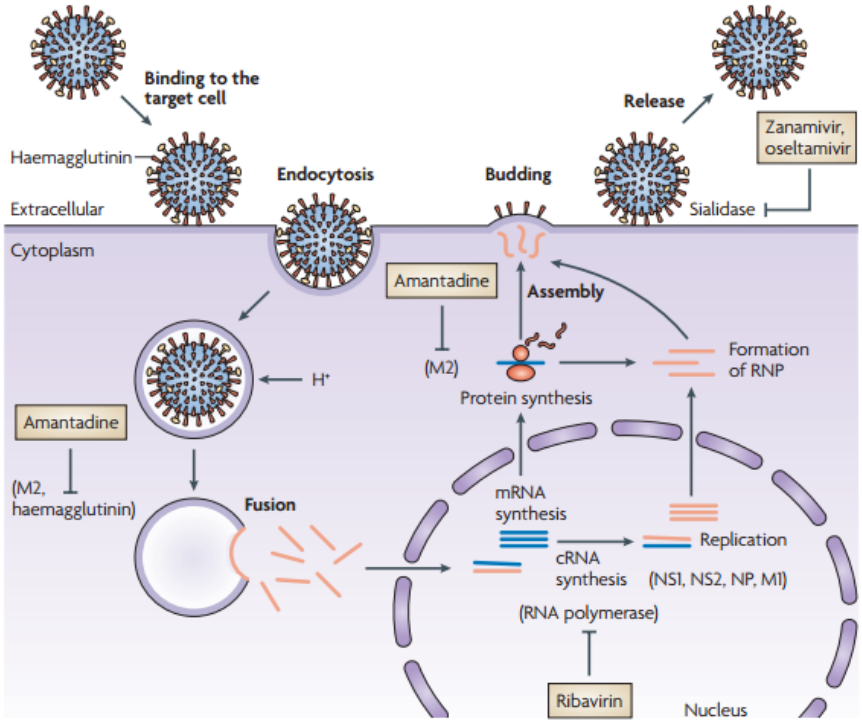

Figure 1.1 Influenza virus life cycle and targets for therapeutics.

First, influenza virus binds to the target cell, second, the virus is endocytosed, third, the virus releases the genome and subsequent viral proteins are synthesized. Fourth, new viruses are assembled. Fifth, NA cleaves the terminal sialic acid to help the viruses exit from host cell.

Figure is taken from publisher with permission.[5]

The surface of influenza virus is decorated by three surface proteins: M2 ion channel protein, HA, a lectin and NA, which is an enzyme. These proteins play important roles in virus life cycle (Figure 1.1). Briefly, the virus life cycle has several steps. 1). Influenza virus bind to the target host cell by recognizes its surface glycan (terminal linked *N*-acetyl Neuraminic acid or sialic acid) using virus surface protein HA. The binding process helps the virus gain entry into

the cell. 2). The virus is endocytosed through a fusion process to allow the virus to enter the host cell. 3). The virus releases the genome and subsequently viral protein are synthesized. 4). After cRNA (complimentary RNA) synthesis, genome is replicated, new virus is assembled. 5). Budding process helps the virus exit the host cell. 6). The enzyme NA cleaves the terminal sialic acid residues from the host cell surface. The virion progeny seeks new host cell for subsequent infections.

HA, NA and the M2 channel are essential for viral infection, therefore, HA, NA and M2 channels have been proposed as potential targets to treat influenza virus infection because of their integral role in viral replication.

Influenza A virus is a negative-sense single stranded RNA virus. The genome is composed of eight viral RNA segments which is used to encode 11 major proteins.[6] We describe the major proteins in the following subsections.

1.1.1 Hemagglutinin (HA)

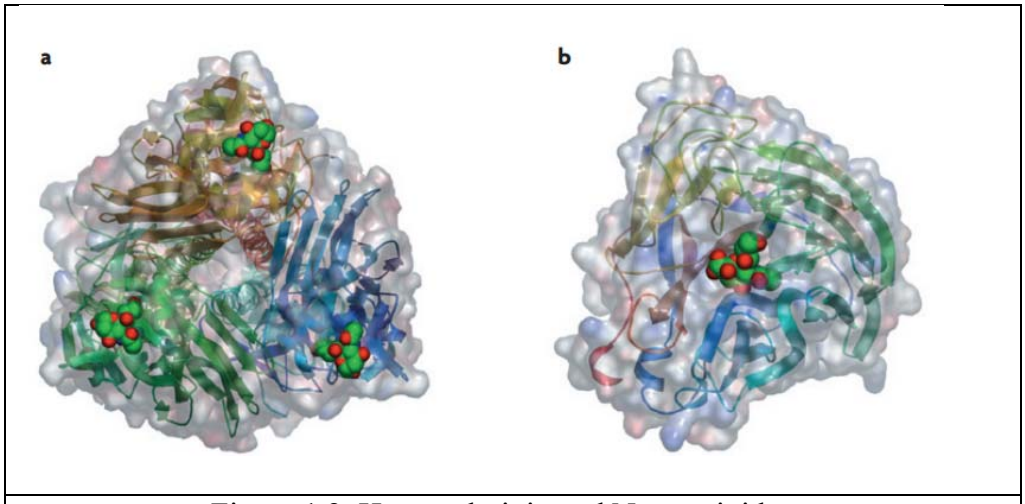

Figure 1.2 Hemagglutinin and Neuraminidase.

a) A view of HA trimer complexed with Neu5Ac. The sialic acid is represented as ball and stick model and the proteins are represented as

ribbons with the space filling model merged into the background. Each part of the trimer is represented in three different colors, green, brown and blue. b) A view of NA monomer, complexed with Neu5Ac.

Figure is taken from publisher with permission. [5]

HA is a glycoprotein. HA is formed by three identical subunits (Figure 1.2) and is presented as spikes on the lipid membrane of influenza virus. There are two functions of HA, the first function is its involvement in binding process,[7] HA binds with sialic acid on the surface of the host cell to anchor the virus on the surface to help the fusion. The second function is to trigger the internalization of the virus through a fusion process.[8]

There are two subunits HA1 and HA2 formed by HA0 which is a HA precursor. HA1 contains a binding domain of the HA for sialic acid, while HA0 contains the fusion peptide.[9] These two domains both contribute to the biological functions of HA. Although HA binds with sialic acid and sialic acid terminated glycans, the binding affinity is also dependent on the linkage between the sialic acid and the penultimate unit, which is typically a galactose unit. Two major glycosylation linkages are recognized by HA: an α (2,3) linkage (Figure 1.3) predominately in avian and equine viruses, and an α (2,6) linkage found in the human influenza viruses.[10] Pigs have both α (2, 3) and α (2, 6) linkage, and are often considered as a resource for "virus mixing". A highly pathogenic avian influenza stains, H5N1, that has preference for α (2, 3) and α (2, 6) linkage has been found recently.[11] The reason for increased pathogenicity is that a single amino acid mutation in this avian strain, which endows the virus the ability to infect human host cells.[12] This finding explains that H5N1 avian influenza virus did not infect humans when it first emerged, but now possesses that ability.

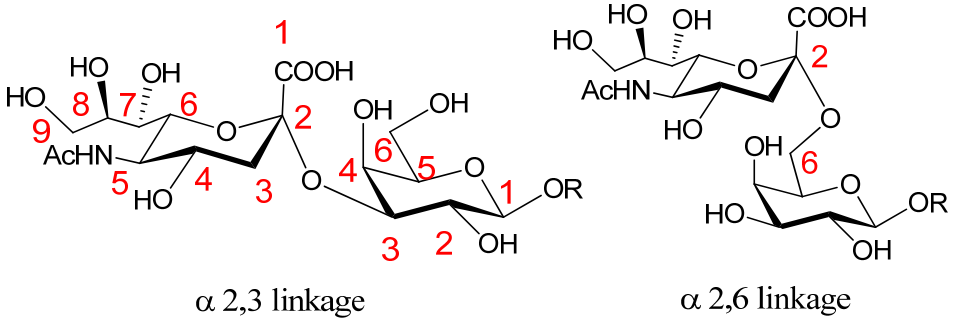

Figure 1.3 α (2,3) linkage and α (2,6) linkage of sialic acid.

The numbering scheme is represented on the figure as red color.

Upon binding to the sialic acid unit on the host cell, a receptor-mediated endocytosis process helps the virus get into the host cell. The pH (typically 5~6) of the endosome will trigger the fusion process, and induce the conformational changes in HA0 to expose the HA2 fusion domain. The HA2 is released to the endosomal membrane and helps the endosomal membrane contact with the viral.[13]

The low pH (5~6) environment of the endosome is important to induce the HA0 conformation changing to expose the HA2 fusion peptide. Another biological process is also triggered by the low pH environment of the endosome, the M2 ion channel on the surface of the virus opens up in low pH environment. This process will acidify the virus core, and help the release of the vRNP (viral ribonucleoproteins) from M1, which is the M1 part of the ion channel. Consequently, the vRNP is free to enter to the cytoplasm of the host cell.[14].

1.1.2 Neuraminidase (NA)

Neuraminidase is another important surface protein of the influenza virus. It plays an essential role in the virus life cycle. NA is a surface protein that made up by four identical

subunits. The entire protein is anchored to the viral membrane.[15] The NA structure is shown in Figure 1.2. On the surface of influenza virus, NA is presented as a tetramer. The shape of NA could be described as a mushroom, a head stick on the thin stem. One virus has approximately 50-100 NAs, as determined by cryo-electron microscopy. [16]

The biological function of NA is that it catalyzes the cleavage of the terminal sialic acid residue. The cleavage mechanism of the terminal sialic acid residue is shown in Figure 1.4. There are four steps in the catalytic processes. In the initial step, the carboxylate group changes from an axial position to a pseudo equatorial position. Second, the lone pair electron of oxygen on the sugar ring triggers the electron transfer to the anomeric carbon, and forms the endocyclic sialoyl cation transition state intermediate. Next, tyrosine residue in the active site attacks the sialosyl cation. Finally, the lone pair electron from the water molecule attacks the sialosyl cation to release Neu5Ac in the glycosylic enzyme intermediate. The major function of NA in the virus life cycle is that it can facilitate the virion release from the infected cell by cleaving the sialic acid from the host cell.[17] Without NA, the emerging virion aggregates on the infected host cell and cannot infect more cells. Recently, a mechanism has been proposed based on tyrosinyl-bound intermediate to explain the resistance of emerging strains to Oseltamivir.[18]

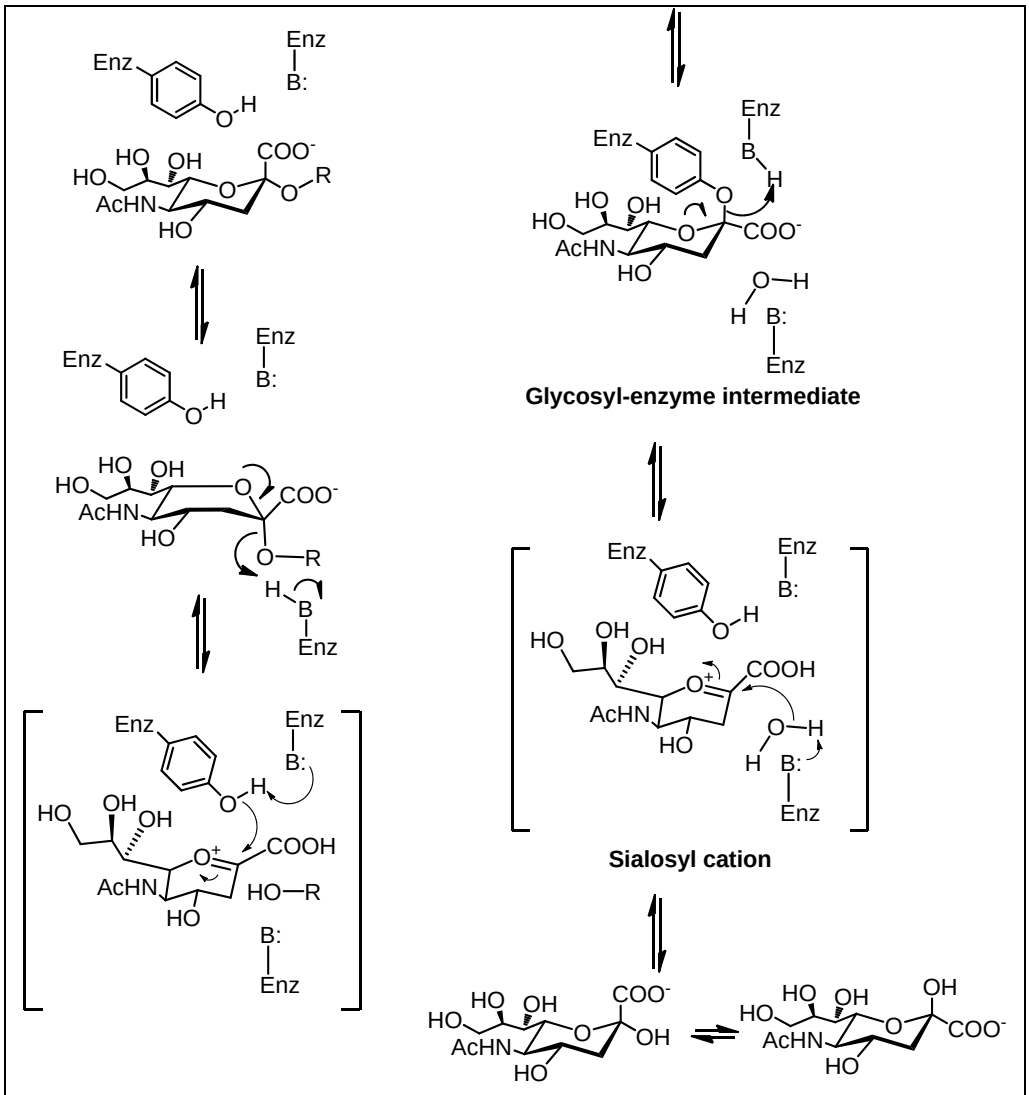

Figure 1.4 Proposed mechanism of NA.

1.1.3 M2 Proton Channel Protein

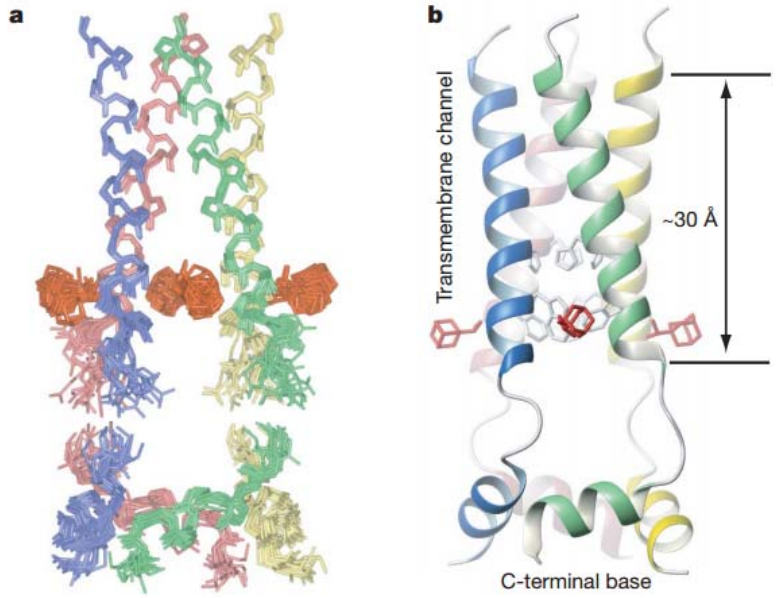

Figure 1.5 M2 Proton Channel Structure

a). An ensemble of 15 low energy structure derived from NMR restraints. b). A ribbon structure represents the ensemble of part a, showing the side chains of His 37 and Trp 41.

Figure is taken from publisher with permission. [19]

M2 is the third surface protein. It is a single-pass membrane protein and is composed of 97-residues.[19] It forms a tetramer in the native state. The amino termini are directed towards the outside of the virus capsid, and carboxyl termini are directed towards inside of the virus capsid.[20] The main biological function of M2 proton channel is that it forms pH-gated proton channels in the viral lipid. This proton channel is formed by four transmembrane helices. Based on the structure of the M2 channel, the His 37 assists in sensing the pH and the Trp 41 acts as the gatekeeper to control the proton flow.[21]

The structure model of the M2 channel has been elucidated based on several technologies such as sequence analysis, mutagenesis and solid state NMR.[20, 22] The M2 channel is inherently unstable and therefore, different analytical methods led to different conclusions in the past. However, the construction of residues 18-60 forms a stable tetramer and this helped determine the correct structure, which was determined by high-resolution NMR spectra.[19] A four helix bundle forms the transmembrane helices as shown in Figure 1.5.

The structure of the M2 proton channel reveals the biological function. Four transmembrane helices pack tightly to each other to form a "gate". The gate can be closed or open depending on the pH of the surroundings as shown in Figure 1.6 because of a conformational change of the transmembrane helices. Different pH triggers the conformation change of the transmembrane helices. The conformation changes are mainly contributed by Trp 41, Asp 44 and His 37. The channel gate is formed by indole rings of Trp 41, and stabilized by inter subunit hydrogen bonds with Asp 44. Thus, when pH is high, the gate is closed due to the interaction between tryptophan and Asp 44. However, at low pH, His 37 is protonated, and the imidazole of His 37 destabilizes the transmembrane helix, thus, the interactions between Trp 41 and Asp 44 is broken and the gate opens.[19] Consequently, proton can flow through the M2 proton channel across the viral envelop.

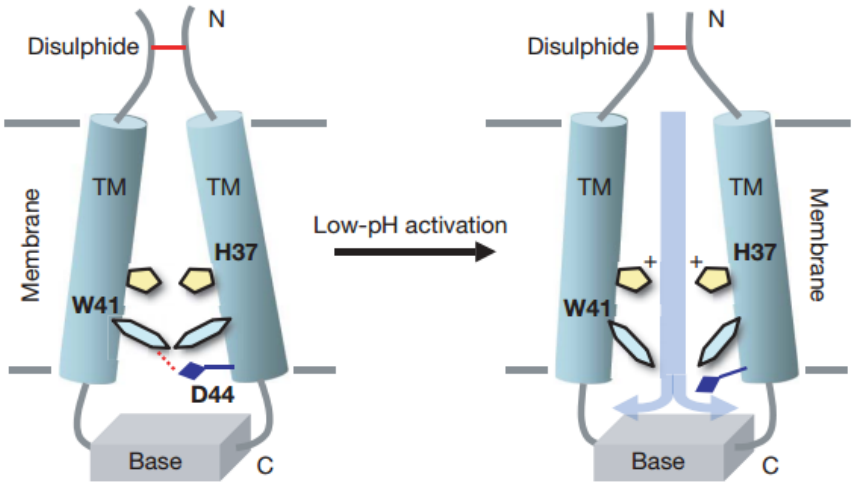

Figure 1.6 The Activation process of M2 channel

At high pH, the transmembrane helices are tightly packed, the tryptophan gate is closed, at low pH, His 37 inidazoles is protonated, this could destabilize the transmembrane helix packing, the gate is opened.

Figure is taken form publisher with permission. [19]

1.1.4 Influenza Viral Polymerase

The RNA dependent RNA polymerase is encoded by three largest vRNAs. The RNA dependent RNA polymerase is mainly composed of three subunits, the acidic subunit PA and the basic subunits PB1 and PB2. There are two biological functions for the influenza virus polymerase. First, it helps the viral replication in the host cell by replicating the RNA segment and transcribing the gene. Second, it causes the virus mutations through its error prone replication due to the lack of proofreading activity. In the viral particle, each ribonucleoprotein contains a single polymerase complex, which is consisted of PA, PB1 and PB2. Since the

negative sense RNA cannot be directly translated, the pre-existence of the polymerase can initiate the first RNA replication and transcription. Once the replication and transcription is finished, more polymerase subunits can be synthesized in the cytoplasm, assembled into a trimer, and involved in further replication and transcription.[23] Biochemical studies show that PA, PB1 and PB2 interact with each other from the *C*-terminus to the *N*-terminus to form an *N*-terminal to *C*-terminal linear PA-PB1-PB2 arrangement as shown in Figure 1.7. [24]

There is no proofreading activity from the influenza virus polymerase, leading to an influenza virus mutation rate, approximately one error per replicated genome.[25] The continual mutations of the genome leads to the virus to mutate fast, especially for the M2 protein and NA, which are major targets for the antiviral therapy. Therefore, the lack of proofreading activity of the viral polymerase is one of the major reasons that make the virus resistant to antiviral drugs and help the virus better to adapt to new host species.[26]

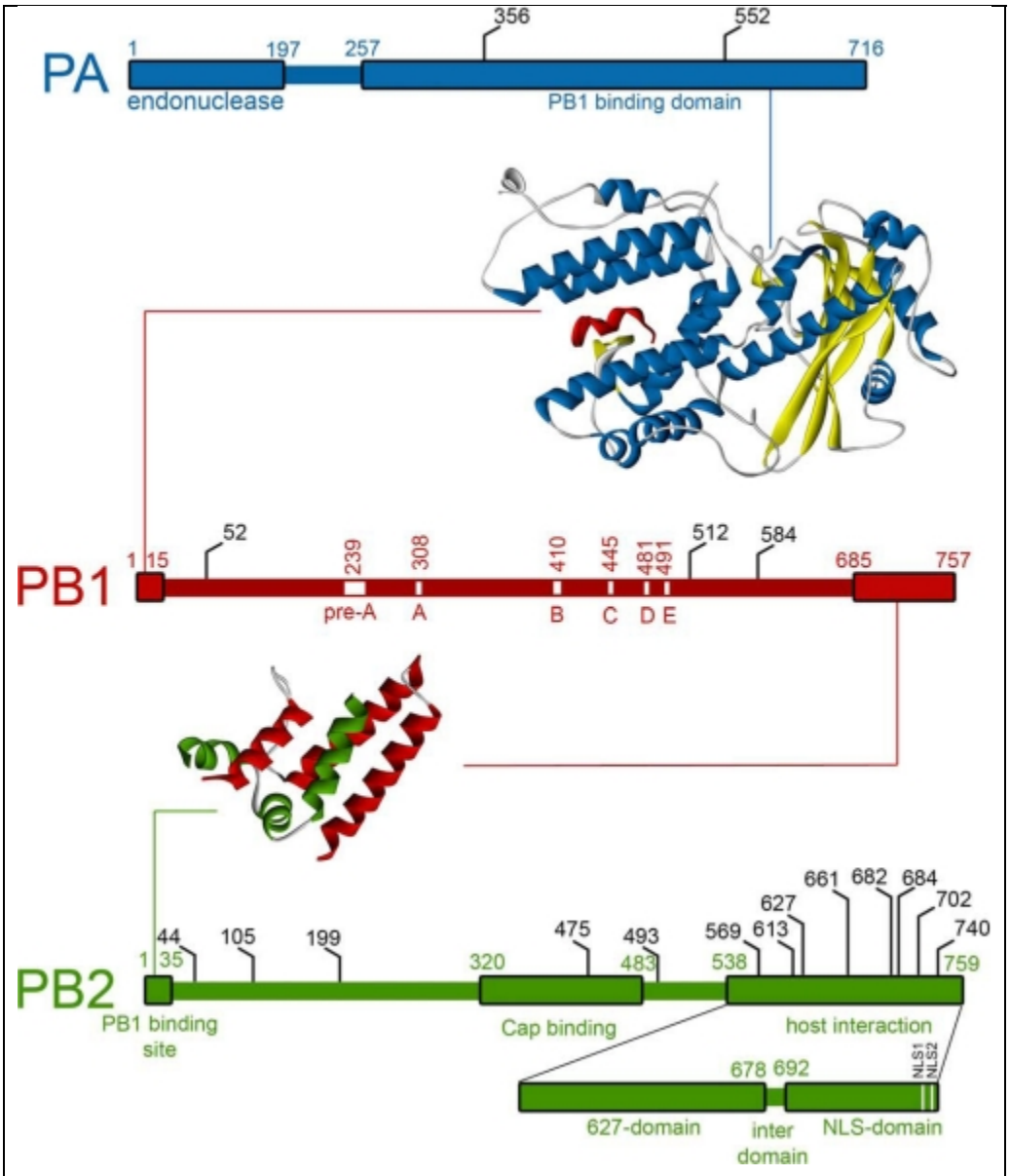

Figure 1.7 Features of the polymerase subunits.

Linear representations of the three polymerase subunits, PA, PB1 and PB2. PA, PB1 and PB2 interact with each other from *C* terminus to *N* terminus. The blue, red and green box represent different domain. The X ray crystal structures of the protein represent the interaction regions of PA-PB1, and PB1-PB2. [27]

Figure is taken from publisher with permission. [23]

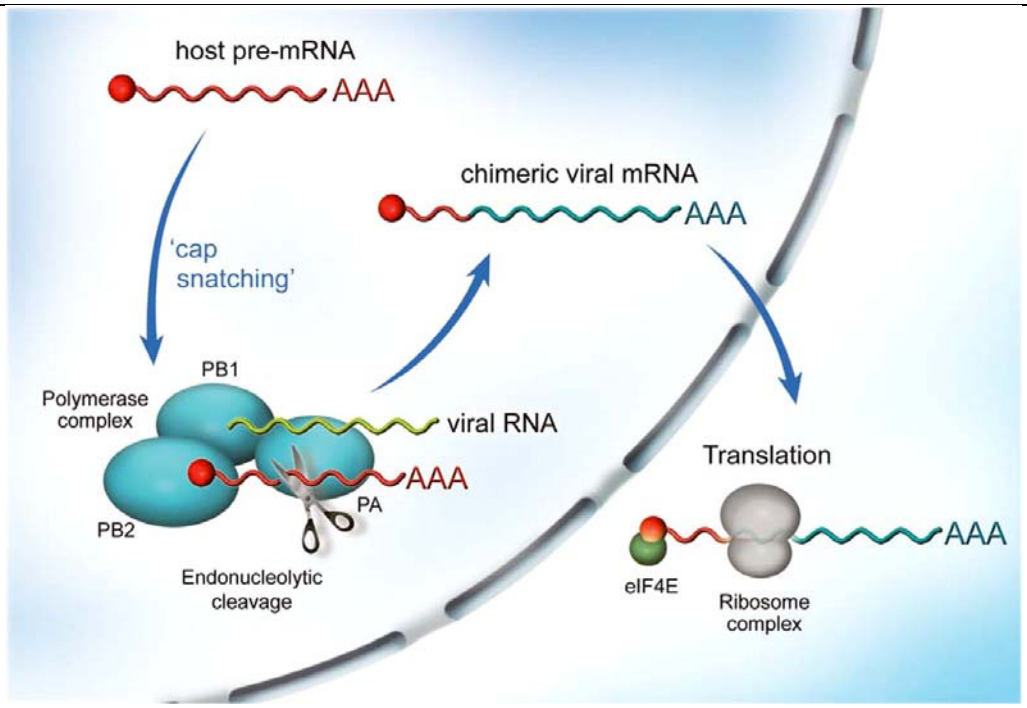

Figure 1.8 Cap-snatching transcription mechanism of influenza polymerase.

In transcription, first, PB2 subunit binds with a host pre-mRNA molecule (red), which can be cleaved 10-15 nucleotides downstream by the PA endonuclease. The short RNA primer is used to initiate polymerization by PB1 subunit using vRNA as the template to generate the chimeric viral mRNA (red and blue), which can be used to translate viral protein.

Figure is taken from publisher with permission. [23]

All of three subunits are essential for the transcription and replication process of the virus life cycle. The initial step of the transcription process is triggered by cap snatching, in which 5'-capped RNA fragments are cleaved from host pre mRNAs. [28] The replication process is composed by two steps. First, complementary RNAs (cRNA) are synthesized, and are used as replication intermediates to generate more virus ribonucleoprotein, they can also act as templates

to the next transcription. Eventually, all of the RNAs are exported from the nucleus to form virions at the plasma membrane.[29] (Figure 1.8)

The function of PA was unclear in the past and several functions were proposed [30] until two groups have determined the structure of the N terminal domain of PA [31] which shows that the main function of PA subunit is that of an endonuclease.[32] There are two subunits labeled as *N*-terminal (25k Da) and *C*-terminal (55k Da). The *C*-terminal fragment serves as a binding site to PB1 to form the polymerase complex, while the *N*-terminal subunit contributes to the cleavage of the cap peptides from the host pre mRNA.[23]

Previous research demonstrated that the *N*-terminal of PB1 binds with the *C*-terminal of PA where the short *N*-terminal of PB1 is co-crystallized as shown in Figure 2.6. At the other end of PB1, the interaction of *C*-terminal with *N*-terminal of PB2 has been demonstrated.[33] The X-ray structure of the *C*-terminal fragment of PB1 with *N*-terminal of PB2 was determined and showed that these α helical subunits are tightly folded.[27b] This interaction interface is highly conserved in different avian and human strains, which make this part a possible drug target.[23] The central role in of PB2 is represented in the RNA replication process. It acts as the backbone of the polymerase, and holds the catalytic site to help the RNA polymerase complete the replication process.[34]

PB2 plays an essential role in the transcription initiation. It is a major virulence determinant of the influenza virus [35] and has been found to affect host range of viruses. [36] It binds to the pre mRNAs to generating 5' capped RNA fragments, which are used as primers for the virus transcription.[37] Most of PB2 proteins are found in the nucleus of the host cell in complex formation with PB1 and PA polymerase subunits. They have been detected in the

mitochondria.[38] It is proposed that the PB2 in mitochondria can contribute to the preservation of mitochondrial function by stabilizing its membrane potential when the host cell is infected by influenza virus. However, the function of the PB2 protein in mitochondrial has not been elucidated in detail.[35]

1.1.5 Antiviral Development Strategies

A virus is composed by genetic material (DNA or RNA), functional proteins such enzymes and polymerases, and wrapped in a protein coat. Viruses lack a cell wall, ribosomes, and other structures, and therefore, they do not respond to antibiotics. The strategies to design an antiviral drug are typically to arrest a specific stage of the virus life cycle. The life cycle of viral follow a general pattern: 1. Attachment to the host cell. 2. Inject the genome and possibly enzyme such as polymerase into the host cell. 3. Replication of the genome by using the host cell machinery. 4. Translation of the protein which is essential to grow new viral progeny. 5. Assembly all of the components to form the new virus. 6. Release from the host cell to infect new targets.

One antiviral strategy is to block the interaction of the virus with host cell. The virus must attach to the host cell by binding to a specific receptor on the host cell surface. Therefore, the method to block the interaction is developing a synthetic protein that blocks the virus from interacting with the host cell receptor or developing small molecules to mimic the receptor of the host cell. Several antiviral drugs have been developed to fight HIV based on "entry inhibiting" or "entry blocking".[39] Amantadine and Rimantadine have been used to combat influenza. [40] Pleconaril has been used to against rhinoviruses by blocking the virus surface pocket which is used to stop the virus uncoating process from releasing its genomic material.[41] These approaches

have not worked well for influenza thus far, because HA is a lectin; however, some reports that target HA have emerged. [42]

Another approach to design the antiviral drug is to develop nucleotide or nucleoside analogous that mimic the building blocks of the RNA or DNA, which deactivates the enzyme activity once the antiviral drug stops the replication process. This method has been wildly applied to inhibit the reverse transcriptase. The antiviral drug Acyclovir used to against herpesvirus is a nucleotide analogue[43], and the antiviral drug Zidovudine used to treat HIV infection is a nucleotide analogue also.[44] Several antiviral drugs have been designed to target the translation process. Antisense drugs and ribozymes are developed based on this strategy.[45] The last step of virus in the life cycle is the release process form the host cell. Two antiviral drugs name Zanamivir and Oseltamivir have been developed to treat influenza virus infection by inhibiting the NA on the virus surface to prevent the release of viral progeny.[23, 25-26]

1.1.6 Development of Antivirals for influenza

There are five licensed influenza antivirals approved by FDA in the United States. Three of them are NA inhibitors, which can inhibit NA to prevent the new virus release process. They are Oseltamivir (Tamiflu®), Zanamivir (Relenza®) and Peramivir (Rapivab®). All of them have activity against influenza A and B viruses. Amantadine and rimantadine are used as antiviral drugs as they are active against influenza A virus by inhibiting M2 channel, however, most circulating strains are resistant to amantadine and rimantadine.

1.1.6.1 M2 Inhibitors

As mentioned previously, M2 proton channel is essential for the virus life cycle. It equilibrates pH across the viral membrane during the virus entry into the host cell and the trans-

Golgi membrane of the host cell during viral maturation.[46] Adamantane is the first synthetic compound that was shown to inhibit influenza virus replication process.[47] Two adamantane derivatives, amantadine and rimantadine,(Figure 1.9) have been developed as licensed antiviral drugs for influenza infection treatment and they are trademarked as Symmetrel® and Flumadine®, These two antiviral drugs were used as the first effective licensed antiviral drugs against outbreak of influenza A drugs in past decades.[46] However, in recent flu seasons, both of them showed a high level of resistance to influenza A (H3N2) and influenza A (H1N1). Therefore, they are no longer recommended for antiviral treatment or chemoprophylaxis in the 2015-2016 influenza seasons.

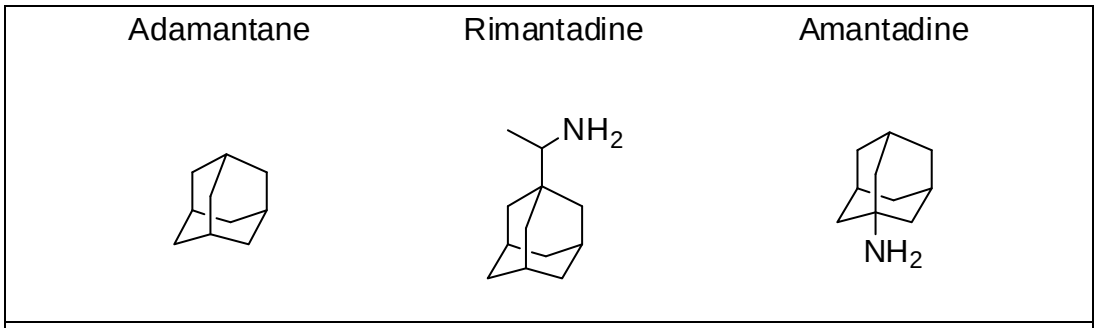

Figure 1.9 Structure of Adamantane, Rimantadine and Amantadine

1.1.6.2 NA Inhibitors

The first NA inhibitor was developed in 1966,[48] and at that time the catalytic mechanism of the NA was still unclear. In early 1990s, the crystal structure of the influenza virus surface proteins was determined and the active site of the NA was discovered, which provided more structural details and strategies to design new and specific NA inhibitors. [49] The mechanism of NA has been discussed in section 1 and shown in figure 1.4.

Four NA inhibitor antiviral drugs have been developed, two of them are FDA approved, Zanamivir and Oseltamivir. Peramivir is approved for use in South Korea and Japan, while Laninamivir is approved for use in Japan.[50] The structures of these four NA inhibitors are shown in Figure 1.10.

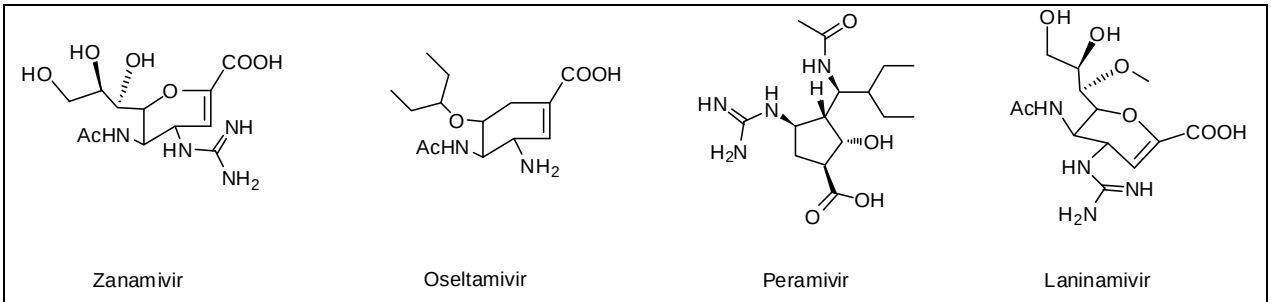

Figure 1.10. Structures of NA inhibitors.

1.1.7 Influenza Virus Detection

In addition to antiviral strategies and vaccines, early diagnosis can help arrest spread of influenza virus. There is a critical need for rapid detection method of influenza virus. Current detection methods are inadequate. A comparison of different tests based on the ASSURED (Affordable, Sensitive, Specific, User-friendly, Rapid and robust, Equipment-free and Deliverable to end-users) criteria set forth by the World Health Organization (WHO), is given in Table 1.1. Briefly, there are four major detection methods: rRT-PCR (real time Reverse Transcription Polymerase Chain Reaction), virus culture, antibody based test, and fluoro/ colorimetric test. rRT-PCR detection is expensive and require sophisticated instruments, trained personnel and the right primers. [51] In addition, testing multiple samples takes time and it is not possible to apply this detection method in resource-poor areas. Although large hospitals can afford sophisticated multiplexed PCR systems, multiple testing takes time, effort and money. Virus culture takes days and is expensive to test hundreds of samples. Fluorescence tests require

a laboratory setting. [52] Antibody tests are rapid and use friendly, but are not sensitive and antibodies suffer from stability and quality control issues. [53] The CDC does not recommend using antibody based tests because they are not sensitive. Additionally, drug susceptibility cannot be determined using antibody based tests.

ASSURED Criteria	**Detection methods**			
	Culture	**Nucleic Acid**	**Fluoro/ Colorimetric**	**Antibody**
Affordable	No, requires laboratory equipment	No, Cepheid and Biomeriux sell point of care system, but cost thousands of dollars.	No, an instrument costs thousands and the reagents are expensive.	Yes, but cost varies. Typical cost is ~ 18-20 $ per test. e.g. Quidel Flu A&B test is 450 $ for a pack of 25. However, the cost of these tests is coming lower.
Sensitive	High	High	High	No, very low sensitivity (20-80%), especially at low concentrations. [54]
Selective	High, can distinguish between live and dead virus.	High, but requires the correct primers and cannot distinguish between dead and live virus	Medium/High but cannot distinguish between live and dead viruses.	High, > 90%, but cannot distinguish between live and dead virus.
Rapid	No, requires days.	No, sample preparation takes hours, but newer systems are integrated to yield results in 1-2 hours.	60 minutes.	15 minutes
Robust	No, requires several reagents, which are not stable	Yes/No, some reagents may require refrigeration	No, requires refrigeration.	Yes/No, depends on antibody stability. May require refrigeration

User friendly	No, requires trained personnel.	Yes/No, newer systems are becoming simpler, but still require trained personnel.	No, requires trained personnel.	Yes
Equipment free	No	No	No	Yes
Deliverable to end users	No, requires a laboratory.	No, requires space	No, requires space	Yes, small footprint, portable
Drug susceptibility	Yes, but takes days	Yes, but takes days	Yes, but requires hours	No

Table 1.1 A comparison of different tests for influenza virus based on the ASSURED

Clearly, there is a great need to develop new diagnostics for influenza viruses. We have been developing receptor (sialic acid) mimics as novel recognition molecules to capture influenza viruses. These efforts are described below.

1.2 Glycan Based Detection and Drug Susceptibility of Influenza Virus Using Microarray

This part of the thesis has been published (Xiaohu Zhang, *et al*. "Glycan based detection and drug susceptibility of influenza virus." Analytical chemistry. **86**.*16*. **2014**, 8238-8244.)

1.2.1 Abstract

In this project, a panel of synthetic glycans has been developed as receptor mimics for the specific capture of influenza viruses. The glycans were printed onto commercial glass slides using a free amine at the end of a spacer to generate a small focused microarray. The microarray was evaluated for its ability to capture three different strains of influenza A virus, two H1N1, A/Brisbane/59/2007 and A/Solomon Islands/3/2006 and one H3N2, A/Aichi/2/1968. We observed excellent detection ability with some compounds exhibiting clinically relevant (10^1 plaque forming units) limit of detection. We also tested the drug susceptibility of current antivirals, Zanamivir and Ostelamivir using this microarray and could determine antiviral resistance for these strains (Figure 1.11).

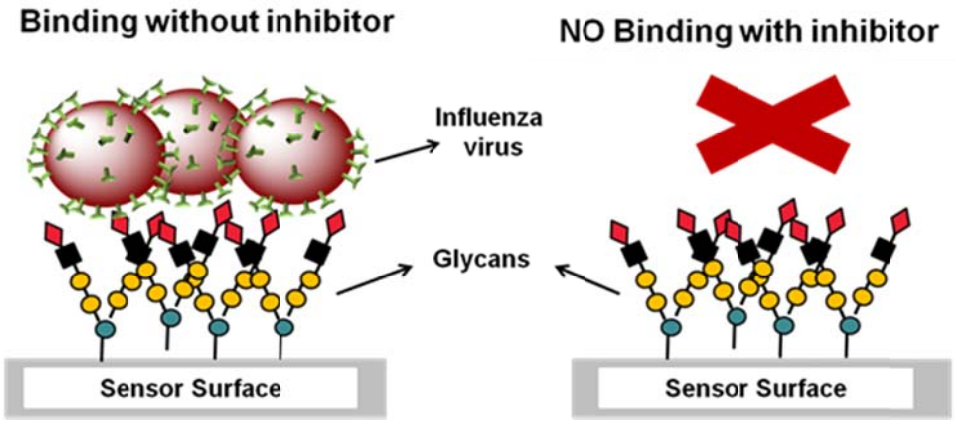

Figure 1.11 Influenza virus detection and measuring drug susceptibility using microarray Left: Influenza virus can be captured by glycans. Right: Influenza virus cannot be captured by glycans when NA is inhibited by antiviral drug.

1.2.2 Introduction

Our first approach was to develop a highly focused glycan microarray to capture and detect influenza viruses. Since printing the glycans to generate a microarray is part of the project, we describe the fabrication of glycan microarrays in the next section. This will be followed by the design and synthesis of NA specific glycans, followed by biological evaluation.

1.2.3 Glycan microarray

The surface of living cell is decorated with highly diverse structures of glycans, these glycans are involved in many biological process by recognizing the glycan binding proteins. Glycan microarray has been introduced since 2002 to detect the binding pattern for this class of biological molecules.[55] Glycan microarray was successfully developed based on the printed arrays of other biomolecules such as DNA arrays.[56] It filled a critical need for the biological molecular recognition detection with the synthetic glycan libraries. The glycan libraries could be high throughput screened by different glycan binding proteins to identify their biological roles. Publications based on glycan microarray have grown exponentially since the glycan microarray is introduced to detect the binding pattern of the glycans. It is widely used in the research area including functional glycomics, diagnosis and drug discovery.

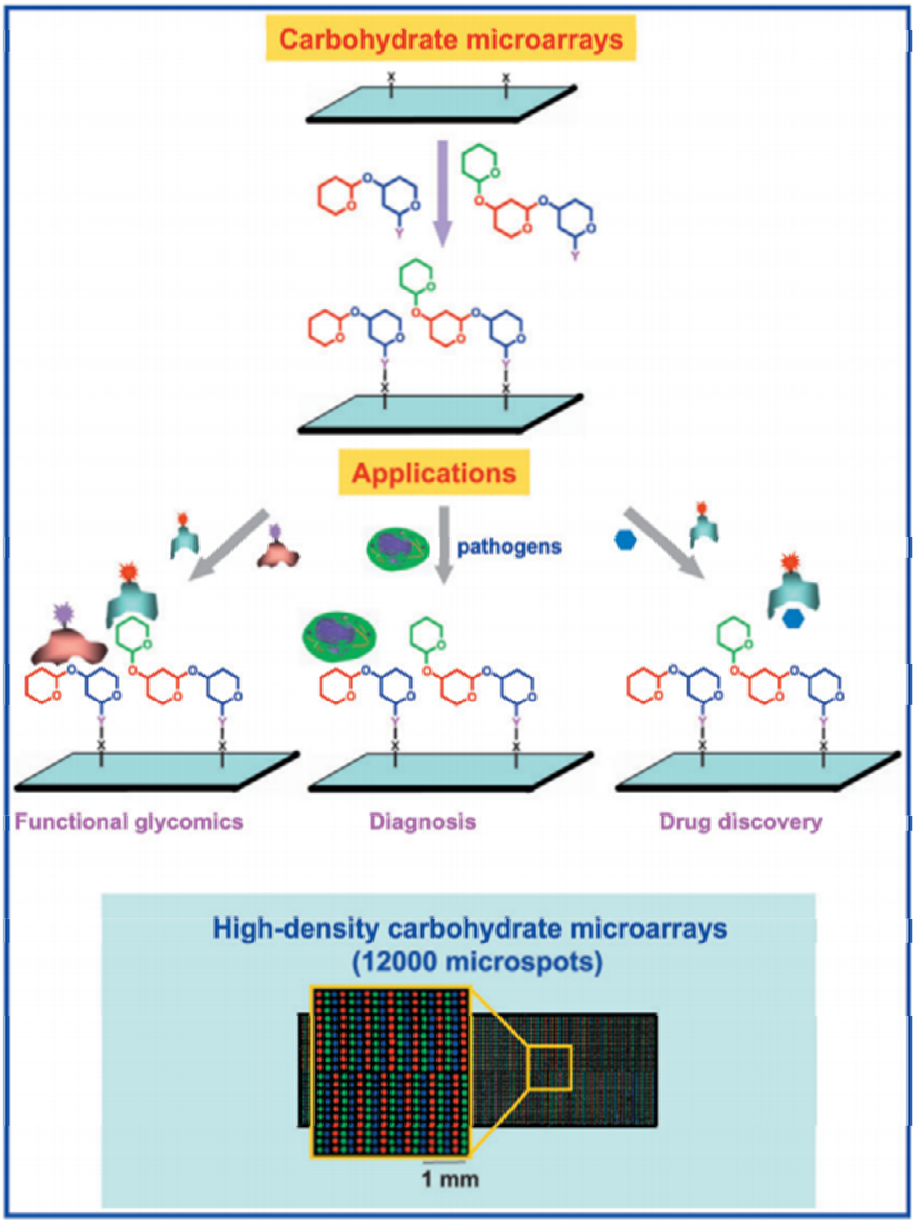

Figure 1.12 Glycan Microarrays

Glycan microarrays can be generated by different strategies and the binding pattern of pathogens or antibody will be evaluated by fluorescent intensity.

Figure is taken from publisher with permission. [57]

The printed glycan microarray detection method is shown in Figure 1.12. First, glycans are prepared to printed on the surface of the slide, thus, the glycan could be anchored on the surface of the slide, second, unmodified area of the slide will be covered by other molecular such as PEG to avoid the detection signal noise. Next, analyte such as glycan recognition protein or pathogens are incubated with the array of glycans and the unspecific binding will be washed away. If the analyte had a fluorescent tag, the slide will be scanned on a microarray scanner and further analyzed by special image software, if not, another molecule such as fluorescent tag marked antibody will be introduced to incubate with the array. Finally, the image of the microarray will be analyzed to generate the binding pattern of the analyte. Glycan microarray has been widely used in binding pattern test as shown in Figure 1.13.

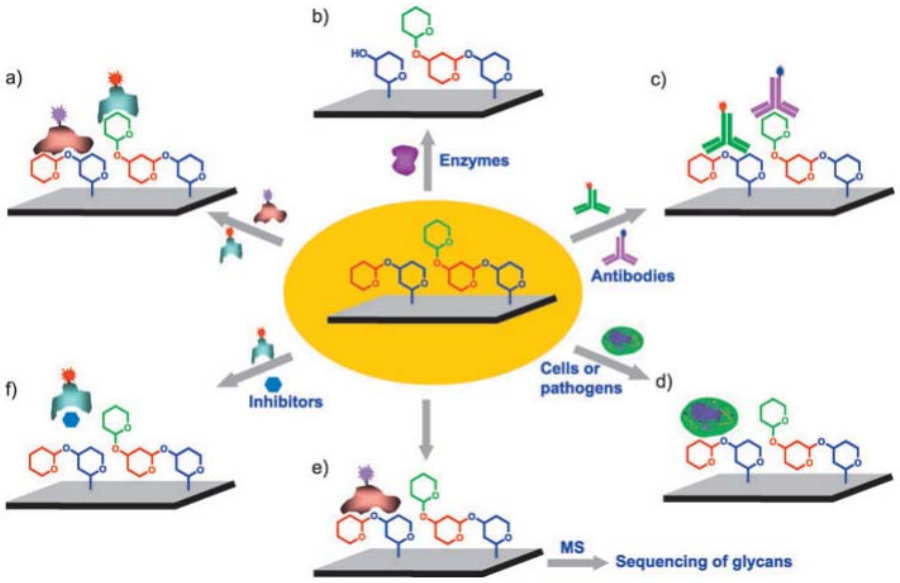

Figure 1.13 Applications of glycan microarray

Glycan microarray has been widely used to test the binding pattern of carbohydrates with enzymes, antibodies, cells or pathogens and inhibitors.

Figure is taken from publisher with permission. [57]

Common strategies to generate glycan libraries are mainly based on three methods: synthetic, enzymatic, and naturally derived glycans as shown in Figure 1.14. The synthetic and enzymatic methods have been widely used to generate the large number of the glycan libraries. Unfortunately, although great strides have been made to develop more convenient methods for the synthesis of glycans in the last 30 years, [58] unlike DNA and protein synthesis, there are no systematic ways for routine synthesis of glycans. Complicated glycans are still hard to obtain from synthetic and enzymatic methods. Releasing from glycoproteins and glycolipids is another major method to obtain glycans for array constructions. However, the major challenge to set up glycan libraries from natural sources is the purification of individual glycans and their structure verification.

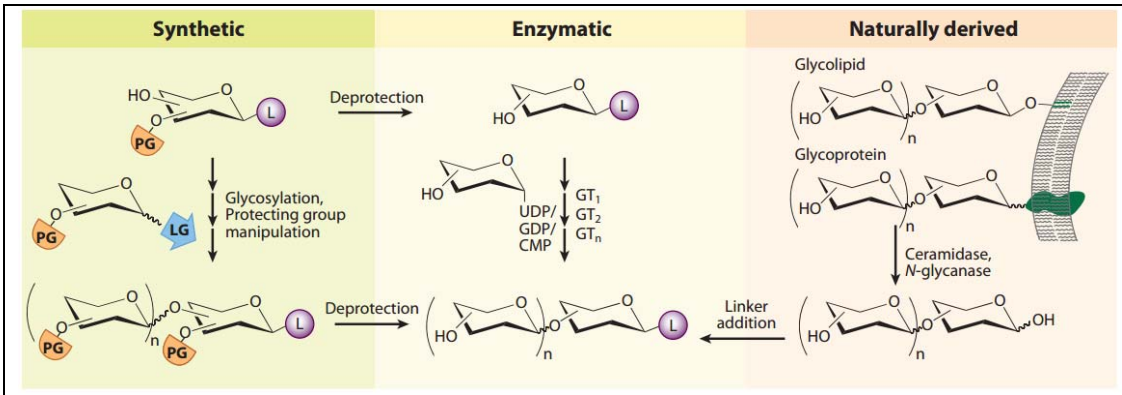

Figure 1.14 Three methods to generate glycan libraries

Synthetic method, glycan is synthesized by different method using PG (protection groups), L (linker) is introduced at the terminal of glycan. Enzymatic method, glycan is obtained by enzymatic catalytic reaction. Naturally derived method, glycan is cleaved and isolated from naturally product such glycolipid or glycoprotein.

Figure is taken from publisher with permission. [59]

To anchor the glycans on the surface of the array slide, the glycan need to be modified with a functional linker. Several strategies have been applied to modify the glycan including reductive amination[60], glycosylamine formation and trapping[61], hydrazide chemistry[62], oxyamine and N-alkyl oxyamine condensations[63] as shown in Figure 1.15.

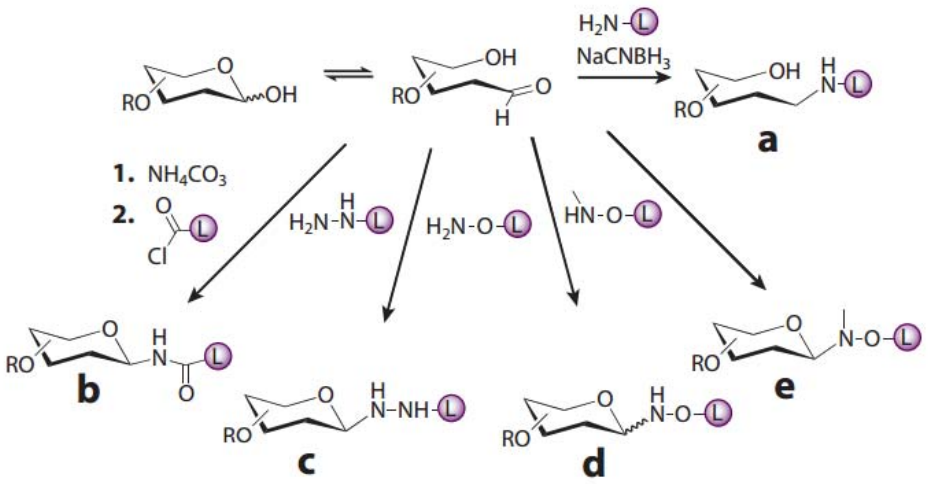

Figure 1.15 Strategies applied to modify the glycan libraries.

Briefly, several strategies have been applied to modify the glycan such as reductive amination, glycosylamine formation, hydrazide chemistry, oxyamine and N- alkyl oxyamine condensations. The aim of the modification is to introduce the linker to the glycan.

Figure is taken from publisher with permission. [59]

To finally anchor glycan on the surface of the array slide, the solid surface needs to be modified to introduce the spacer of the glycan. Strategies used to modify the slide surface include the methods that have been used to prepare DNA and protein microarrays, and the novel methods that developed specifically for glycan microarrays. The modification of the surface will

be finally used to immobilize or fabricate the glycan on to it. The modification methods are shown in Figure 1.16.

We have used two different methods to fabricate glycan microarrays. For influenza detection, we have attached the linker to the glycans. The linkers are terminated with an amine, which is printed on activated carboxylic acid slides. For norovirus detection, we have glycans attached to BSA, which is printed onto glass slides. The two different strategies and the biological evaluation are described in the following sections.

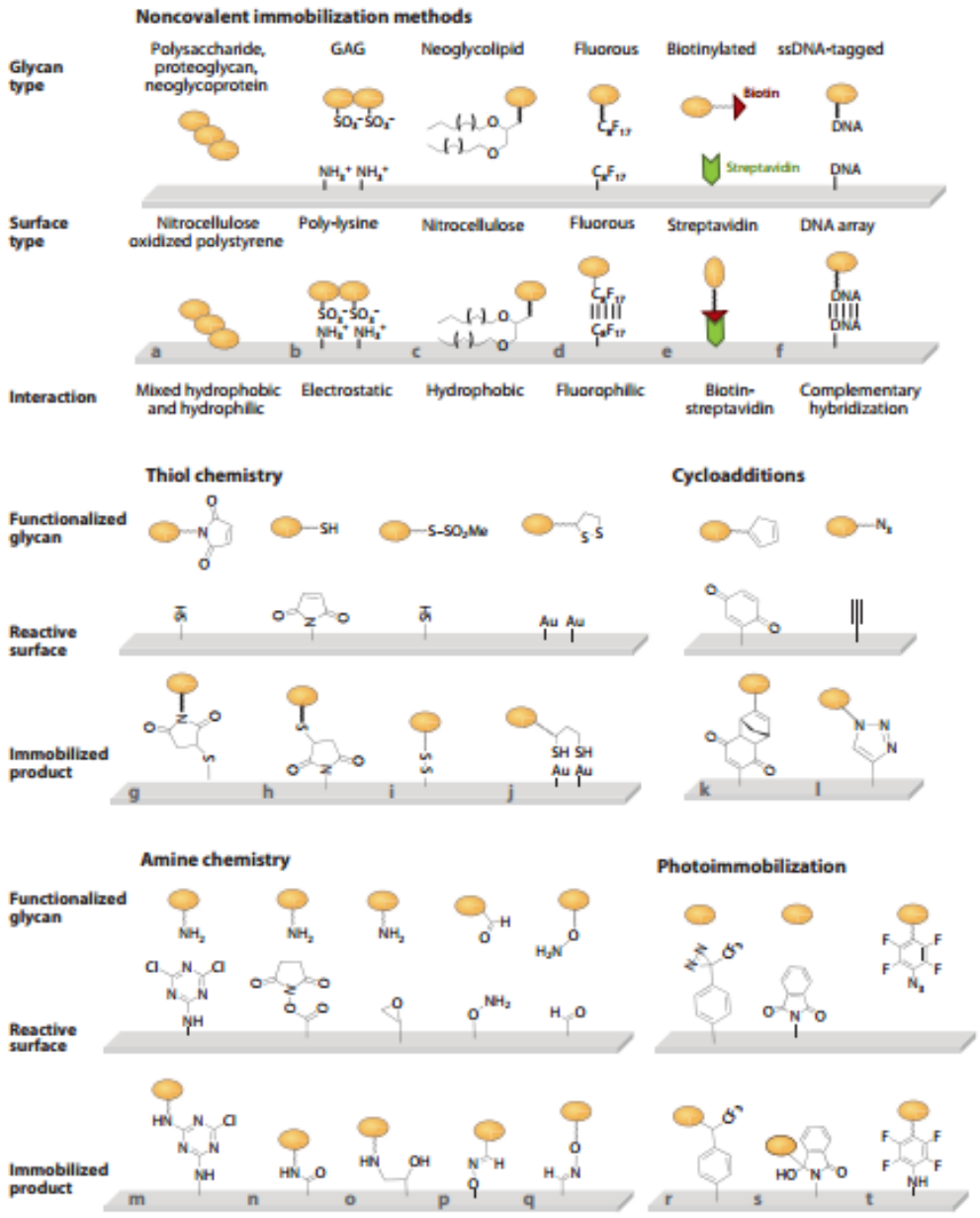

Figure 1.16 Methods to modify the surface of the array slide

Based on different linker of the glycans, different methods are applied to immobilize glycans on the surface of microarray chips. Function groups show on the surface of the chips and the corresponding glycans are shown on the top of the chips.

Figure is taken from publisher with permission. [59]

1.2.4 Design and Synthesis

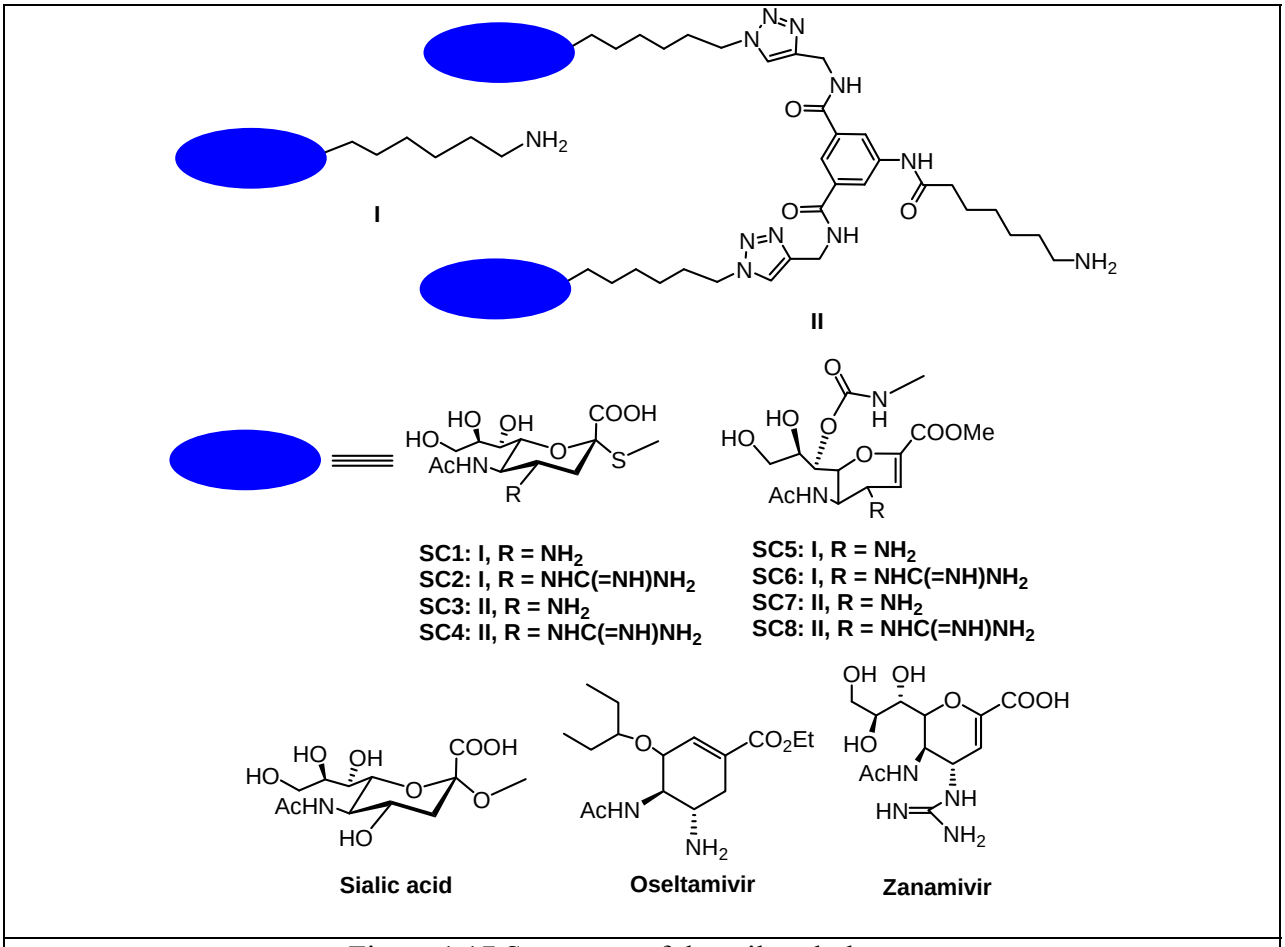

Figure 1.17 Structures of the tailored glycans.

The blue ellipse represents the two glycan headgroups, and I and II represent mono and bivalent derivatives. The natural receptor, N-acetyl neuraminic acid (sialic acid), and the FDA approved antivirals, Zanamivir and Oseltamivir, are also shown.

The structures of the eight molecules used to develop the focused microarray are shown in Figure 1.17. There are several salient features of the designer molecules. First, all eight molecules are derived from the natural receptor, namely sialic acid. Second, the molecules have a free amine at the end of a spacer which is necessary for facile attachment to an activated carboxyl acid group on any surface. Third, the molecules also have an amine or a guanidine

group at the four position; introduction of a polar group at the four position has been demonstrated to be highly specific to influenza virus as X-ray structures have shown that the polar group fits very well into a binding pocket of influenza virus NA, but doesn't fit well into human or bacterial NA. [64] Fourth, we designed two types of molecules; **SC1-4** are sialic acid analogues that have spacers attached to the 2 position via a thiol linkage, in contrast, **SC5-8** are analogues derived from Zanamivir® and attached to the spacer at the 7 position. [65] Finally, since we recently demonstrated that molecules similar to **SC1-4** and bivalent molecules thereof, inhibited two H1N1 and H3N2 strains at low nanomolar concentrations, we designed monovalent and bivalent derivatives.[65c] The bivalent derivatives were synthesized for two reasons. First, the bivalent scaffold provides additional distance from the microarray surface for the NA's of the virus to bind. Second, NA exists as a tetramer with four binding sites, the distances between the two glycan headgroups are spaced such that a single molecule could fit into to two binding sites from a single NA tetramer or alternatively, fit into the pockets of two adjacent NA tetramers on a single virion. [66] When these mono and bivalent molecules are tethered to a surface, the overall binding affinity of multiple glycans with influenza viruses is expected to increase exponentially, leading to a higher capturing efficiency.

The syntheses of the molecules are shown in Scheme 1.1 and 1.2. For **SC1-4**, the thioacetate group of the known azido compound **1** was reacted with a suitable six carbon spacer, which had a chloride at the terminus to yield **2** in appreciable amounts. The azide was reduced under mild conditions using triphenylphosphine and the amine group was either protected by a tert-butoxy group or a suitably protected guanidine group followed by replacement of the chloride by an azide using sodium azide to yield **3a** and **3b** in decent yields. Zemplén deprotection to remove the acetates and methyl ester was followed by acidic removal of the tert-

butoxy groups and subsequent reduction of the azide using standard hydrogenation conditions yielded the monovalent compounds **SC1** and **SC2** which had an amine and a guanidine group at the four position of the sialic acid, respectively. Copper(I) catalyzed 1,3 dipolar addition of **3a,b** with a dimeric scaffold, **4** bearing two alkyne groups resulted in the fully protected bivalent compounds, **5a,b** in good yields. The protecting groups were removed using the same conditions as described for the monovalent derivatives to yield the bivalent compounds, **SC3-4**. For the Zanamivir analogues, **SC5-8**, we attached the spacer to the seven hydroxyl group as modifications at this position are well tolerated by NA, indeed this approach has been used to attach a biotin to Zanamivir. To this end, we elaborated the known azido compound **6** by reducing the azide and protecting the free amine group using a tert-butoxy group to yield **7** in high yields. This was followed by base induced deprotection of the acetate groups and acetonide protection of the 8, 9 hydroxyl groups leaving the hydroxyl group at the 7 position open for conjugation to the spacer. The terminal amine of a six carbon spacer bearing an azide group at the opposite end was conjugated to **8**, in a two-step procedure using p-nitrochloroformate as the coupler to yield the carbamate **9**. The acetonide group was removed under mild acidic conditions to produce **10a**. The guanidine derivative, **10b** was synthesized from **10a**, the tert butoxy group was removed and a suitably protected guanidine group was attached to the free amine to yield **10b** in significant amounts. This strategy of installing the guanidine group at this later stage was more successful in our hands as opposed to introducing the guanidine group early in the synthesis, the latter strategy gave us undesirable products and variable results. Global deprotection of **10a, b** was performed as described for **SC1,2** to yield **SC5,6** in good yields. The bivalent derivatives **SC7,8** were synthesized from **10 a,b** in a manner similar to the synthesis of **SC3,4** by coupling to the scaffold **4**, followed by global deprotection. The final compounds were

purified using size exclusion chromatography using Biogel P2 and the appropriate fractions containing the compounds were freeze dried to produce colorless foamy solid material.

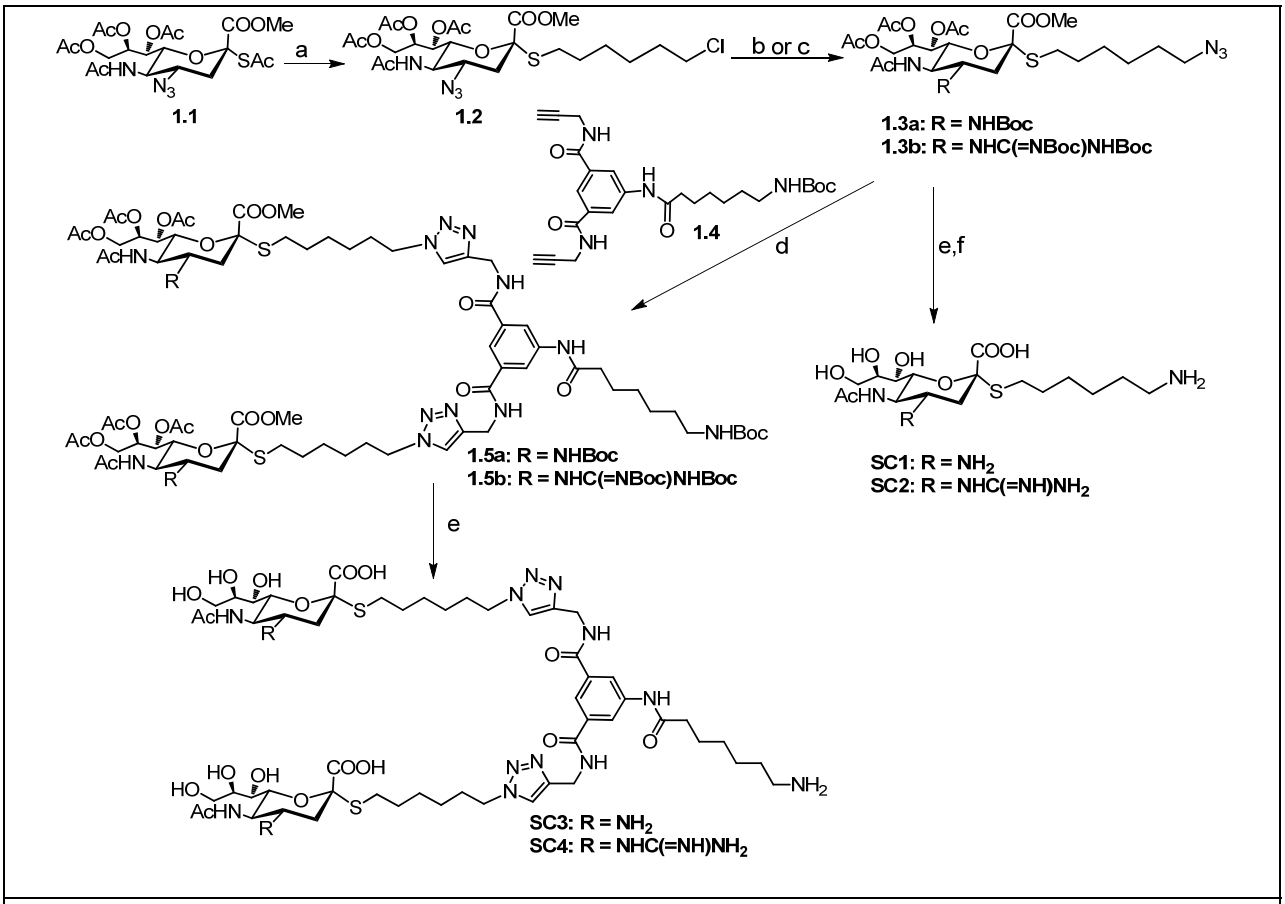

Scheme 1.1 Synthesis route for **SC1**, **SC2**, **SC3** and **SC4**.

(a) 6-Chlorohexyl 4-methylbenzenesulfonate, DEA, DMF, rt, 4 h. 80% (b) i. PPh_3, THF/H_2O (1:1), 40 °C, 12 h. ii. (t-Boc)$_2$O, TEA, THF, 60%. iii. NaN_3, DMF, 60 °C. 90%. (c) i. PPh_3, THF/H_2O (1:1), 40 °C, 12 h. ii. 1,3-Bis(*tert*-butoxycarbonyl)-2-methyl-2-thiopseudourea, TEA, $HgCl_2$, 85%. iii. NaN_3, DMF, 60 °C. 93%. (d) Na-*L*-ascorbate, $CuSO_4$, THF/H_2O. 12 h, 60% for **5a**; 65% for **5b**. (e) i. NaOMe, MeOH. ii. DCM/TFA. iii. NaOH, MeOH, 80% yield for **SC3**, 70% yield for **SC4**. (f) H_2, Lindlar catalyst, EtOH/H_2O, 4 h, 75% yield for **SC1**, 70% yield for **SC2**.

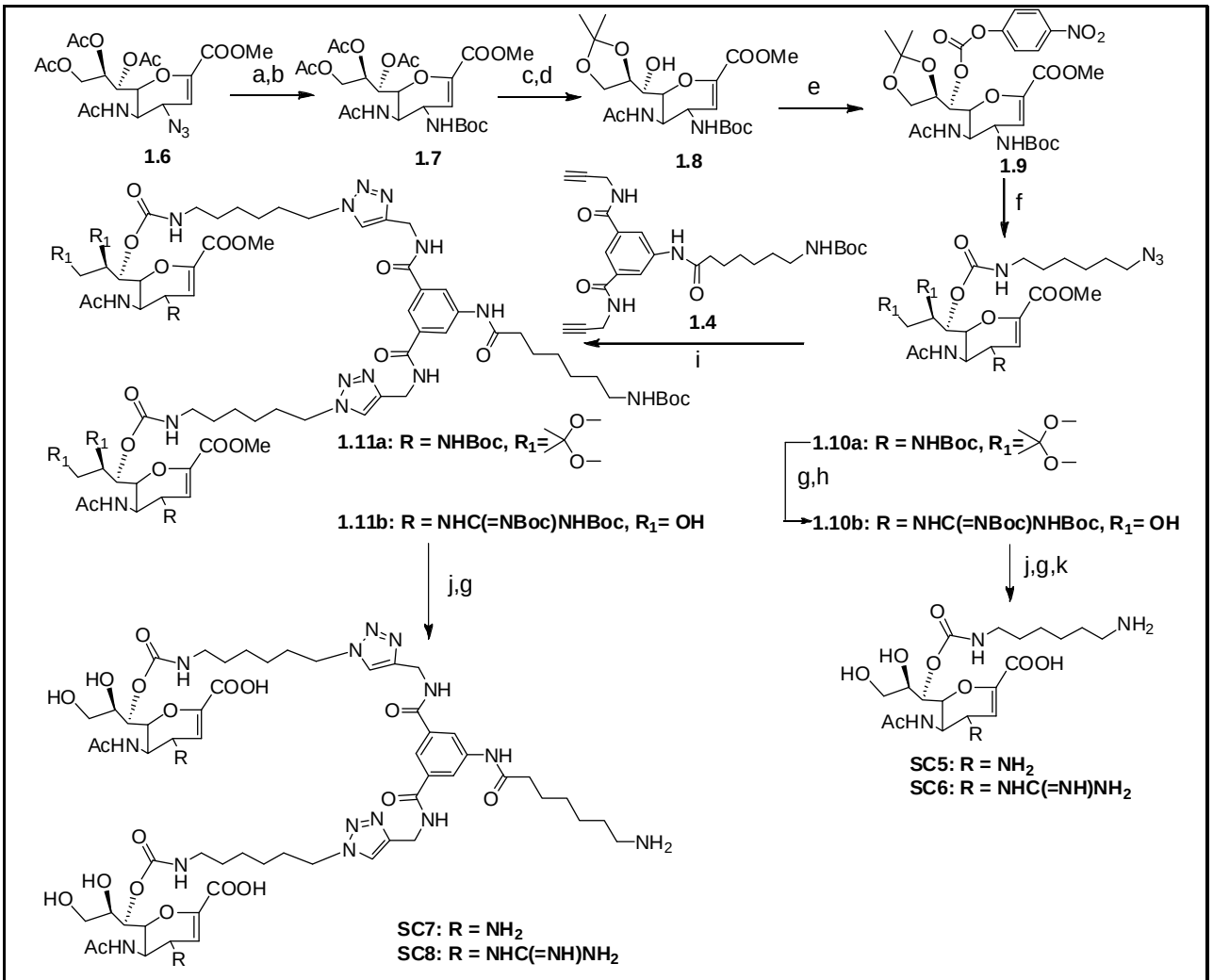

Scheme 1.2 Synthesis route for SC5, SC6, SC7 and SC8.

(a) H_2, Lindlar catalyst, EtOH, 4 h, quant. (b) Boc_2O, TEA, THF, 12 h, 86%. (c) NaOMe, MeOH, 1 h, quant. (d) H^+ resin, acetone, 12 h, 88%. (e) DMAP, pyridine, *p*-$NO_2C_6H_4OCOCl$, 12 h, 80%. (f) 6-Azido-hex-1-amine, CH_3CN, TEA, 3 h, 89%. (g) TFA, DCM. (h) 1,3-Bis(*tert*-butoxycarbonyl)- 2-methyl-2-thiopseudourea. $HgCl_2$, TEA, DCM, 12 h, 84%. (i) Na-*L*-ascorbate, $CuSO_4$, THF/H_2O, 12 h. 78% for **11a**; 80% for **11b**. (j) NaOH, MeOH. 1 h. 70% for SC7; 79% for SC8. (k) H_2, Lindlar catalyst, EtOH, 4 h. 76% for **SC5**; 72% for **SC6**.

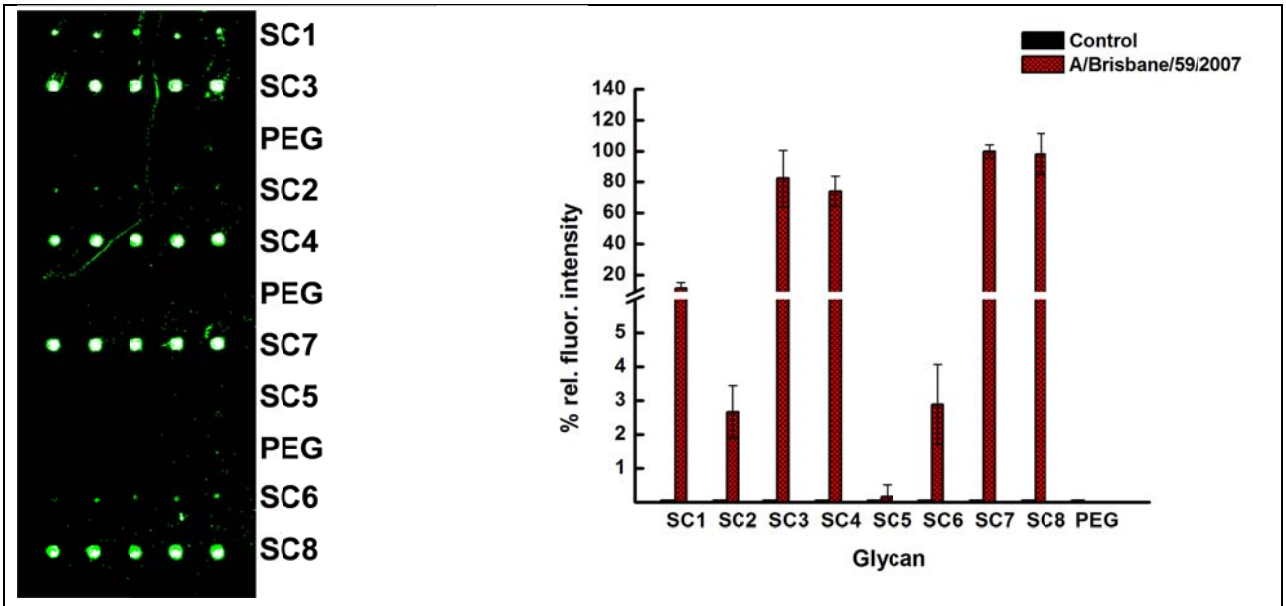

Figure 1.18 Influenza virus binding studies.

Left: Fluorescence image of microarray containing eight glycans (**SC1−SC8**) after exposure to 10^5 PFU of H1N1 Influenza A/Brisbane/59/2007, followed by ferret hyperimmune sera and antiferret rhodamine labeled secondary antibody for A/Brisbane/ 59/2007 and scanned by Genepix scanner at 532 nm. Right: Fluorescence detection of H1N1 (A/Brisbane/59/2007) influenza A virus using synthetic glycans. Glycans, PEG (negative control) and biotin (positive control) were printed at 200 μM. Virus concentration was 10^5 PFU. Fluorescence intensity was measured by the Genepix scanner using ferret hyperimmune sera to influenza A/Brisbane/59/2007 (H1N1) and antiferret rhodamine labeled antibody. A/Brisbane/59/2007 was scanned at 532 nm. The experiment was performed in triplicate.

The synthetic glycans were printed onto commercial glass slides bearing activated carboxyl groups for conjugation to the free amines of **SC1-8** to produce a focused microarray. Printing was performed at various concentrations; we used a concentration of 200 μM for all assays in this report as it gave us excellent signal to noise ratio. Amine terminated PEG was printed as a negative control. Amine terminated biotin was included as a positive control. The microarray was exposed to three different strains of influenza virus, two H1N1, A/Brisbane/59/2007 and A/Solomon Islands/3/2006 and a H3N2, A/Aichi/2/1968. The strains were incubated at rt for 60 min, followed by incubation of the appropriate primary and fluorescently labeled secondary antibody. The slides were washed at every stage extensively and the slides were scanned using a Genepix scanner at 532 or 635 nm. Reproduced in Figure 1.18 is the fluorescence image where the microarray was exposed to 10^5 PFU of H1N1 Influenza viruses A/Brisbane/59/2007. The image clearly shows that the bivalent compounds, **SC3,4,7,8** captured the virus very well, however, most of the monovalent compounds, **SC1,2,5,6** bind weakly to this strain, suggesting that the bivalent derivatives provide the required distance from the surface for the virus to bind. We and others have observed this phenomenon before, binding of glycans to their respective analytes are highly dependent on glycan density and presentation. Exposure to H3N2 strain A/Aichi/2/1968, resulted in similar results (Figure 1.19-1.21), however, all compounds bound well to H1N1, A/Solomon Islands/3/2006, indicating that this virus strain is more accommodating in its binding preferences. (Figure 1.19-1.21). Non-specific binding to the control ligand, PEG, was negligible, which is a very important aspect of biosensor development as viruses are notorious in terms of non-specific binding. Several other controls (with buffer only, using other synthetic glycans) were performed and all of these control experiments resulted in no binding. We observed a differential response to the ligands for each viral strain, for example, the

A/Aichi/2/1968 strain exhibits similar binding to all four bivalent compounds, the A/Brisbane/59/2007 strain binds better to the bivalent compounds, **SC4** and **SC8**, with the guanidine group at the four position, with the best binder being **SC4**. With more ligands and slight differences in the binding affinities, this differential pattern could potentially be used to develop a "fingerprint" pattern of recognition for each strain, including emerging strains. [67]

Next, we determined the analytical limit of detection using different concentrations of the different strains from 10^6 to 10^1PFU. As shown in Figure 1.19-1.21, the bivalent compounds bind to the three different strains at higher concentrations very well with high relative fluorescence intensities. At the lowest tested concentration of 10^1 PFU, the bivalent compounds **SC3** and **SC7** bind well to the H1N1 A/Brisbane/59/2007 and the A/Solomon Islands/3/2006 strains, however, only **SC3** binds to the H3N2 A/Aichi/2/1968 strain. Known differences in the binding pockets of N1 and N2 could be a possible reason for this difference in binding at lower concentrations in addition to the number of NAs present on the surface of each strain. [68] We note that these first generation ligands can capture extremely low clinically relevant concentrations of viruses and further optimization could lead to lower limits of detection. Finally, we tested the microarray for susceptibility to FDA approved antivirals, Zanamivir® and Oseltamivir® (Figure 1.22-1.24). Briefly, known concentrations of the three strains were premixed with either one of the antivirals and exposed to the microarray. Washing to remove unbound virus was followed by detection using the appropriate primary and labeled secondary antibody. It was gratifying to observe no binding to any of the compounds for all three strains, which indicates that the antiviral blocks the NA leading to loss of signal. There are two outliers, **SC3** and **SC7**. In the presence of antivirals, **SC3** binds H3N2 A/Aichi/2/1968 strain and **SC7** binds both H1N1 strains. A possible explanation for these observations could be that the binding pocket of HA for each

particular strain could accommodate sialic acid with an amine at the 4 position, which is similar to the structure of the glycan head groups in **SC3** and **SC7**.

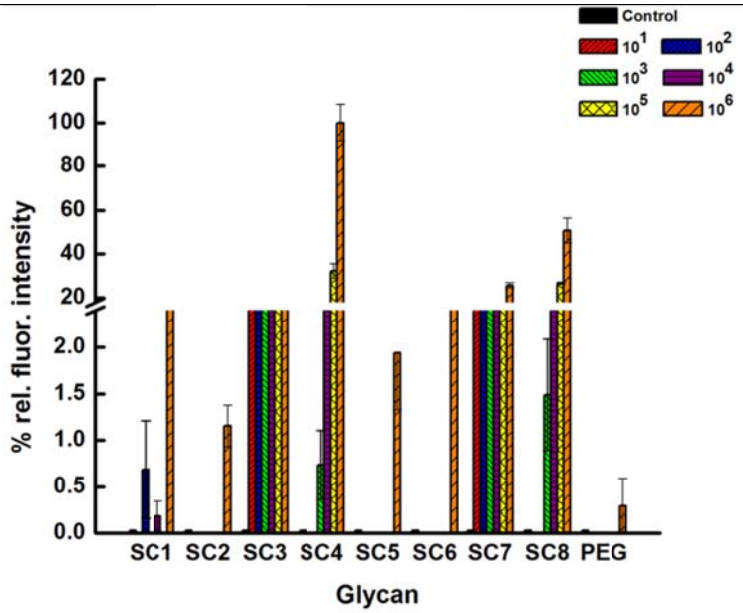

Figure 1.19 Limit of detection for H1N1 Influenza A/Brisbane/59/2007.

Figure 1.19-1.21, fluorescence intensity for A/Brisbane/59/2007 was measured as previously described for Figure 1.18. Fluorescence intensity was measured by the Genepix scanner using ferret hyperimmune sera to influenza A/ Solomon Islands/3/2006 (H1N1) and antiferret rhodamine labeled antibody; polyclonal antiserum chicken to A/Aichi/2/1968 (H3N2) and Alexa Fluor 633 labeled antichicken. A/Solomon Islands/3/2006 was scanned at 532 nm and A/Aichi/2/1968 at 635 nm. All experiments were performed in triplicate.

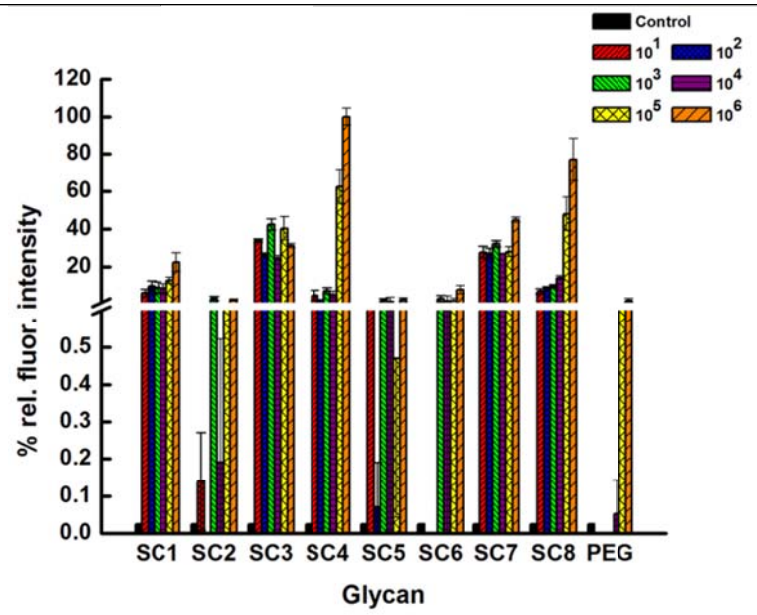

Figure 1.20 Limit of detection for H1N1 Influenza A/Solomon Islands/3/2006.

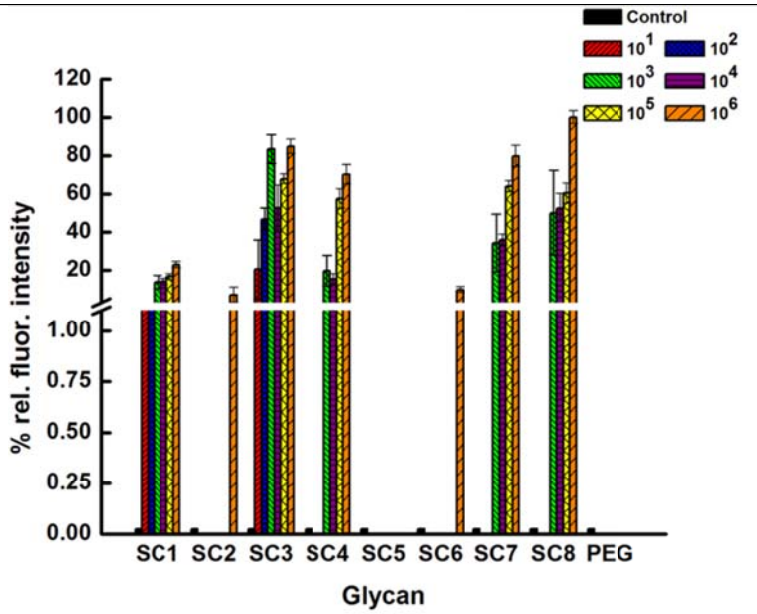

Figure 1.21 Limit of detection for H3N2 Influenza A/Aichi/2/1968.

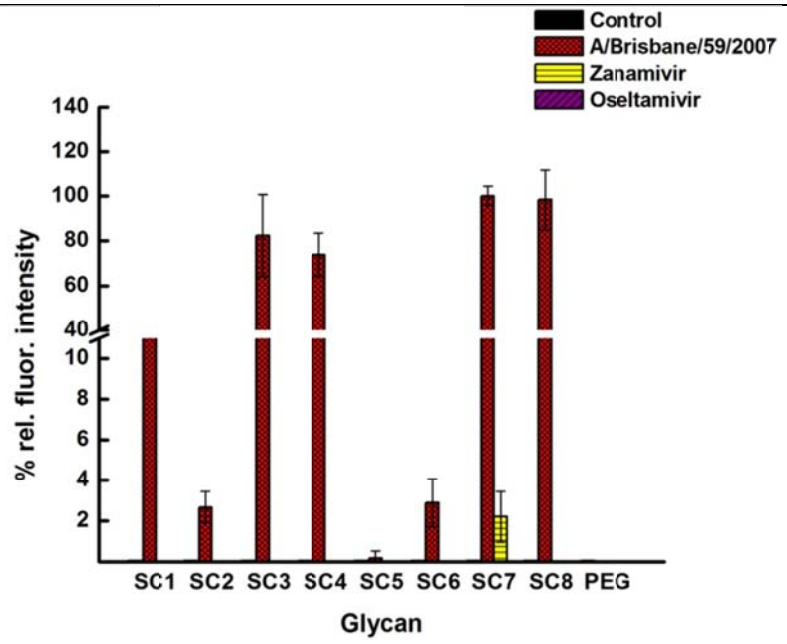

Figure 1.22 Drug susceptibility studies for H1N1 Influenza A/Brisbane/59/2007.

Figure 1.22-1.24, ten nanograms of antivirals Zanamivir or Oseltamivir were premixed with the strains at 10^5 PFU for 30 min at rt and subsequently added to the microarray. Fluorescence intensity was measured as previously described in Figures 1.18. All experiments were performed in triplicate.

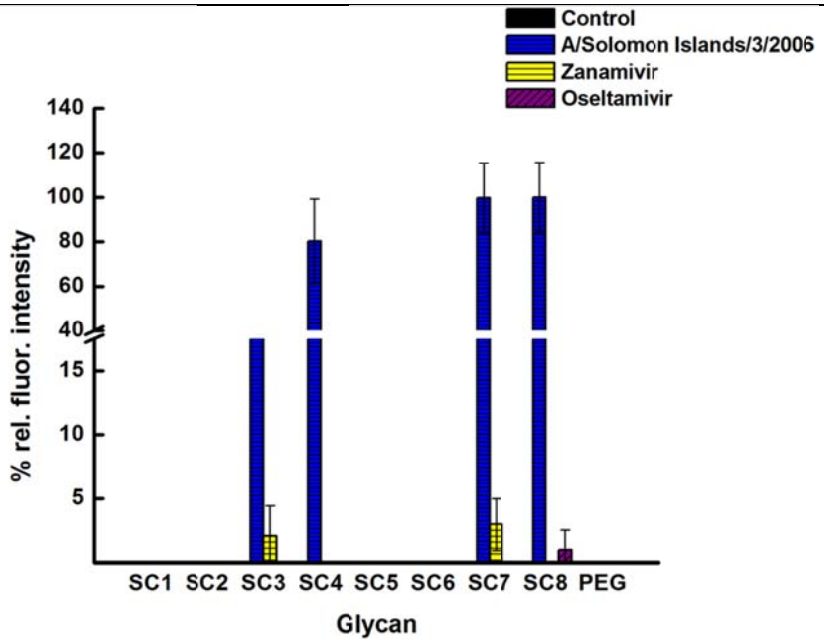

Figure 1.23 Drug susceptibility studies for H1N1 Influenza A/Solomon Islands/3/2006.

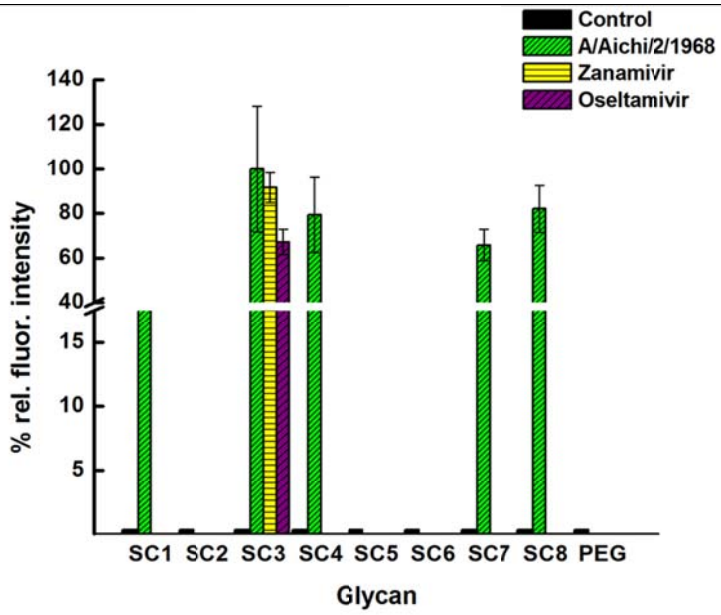

Figure 1.24 Drug susceptibility studies for H3N2 Influenza A/Aichi/2/1968.

1.2.5 Conclusion

We have synthesized tailored glycans, printed them onto glass slides and demonstrated the ability of a focused microarray to capture three influenza strains at different concentrations. We determined the limit of detection to be 10^1 PFU, which indicates that the assay is clinically relevant. We also demonstrated that the assay can be used to test drug susceptibility of current FDA approved antivirals, Zanamivir® and Oseltamivir®, by premixing the antivirals with the strains and performing the assay. Thus, the assay reported in this article can be performed rapidly within hours using minimal tools. In contrast, current genotyping methods to determine antiviral resistance is typically performed in a clinical laboratory using molecular markers by trained

personnel, specialized equipment and days to accomplish. We are currently expanding our efforts to develop second generation ligands and include more strains to demonstrate broad applicability. By further optimization of ligand structure, testing different conditions and biosensor platforms, this assay has the potential to be translated to rapid diagnostic tests.

1.2.6 Experiment Section

1.2.6.1 General Information

All reagents and solvents were of reagent grade or were purified by standard methods before use. Column chromatography was carried out on flash silica gel (Sorbent 230–400 mesh). TLC analysis was conducted on silica gel plates (Sorbent Silica G UV254). NMR spectra were recorded at ^{1}H (400 MHz) and ^{13}C (100 MHz) on a Bruker instrument. Chemical shifts and coupling constants (J values) are given in ppm and hertz, respectively, using solvents (^{1}H NMR, ^{13}C NMR) as the internal standard. All reactions were performed under argon atmosphere using degassed solvents.

1.2.6.2 Abbreviation

N,*N*-Dimethyl formamide, DMF; Ethyl acetate, EtOAc; Trifluroacetic acid, TFA; Acetonitrile, CH_3CN; Azidotrimethylsilane, $TMSN_3$; Diethylamine, DEA; Trimethylsilyltrifluoromethanesulfonate, TMSOTf; p-Toluene sulfonyl, Tos; Di-tert-butyl dicarbonate, $(Boc)_2O$; *tert*-Butyl alcohol, *t*-BuOH; Methanesulfonyl chloride, MsCl; Methanol, MeOH; Tetrahydrofuran, THF; Dichloromethane, DCM; Hydrochloric acid, HCl; Triphenylphosphine, PPh_3; Sodium sulfate, Na_2SO_4; Sodium azide, NaN_3; *N*-methyl morpholine, NMM; 2-Chloro-4,6-DiMethoxy-1,3,5-Triazine, CDMT; Sodium methoxide, NaOMe; Cupric sulfate, $CuSO_4$; Triethylamine, Et_3N; De-ionized water, DI water; Hydrogen gas, H_2; , H_2O;

Triethylamine, Et_3N; Mercury(II) chloride, $HgCl_2$; Dimethylamino pyridine, DMAP; Sodium bicarbonate, $NaHCO_3$; Acetonitrile, CH_3CN.

1.2.6.3 Synthesis and Characterization

Compound 2: 6-S-[Methyl 5-acetamido-7, 8, 9-*tri*-O- acetyl-4-azido-3, 4, 5-trideoxy -D-glycero-α-D-galacto-non-2-ulopyranosyl) onate]-1-chloro-hexane.

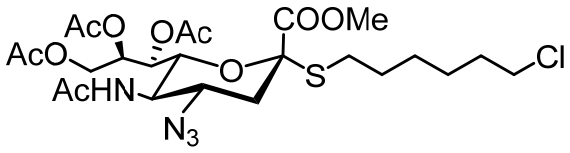

To a stirring solution of compound **1**[66] (0.50 g, 0.94 mmol) in DMF (1.0 ml), DEA (0.95 ml, 9.4 mmol) was added. The reaction mixture was stirred for 10 min at rt. 6-Chlorohexyl 4-methylbenzenesulfonate (0.35 g, 1.1 mmol) was added and the reaction stirred for additional 12 h. The reaction mixture was quenched using brine solution (0.20 L, 1x) and extracted with ethyl acetate (0.050 L, 3x). Organic layers were combined and washed with HCl solution (0.05 ml, 1M, 1X), dried over Na_2SO_4 and concentrated in vacuo. The title compound was purified using column chromatography with hexane:acetone (3:1) as eluent to yield a yellow oil (0.46 mg, 80% yield). ^{1}H NMR (400 MHz, $CDCl_3$) δ 5.57 (d, J = 8 Hz, 1H), 5.39-5.36 (m, 1H), 5.31 (d, J = 7.6 Hz, 1H), 4.34-4.30 (m, 1H), 4.25-4.19 (m, 1H), 4.11 (d, J = 10.8 Hz, 1H), 4.06-4.02 (m, 1H), 3.83 (s, 3H), 3.56 (vt, J = 6.4, 13.2 Hz, 2H), 3.33-3.25 (m, 1H), 2.82-2.73 (m, 2H), 2.59-2.53 (m, 1H), 2.18 (d, J = 3.2 Hz, 6H), 2.06 (s, 3H), 2.01 (s, 3H), 1.81-1.73 (m, 3H), 1.55-1.39 (m, 6H). ^{13}C-NMR (100 MHz, $CDCl_3$) δ 170.8, 170.7, 170.6, 170.0, 168.3, 82.9, 72.8, 68.3, 68.0, 62.0, 58.0, 52.3, 45.0, 38.2, 32.4, 29.1, 28.7, 28.0, 26.3, 23.4, 21.1, 21.0, 20.7. HRMS (ESI): Calculated for: $C_{24}H_{37}ClN_4O_{10}SH$, 608.1919; found, 609.1975 (M+H).

Compound 3a: 6-S-[Methyl 5-acetamido-7, 8, 9-*tri*-O- acetyl-3, 4, 5-trideoxy -4-(N-tert-butyloxycarbonyl)-amino-D-glycero-α-D-galacto-non-2-ulopyranosyl)onate]-1-azido-hexane.

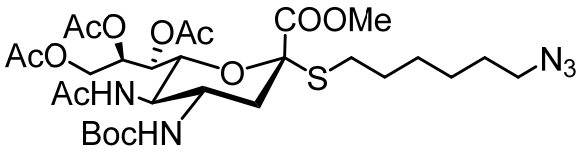

To a stirring solution of compound **2** (0.20 g, 0.33 mmol) in a mixture of THF: H_2O (5.0 ml, 1:1), PPh_3 (0.10 g, 0.39 mmol) was added and the reaction was heated at 40 °C for 12 h. The solvent was removed in vacuo and the residue purified by column chromatography to obtain a clear oil. This compound was directly taken to the next step without further purification. To a stirring solution of the crude product (0.18 g, 0.31 mmol) in THF (0.010 L) and TEA (31 mg, 0.31 mmol), di-*t*-butyl carbonate anhydride (0.10 g, 0.47 mmol) was added. Reaction mixture was stirred for 12h at rt. The white solid was filtered and the residue was concentrated, dissolved in DCM (25 ml) and washed with HCl (25 ml, 1M, 1x). The organic layer was dried over Na_2SO_4 and concentrated in vacuo. Product was purified via column chromatography with hexane: acetone (5:1) to yield clear yellow oil (0.13 g, 60% yield for two steps). ^{1}H NMR (400 MHz, $CDCl_3$) δ 5.46 (s, 1H), 5.33 (s, 2H), 4.75 (d, *J* = 8.8 Hz, 1H), 4.28 (d, *J* = 12 Hz, 1H), 4.09 (d, *J* = 8.8 Hz, 1H), 3.88 (d, *J* = 10.4 Hz, 1H), 3.79-3.73 (m, 5H), 3.52 (t, *J* = 6.4, 3H), 2.72 (d, *J* = 11.6 Hz, 2H), 2.54-2.48 (m, 1H), 2.15 (s, 3H), 2.11 (s, 3H), S-4 2.03 (s, 3H), 1.88 (s, 4H), 1.77-1.71 (m, 4H), 1.38 (s, 19H). ^{13}CNMR (100 MHz, $CDCl_3$) δ 171.0, 170.7, 170.0 169.9, 168.7, 156.0, 83.4, 80.0, 68.5, 67.5, 62.2, 52.9, 50.2, 50.0, 45.0, 39.2, 32.4, 29.1, 28.7, 28.3, 26.4, 23.2, 21.2, 20.8, 20.7. HRMS (ESI): Calculated for $C_{29}H_{47}ClN_2O_{12}S$: 682.2538; Found: 683.2613 (M+H).

To a stirring solution of the chloro derivative (71 mg, 0.10 mmol) in DMF (1.0 ml) NaN_3 (65 mg, 1.04 mmol) was added and the reaction was stirred at 60 °C. After 12 hr, the reaction mixture was quenched with DI water (25 ml) and extracted with DCM (25 ml, 3x). The organic layers were combined, washed with brine (25 ml, 1x), dried over Na_2SO_4 and concentrated in vacuo, to yield a clear oil (64 mg, 90% yield). ^{1}H NMR (400 MHz, $CDCl_3$) δ 5.47 (d, *J* = 12 Hz, 1H), 5.33 (s, 2H), 4.75 (d, *J* = 8 Hz, 1H), 4.29 (d, *J* = 12 Hz, 1H), 4.09 (d, *J* = 8 Hz, 1H), 3.87 (m, 1H), 3.79 (s, 3H), 3.60 (m, 1H), 3.52 (vt, *J* = 12, 8.0 Hz, 2H), 2.73 (d, *J* = 12 Hz, 2H), 2.54-2.48 (m, 1H), 2.15 (s, 3H), 2.11 (s, 3H), 2.03 (s, 3H), 1.88 (s, 3H), 1.77-1.74 (m, 3H), 1.5-1.40 (m, 2H), 1.38 (s, 14H). ^{13}C NMR (100 MHz, $CDCl_3$) δ 171.0, 170.7, 170.1, 170.0, 168.7, 156.0, 83.4, 80.0, 68.5, 67.4, 62.2, 52.9, 50.2, 50.0, 45.0 39.2, 32.4, 28.3, 26.4, 23.2, 21.2, 20.84, 20.80. HRMS (ESI): Calculated for $C_{29}H_{47}N_5O_{12}S$: 689.2942; Found: 690.3004 (M+H).

Compound 3b: 6-S-[Methyl 5-acetamido-7, 8, 9-tri-O- acetyl-3, 4, 5-trideoxy-4-(bis-N, N'-tert-butyloxycarbonyl)-guanidino-D-glycero-α-D-galacto-non-2-ulopyranosyl)onate]-hexane

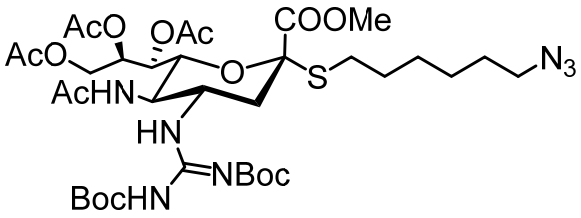

To a stirring solution of compound **2** (0.11 g, 0.20 mmol) in a mixture of THF and H_2O (2.0 ml, 1:1), PPh_3 (62 mg, 0.24 mmol) was added and the reaction was heated at 40 °C for 12 h. The solvent was removed in vacuo and purified by column chromatography using DCM:MeOH (10:1). To this compound (0.10 g, 0.16 mmol) in DCM (0.01 L), TEA (0.3 ml, 1.6 mmol) was added and the reaction was stirred for 10 min at rt. Then 1,3-bis(*tert*-butoxy-carbonyl)-2-methyl-

2-thiopseudourea (55 mg, 0.19 mmol) and $HgCl_2$ (51 mg, 0.19 mmol) were added and the reaction was stirred for 12 h. Next, the reaction mixture was washed with H_2O (25 ml, 1x) and brine (25 ml, 1X). The organic layers were separated, dried over Na_2SO_4 and concentrated in vacuo. Product was purified using column chromatography with hexane:acetone (3:1 ratio) to yield a clear oil (0.12 g, 80% yield). ^{1}H NMR (400 MHz, $CDCl_3$) δ 11.30 (s, 1H), 8.35 (d, *J* = 8.0 Hz, 1H), 6.05 (d, *J* = 8.0 Hz, 1H), 5.37-5.29 (m, 2H), 4.36-4.33 (m, 1H), 4.06 (s, 3H), 3.54 (t, *J* = 12, 4.0 Hz, 2H), 2.82-2.74 (m, 2H), 2.56-2.53 (m, 1H), 2.17 (s, 3H), 2.14 (s, 3H), 2.04 (s, 3H), 1.83 (s, 4H), 1.48 (s, 24H). ^{13}C NMR (100 MHz, CDCl3) δ 170.8, 170.7, 170.2, 170.1, 168.8, 163.0, 156.8, 152.7, 83.8, 83.3, 79.5, 75.4, 69.0, 67.8, 62.4, 52.9, 50.5, 49.7, 45.0, 38.8, 32.4, 29.1, 28.7, 28.3, 28.0, 27.9, 26.4, 23.0, 21.2, 21.0, 20.8. HRMS (ESI): Calculated for $C_{35}H_{57}ClN_4O_{14}S$: 824.3281; Found: 825.3348 (M+H).

To a stirring solution of the chloro compound (47 mg, 0.06 mmol) in DMF (1.0 ml), NaN_3 (39 mg, 0.60 mmol) was added and stirred at 60 ^{o}C. After 12 h, the reaction mixture was quenched with H_2O and extracted with DCM (25 ml, 3x). The organic layers were collected and washed with brine (25 ml, 1x), dried over Na_2SO_4 and concentrated in vacuo, to yield a clear oil (40 mg, 85% yield). ^{1}H NMR (400 MHz, $CDCl_3$) δ 11.31 (s, 1H), 8.40 (d, *J* = 7.0 Hz, 1H), 6.03 (d, J = 8.7 Hz, 1H), 5.33 (t, *J* = 15.6 Hz, 4H), 4.35 (d, *J* = 12.4 Hz, 2H), 4.14 – 3.94 (m, 4H), 3.91 – 3.69 (m, 7H), 3.27 (t, *J* = 6.8 Hz, 4H), 2.99 – 2.47 (m, 9H), 2.17 (s, 5H), 2.15 (s, 5H), 2.05 (s, 6H), 1.84 (s, 5H), 1.60 (d, *J* = 6.3 Hz, 6H), 1.49 (s, 22H), 1.39 (s, 10H), 1.26 (s, 8H). ^{13}C NMR (100 MHz, $CDCl_3$) δ 170.8, 170.6, 170.2, 170.1, 168.8, 162.9, 156.8, 152.7, 83.8, 83.3, 79.5, 77.3, 77.0, 76.7, 75.4, 69.0, 67.8, 62.4, 52.9, 51.3, 50.4, 49.7, 38.8, 29.7, 29.1, 28.7, 28.7, 28.3, 28.0, 26.2, 23.0, 21.2, 21.0, 20.8. HRMS (ESI): Calculated for $C_{35}H_{57}N_7O_{14}S$: 831.3684; Found: 832.3695 (M+H).

Compound 4: *tert*-Butyl(7-((3,5-bis(prop-2-yn-1-ylcarbamoyl)phenyl)amino)-7-oxoheptyl) carbamate.

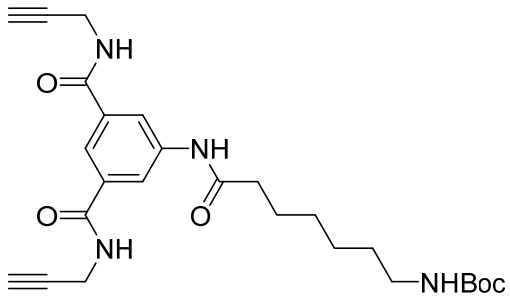

To a stirring solution of the known spacer (64 mg, 0.26 mmol) in THF (5.0 ml), CDMT (91 mg, 0.52 mmol) and NMM (52 mg, 0.52 mmol) was added at 0 ^{o}C. In a separate flask, the known dimeric scaffold **2** was dissolved in THF (5 ml) with NMM (52 mg, 0.52 mmol) at 0 ^{o}C and added to the activated acid and stirred for 12 h. The reaction mixture was quenched with H_2O, extracted with EtOAc (10 ml, 3x), dried over Na_2SO_4 and concentrated in vacuo. The compound was purified using flask chromatography with hexane: acetone (3:1) to yield a white solid (96 mg, 80% yield). ^{1}H NMR (400 MHz, $CDCl_3$) δ 9.39 (s, 1H), 8.27 (s, 2H), 8.04 (s, 1H), 7.75 (s, 2H), 4.80 (s, 1H), 4.17 (s, 4H), 3.00 (d, J = 6.1 Hz, 2H), 2.25 (t, J = 37.5 Hz, 5H), 1.42 (s, 15H). ^{13}C NMR (100 MHz, $CDCl_3$) δ 173.00, 166.66, 159.37, 139.39, 134.58, 121.77, 79.42, 77.36, 77.05, 76.73, 71.69, 56.03, 37.05, 31.58, 30.94, 29.79, 28.60, 28.45, 26.29, 25.27, 22.64, 14.11. HRMS (ESI) Calculated for $C_{26}H_{34}N_4O_5$: 482.2529; Found: 505.2404 (M+Na).

Compound 5a:

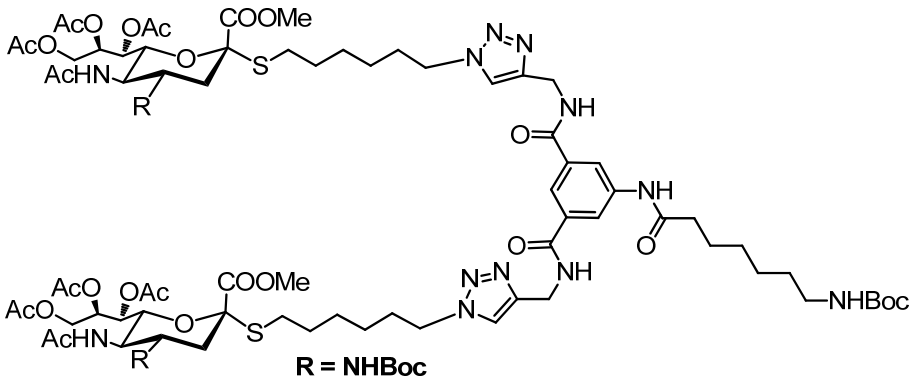

To a stirring solution of **3a** (40 mg, 0.06 mmol) in THF/ H_2O (1.0 ml, 1:1), **4** (9.6 mg, 0.02 mmol) was added. $CuSO_4$ (10 mg, 0.04 mmol) was added along with sodium *L*-ascorbate (7.9 mg, 0.04 mmol) and the reaction was stirred at rt for 12 h. Solvent was removed in vacuo and product was purified using flash column chromatography with DCM:MeOH (10:1) to yield **5a** (33 mg, 60% yield). ^{1}H-NMR (400 MHz, $CDCl_3$) δ 9.21 (s, 1H), 8.35 (s, 3H), 8.07 (s, 3H), 6.08 (s, 2H), 5.53 (d, *J* = 8 Hz, 2H), 5.36-5.31 (m, 5H), 4.70 (s, 5H), 4.32-4.29 (m, 6H), 4.07 (dd, *J* = 4, 12 Hz, 2H), 3.99-3.92 (m, 2H), 3.78-3.75 (m, 3H), 3.71 (s, 6H), 3.55 (d, *J* = 8 Hz, 2H), 3.10 (d, *J* = 4 Hz, 2H), 2.72-2.65 (m, 6H), 2.55-2.51 (m, 2H), 2.38 (s, 2H), 2.19 (m, 3H), 2.13 (s, 6H), 2.02 (s, 6H), 1.98 (s, 6H), 1.93 (s, 6H), 1.45 (s, 12H), 1.36 (s, 27H), 1.27 (s, 12H). ^{13}C NMR (100 MHz, $CDCl_3$) δ 210.8, 172.3, 171.3, 170.7, 170.1, 170.0, 168.8, 166.6, 156.3, 156.1, 139.7, 135.0, 134.9, 123.1, 121.5, 121.44, 121.4, 121.3, 83.5, 79.7, 79.13, 79.11, 77.9, 77.6, 77.5, 77.2, 76.6, 76.5, 74.4, 69.5, 68.4, 68.2, 68.0, 62.4, 53.8, 52.9, 51.0, 50.3, 50.2, 50.15, 50.08, 50.00, 40.5, 40.4, 38.8, 37.2, 37.1, 35.5, 35.4, 31.9, 31.8, 29.9, 29.8, 29.78, 29.7, 29.6, 29.5, 29.4, 29.3, 28.8, 28.7, 28.73, 28.69, 28.65, 28.62, 28.5, 28.4, 28.3, 28.2, 28.18, 28.14, 27,3, 27.2, 26.4, 25.9, 25.6, 25.5, 25.4, 25.3, 25.2, 23.3, 23.2, 22.7, 22.6, 21.1, 21.0, 20.8, 20.7, 14.1. HRMS (ESI) Calculated for $C_{84}H_{128}N_{14}O_{29}S_2$: 1860.8413; Found: 1923.6098 (M+ 3Na).

Compound 5b:

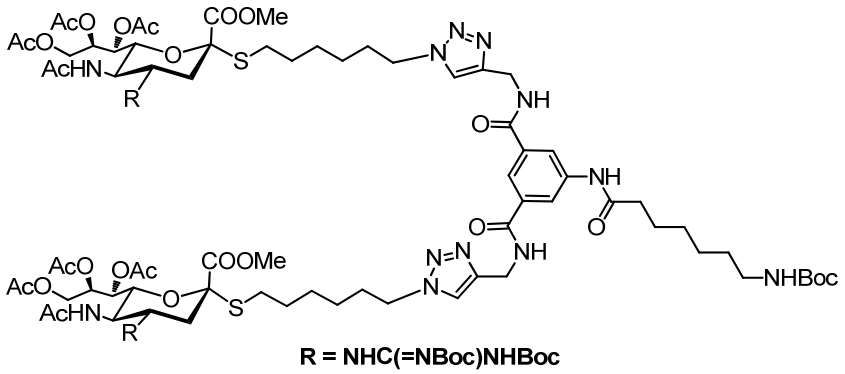

To a stirring solution of compound **3b** (26 mg, 0.04 mmol) in THF: H_2O (1.0 ml, 1:1), 4 (8.6 mg, 0.017 mmol) was added. $CuSO_4$ (7.5 mg, 0.38 mmol) was added with sodium *L*-ascorbate (6.7 mg, 0.28) and the reaction was stirred for 12h at rt. Solvent was removed in vacuo and the product was purified using flash column chromatography with DCM:MeOH (10:1) to yield compound **5b** (84 mg, 65% yield). ^{1}H NMR (400 MHz, $CDCl_3$) δ 11.30 (s, 2H), 8.50 (d, *J* = 27.2 Hz, 3H), 8.38 – 8.19 (m, 2H), 7.86 – 7.59 (m, 6H), 6.25 (s, 2H), 5.33 (m, 5H), 4.72 (m, 6H), 4.34 (m, 7H), 4.21 – 4.01 (m, 9H), 3.88 – 3.69 (m, 10H), 3.11 (d, *J* = 6.1 Hz, 1H), 2.87 – 2.61 (m, 5H), 2.58 – 2.44 (m, 2H), 2.38-1.87 (m, *J* = 7.3 Hz, 22H), 1.57 – 1.14 (m, 67H), . ^{13}C NMR (101 MHz, $CDCl_3$) δ 170.9, 170.7, 170.2, 168.7, 166.3, 162.9, 156.8, 152.5, 144.6, 134.9, 122.9, 121.3, 114.1, 83.5, 77.3, 77.2, 77.0, 76.7, 75.0, 68.8, 67.8, 62.5, 56.1, 53.8, 52.9, 50.2, 35.5, 31.9, 29.8, 29.7, 29.4, 29.3, 28.6, 28.4, 28.2, 27.9, 27.5, 25.8, 23.0, 22.7, 21.2, 20.9, 20.8, 14.1. HRMS (ESI) Calculated for $C_{96}H_{148}N_{18}O_{33}S_2$: 2144.9898; Found: 2145.9985 (M+H).

Compound SC1.

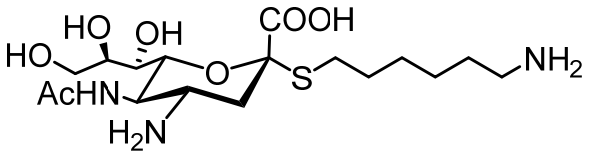

To a stirring solution of compound **3a** (10 mg, 16 µmol) in MeOH(1.0 ml), NaOMe (5.4 M, 0.25 ml) was added. The reaction was stirred for 1 h, neutralized with Dowex H^+ resin until the pH was 7. The resin was filtered, solvent was removed in vacuo and the residue was re-dissolved in DCM: TFA (1.0 ml, 1:1) and stirred for 1 h and solvent removed in vacuo. The residue was dissolved in EtOH with calaytic amount of $Pd(OH)_2$ and stirred for 8 h. Reaction mixture was filtered and solvent removed, re-dissolved in MeOH (1.0 ml), NaOH (10 mM, 1.0 ml) was added and stirred for 1 h. Dowex H^+ resin was used to neutralize to pH 7 and solvent was removed and compounds were purified with Bio-Gel P-2 Gel with DI water as solvent (5.0 mg, 75% yield). ^{1}H NMR (400 MHz, D_2O) δ 3.72 (t, *J* = 11.4 Hz, 2H), 3.62 – 3.32 (m, 5H), 3.22 (s, 1H), 2.87 (t, *J* = 7.6 Hz, 1H), 2.75 – 2.41 (m, 4H), 1.91 (d, *J* = 13.9 Hz, 3H), 1.52 (m, 4H), 1.28 (s, 4H). HRMS (ESI) Calculated for $C_{17}H_{33}N_3O_7S$: 423.2039; Found: 422.1962 (M-1, negative ion).

Compound SC2.

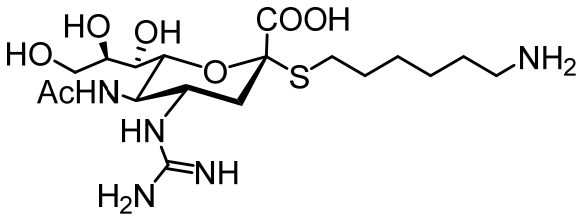

SC2 was synthesized in a manner from **3b** (5.0 mg, 16 µmol) similar to that of **Sc1** and the product was purified using Bio-Gel P-2 Gel with DI water as solvent to give pure **SC2** (1.9 mg, 70 %). ^{1}H NMR (400 MHz, D_2O) δ 4.25-4.08 (m, 3H), 3.99 (m, 3H), 3.58-3.55 (m , 1H), 3.36-3.34 (m, 1H), 3.12-3.07 (m, *J* = 8.2 Hz, 2H), 2.95-2.78 (m, 1H), 2.44-2.35 (m, 3H), 2.15 (s, 1H), 2.03 (s, 1H), 1.87 (s, 5H), 1.69-1.54 (m, 3H). HRMS (ESI) Calculated for $C_{18}H_{35}N_5O_7S$ 465.2257; Found: 464.1987 (M-1, negative ion).

Compound SC3.

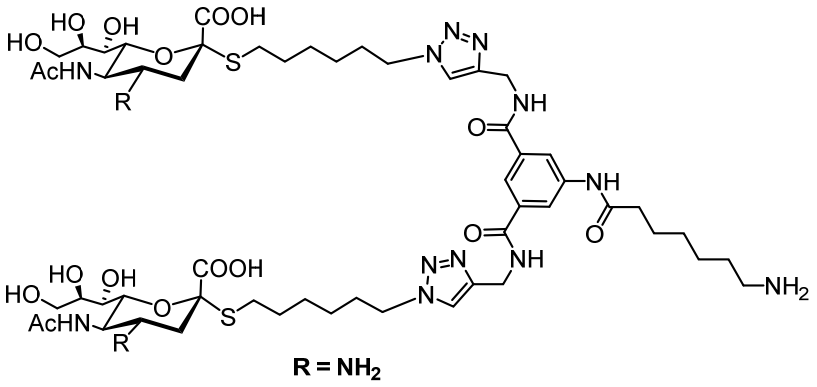

To a stirring solution of compound **5a** (4.0 mg, 2.4 μmol) in MeOH (1.0 ml), NaOMe (5.4 M, 0.25 ml) was added. The reaction was stirred for 1 h, neutralized with Dowex H^+ resin. The resin was filtered, solvent was removed in vacuo and residue was re-dissolved in DCM/TFA (1.0 ml, 1:1) and stirred for 1 h. Solvent was removed in vacuo, re-dissolved in MeOH (1.0 ml) and NaOH (10 mM, 1.0 ml) was added and stirred for 1 h. Dowex H^+ resin was used to neutralized to pH 7 and solvent was removed. The product was purified with Bio-Gel P-2 Gel with DI water as solvent (2.2 mg, 80 % yield). ^{1}H NMR (400 MHz, D_2O) δ 7.88 – 7.69 (m, 5H), 4.21 (q, *J* = 6.6 Hz, 2H), 4.06 – 3.90 (m, 1H), 3.76 – 3.44 (m, 11H), 3.30 – 3.14 (m, 2H), 2.90 – 2.83 (m, 2H), 2.80 – 2.70 (m, 2H), 2.62 – 2.47 (m, 3H), 2.45 – 2.33 (m, 2H), 2.32 – 2.21 (m, 2H), 1.92 (s, 6H), 1.77 (q, *J* = 12.9 Hz, 2H), 1.72 – 1.61 (m, 4H), 1.57 – 1.45 (m, 4H), 1.43 – 0.91 (m, 20H). HRMS (ESI) Calculated for $C_{55}H_{88}N_{14}O_{17}S_2$: 1280.5893; Found: 641.3013 (2M+H).

Compound SC4

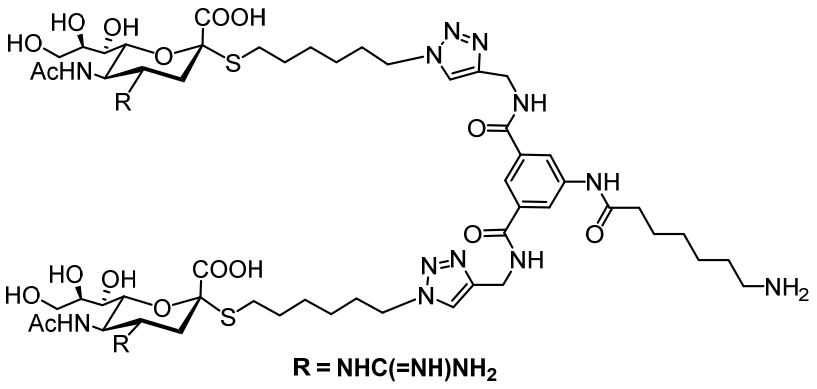

SC4 was synthesized in a manner similar to **SC3** using **5b** (5.1 mg, 2.4 μmol) to yield a white solid (2.3 mg, 70% yield). ^{1}H NMR (400 MHz, D_2O) δ 7.99 – 7.73 (m, 5H), 4.28 (d, *J* = 6.2 Hz, 1H), 4.05 (s, 1H), 3.83 (m, 3H), 3.65 (m, 10H), 3.48 (dd, *J* = 25.8, 14.8 Hz, 10H), 2.68 – 2.43 (m, 5H), 2.46 – 2.23 (m, 4H), 1.87 (s, 6H), 1.81 – 1.46 (m, 10H), 1.42 – 0.98 (m, 18H). HRMS (ESI) Calculated for $C_{57}H_{92}N_{18}O_{17}S_2$: 1364.6329; Found 1365.6420 (M+H).

Compound 7: 5-Acetylamino-4- N-tert-butyloxycarbonyl-6- (1,2,3-triacetoxy-propyl) -5,6-dihydro-4H-pyran-2-carboxylic acid methyl ester.

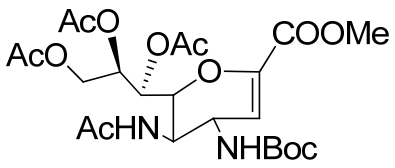

To a solution of compound **6**[65b, 65c] (1.5 g, 3.3 mmol) in EtOH (25 ml), Lindlar catalyst (0.15 g, 0.10 equivalent) was added. H_2 gas was bubbled to the solution and the reaction was stirred at rt for 12 h. After filtering using celite, the filtrate was collected and solvent removed in vacuo to give a white product (1.4 g, quantitative). To this compound (0.53 g, 1.2 mmol) in THF (20 ml), Et_3N (1.6 ml, 1.5 mmol) was added. The solution was stirred rt for 30 min and Boc_2O (0.54 g, 2.5 mmol) was added and reaction stirred for 12h at rt. Upon completion, THF was removed in vacuo. The residue was washed using HCl (1M, 25 ml) and extracted by DCM (30

ml, 3x), the organic phases were combined and dried over Na_2SO_4. DCM was removed in vacuo and the reaction mixture was purified using column chromatography with hexane: acetone (3:1) as eluent to give a white product. (0.56 g, 86% yield). ^{1}H NMR (400 MHz, $CDCl_3$) δ 6.46 (d, *J* = 9.0 Hz, 1H), 5.94 (s, 1H), 5.43 (s, 1H), 5.27 (s, 1H), 4.63 (d, *J* = 12.4 Hz, 1H), 4.44 (d, *J* = 10.0 Hz, 1H), 4.35 (d, *J* = 8.9 Hz, 1H), 4.15 (dd, *J* = 12.3, 7.1 Hz, 1H), 3.95 (d, *J* = 9.2 Hz, 1H), 3.77 (s, 3H), 2.14 (s, 9H), 2.10 (s, 3H), 2.03 (s, 3H), 2.02 (s, 3H), 1.95 (s, 3H). ^{13}C NMR (100 MHz, $CDCl_3$) δ 170.9, 170.6, 170.3, 170.0, 161.8, 156.2, 144.6, 111.0, 80.2, 71.4, 67.8, 62.2, 60.4, 52.4, 50.1, 47.3, 28.2, 23.1, 21.0, 20.9, 20.8, 20.7, 14.2. HRMS. Calculated for $C_{23}H_{34}N_2O_{12}$: 530.2112; Found: 531.2181 (M+H)

Compound 8: 5-Acetylamino-4- N-*tert*-butyloxycarbonyl-6-[(2,2-dimethyl-[1,3]dioxolan-4-yl] 5,6-dihydro-4H-pyran-2-carboxylic acid methyl ester.

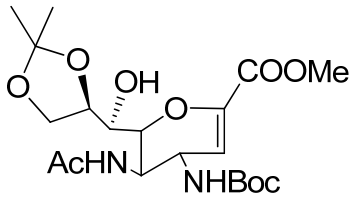

To a solution of compound **7** (0.56 g, 1.1 mmol) in MeOH (0.010 L), NaOMe (0.05 eq) was added. The solution was stirred at rt for 5 h. The progress of the reaction was monitored by TLC. Upon completion, the reaction mixture was neutralized by H^+ resin, the suspension was filtered. The liquid phase was collected and dried in vacuo to give a colorless compound. To a solution of this compound (0.42 g, 1.1 mmol) in dry acetone (0.010 L), H^+ resin was added to adjust the pH to 4. The solution was stirred at rt for 12 h. The suspension was filtered, acetone was removed in vacuo, the residue was washed by saturated $NaHCO_3$, extracted by DCM (3x 0.020 mL), the organic phases were combined and dried over Na_2SO_4, DCM was removed in

vacuo and the reaction mixture was purified by flash column chromatography using hexane: acetone (4:1) to give the 3. (0.41 mg, 88%). ^{1}H NMR (400 MHz, $CDCl_3$) δ 6.65 (d, *J* = 6.4 Hz, 1H), 5.79 (s, 1H), 5.08 (d, *J* = 4.2 Hz, 1H), 4.82 (d, *J* = 9.0 Hz, 1H), 4.59 (t, *J* = 9.4 Hz, 1H), 4.38 (dd, *J* = 13.5, 5.3 Hz, 1H), 4.26 – 4.06 (m, 2H), 4.01 (d, *J* = 10.6 Hz, 1H), 3.91 (td, *J* = 10.1, 6.7 Hz, 1H), 3.76 (s, 3H), 3.50 (dd, *J* = 8.3, 4.3 Hz, 1H), 2.03 (s, 3H), 1.44 (s, 9H), 1.40 (s, 3H), 1.36 (s, 3H). ^{13}C NMR (400 MHz, $CDCl_3$) δ 173.9, 162.0, 157.2, 146.3, 109.2, 107.8, 81.0, 78.3, 77.3, 77.0, 76.7, 74.0, 69.7, 67.3, 52.4, 52.1, 48.7, 28.2, 27.1, 25.3, 23.0. HRMS (ESI) Calculated for $C_{20}H_{32}N_2O_9$: 444.2108; Found: 445.2180 (M+H).

Compound 9: 5-Acetylamino-4-N-*tert*-butyloxycarbonyl-6- [(2,2-dimethyl-[1,3]dioxolan-4-yl)- (4-nitro-phenoxycarbonyloxy)-methyl]-5,6-dihydro-4H-pyran-2-carboxylic acid methyl ester.

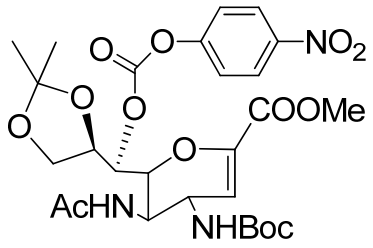

To a solution of compound **3** (35 mg, 0.079 mmol) in pyridine (0.010 L), DMAP (19 mg, 0.16 mmol) was added. The solution was stirred at rt for 30 min and 4-nitrophenylchloroformate (32 mg, 0.16 mmol) was added. The reaction was stirred at rt for 16 h. The reaction mixture was washed by HCl (1 M, 0.025 L) and extracted with DCM (3 x 0.020 L), the organic phases were combined and dried over Na_2SO_4. DCM was removed in vacuo and the product was purified by column chromatography using hexane: acetone (3:1) to give 4. (39 mg, 80% yield). ^{1}H NMR (400 MHz, $CDCl_3$) δ 8.27 (d, J = 8.9 Hz, 2H), 7.50 (d, *J* = 8.9 Hz, 2H), 5.97 (d, *J* = 9.6 Hz, 1H), 5.90 (s, 1H), 5.31 (t, *J* = 5.7 Hz, 1H), 4.81 (d, *J* = 9.6 Hz, 1H), 4.54 (t, *J* = 9.7 Hz, 1H), 4.47 –

4.29 (m, 2H), 4.24 (dd, *J* = 8.9, 5.7 Hz, 2H), 4.17 – 4.05 (m, 1H), 3.79 (s, 3H), 1.95 (s, 3H), 1.42 (s, 9H), 1.41 (s, 3H), 1.38 (s, 3H). ^{13}C NMR (100 MHz, $CDCl_3$) δ 171.3, 161.6, 156.4, 155.7, 152.5, 145.6, 144.8, 125.2, 122.3, 110.5, 108.9, 80.6, 77.3, 77.0, 76.7, 75.1, 74.2, 65.5, 52.5, 49.5, 48.1, 28.2, 26.4, 25.5, 23.2. HRMS (ESI) Calculated for $C_{27}H_{35}N_3O_{13}$: 609.2170; Found: 632.2057 (M+Na).

Compound 10a: 5-Acetylamino-4-N-*tert*-butyloxycarbonyl-6-[(6-azido-hexylcarbamoyloxy) -(2,2-dimethyl-[1,3]dioxolan-4-yl)-methyl]-5,6-dihydro-4H-pyran-2-carboxylic acid methyl ester.

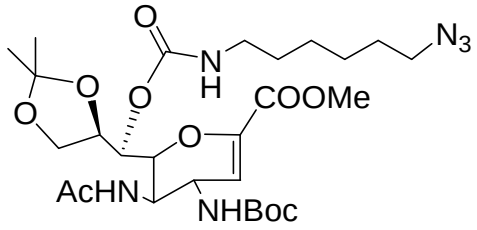

To a solution of 6-azidohex-1-amine (19 mg, 0.13 mmol) in CH_3CN (8.0 ml), Et_3N (20 mg, 0.19 mmol) was added. The solution was stirred at rt for 30 min. 9 (39 mg, 0.064 mmol) in CH_3CN (2.0 ml) was added. The reaction was stirred at rt for 3 h. The progress of the reaction was monitored by TLC. Upon completion, CH_3CN was removed in vacuo and the reaction mixture was washed by HCl (1 M, 0.025 L), extracted by DCM (3 x 0.020 L), the organic phases were combined and dried over Na_2SO_4. DCM was removed in vacuo and the product was purified by column chromatography using hexane: EtOAc (1:1) to give 5. (35 mg, 89%). ^{1}H NMR (400 MHz, $CDCl_3$) δ 6.15 (d, *J* = 9.4 Hz, 1H), 5.90 (s, 1H), 5.24 (d, *J* = 3.7 Hz, 1H), 5.01 – 4.83 (m, 2H), 4.51 (t, *J* = 8.9 Hz, 1H), 4.33 (dd, *J* = 13.6, 7.8 Hz, 2H), 4.19 – 4.04 (m, 2H), 4.04 – 3.92 (m, 2H), 3.76 (s, 3H), 3.73(s, 1H) 3.24 (t, J = 6.9 Hz, 2H), 3.11 (dt, *J* = 20.7, 6.6 Hz, 2H), 1.93 (s, 3H), 1.66 – 1.53 (m, 2H), 1.48 (m, 2H), 1.41 (m, 2H), 1.39 (s, 9H), 1.34(s, 3H),

1.23(s, 3H). ^{13}C NMR (101 MHz, $CDCl_3$) δ 170.8, 162.1, 156.2, 155.5, 144.4, 111.4, 108.9, 80.1, 74.9, 69.7, 65.9, 52.4, 51.3, 50.0, 47.6, 41.1, 29.6, 28.7, 28.3, 26.4, 26.3, 26.3, 25.4, 23.2. HRMS (ESI) Calculated for $C_{27}H_{44}N_6O_{10}$: 612.3119; Found: 635.3006 (M+Na).

Compound 10b: 5-Acetylamino-4-[2,3-bis(tert-butoxycarbonyl)guanidine]-6-[(6-azido-hexyl carbamoyloxy)-2,3 dihydroxy propyl]-5,6-dihydro-4H-pyran-2-carboxylic acid methyl ester.

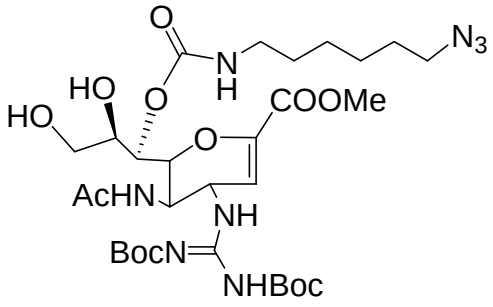

To a solution of compound **10a** (40 mg, 0.084 mmol) in THF (3.0 ml), TFA (3.0 ml) was added, the reaction was stirred at rt for 1 h. THF was removed in vacuo, Et_3N (26 µl, 0.25 mmol) was added. The solution was stirred at rt for 30 min. $HgCl_2$ (27 mg, 0.10 mmol) and 1,3-Bis(*tert*-butoxycarbonyl)-2-methyl-2-thiopseudourea (29 mg, 1.2 mmol) was added. The reaction was stirred at rt for 12 h. The reaction mixture was washed with HCl (1M, 0.025 L), extracted with DCM (3 x 0.010 L), DCM was removed in vacuo and the product was purified by column chromatography using DCM: MeOH (25:1) to give the product 10b. (50 mg, 84%). ^{1}H NMR (400 MHz, $CDCl_3$) δ 11.40 (s, 1H), 8.54 (d, *J* = 8.7 Hz, 1H), 7.39 (s, 1H), 7.28 (s, 1H), 6.85 (s, 1H), 5.89 (s, 1H), 5.32 (s, 1H), 5.20 (t, *J* = 9.5 Hz, 1H), 5.03 (t, *J* = 5.7 Hz, 1H), 4.82 (d, *J* = 9.4 Hz, 1H), 4.49 (d, *J* = 10.5 Hz, 1H), 4.37 (dd, *J* = 19.7, 10.0 Hz, 1H), 4.14 (dd, *J* = 14.2, 7.1 Hz, 1H), 4.05 (d, *J* = 9.2 Hz, 1H), 3.80 (s, 3H), 3.68 (dd, *J* = 24.9, 12.7 Hz, 1H), 3.27 (t, *J* = 6.8 Hz, 2H), 3.17 (ddd, *J* = 19.4, 13.4, 6.8 Hz, 2H), 1.95 (d, *J* = 10.0 Hz, 3H), 1.60 (dd, *J* = 13.8, 6.8 Hz,

2H), 1.50 (s, 18H), 1.38 (s, 4H), 1.27 (dd, J = 7.7, 6.5 Hz, 2H). ^{13}C NMR (100 MHz, $CDCl_3$) δ 171.0, 162.8, 162.4, 162.2, 162.1, 157.1, 157.1, 152.5, 144.9, 118.2, 115.3, 110.5, 83.7, 79.7, 69.4, 68.7, 62.4, 53.5, 52.31, 51.26, 49.4, 47.1, 45.7, 41.2, 29.4, 28.7, 28.3, 28.2, 28.1, 27.9, 27.9, 26.3, 26.2, 22.7, 8.4. HRMS (ESI) Calculated for $C_{30}H_{50}N_8O_{12}$: 714.3548; Found: 715.3627 (M+H).

Compound 11a:

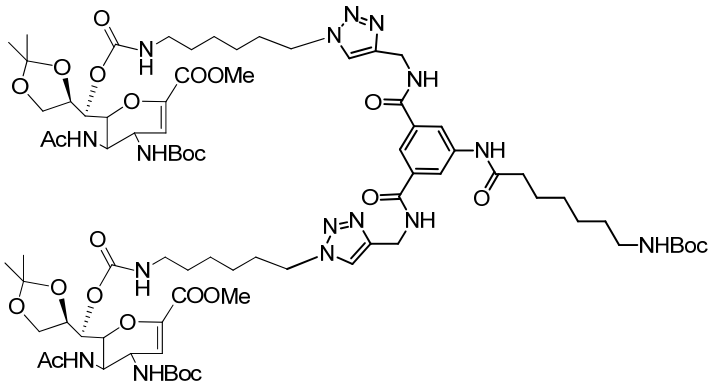

To a solution of **10a** (54 mg, 0.088 mmol) in THF/H_2O (1.0 ml, 1:1), 4 (18 mg, 0.036 mmol) was added. $CuSO_4$ (15 mg, 0.10 mmol) was added along with sodium *L*-ascorbate (0.020 g, 0.10 mmol). The reaction was stirred at rt for 12 h. Upon completion by TLC, solvent was removed in vacuo and the product was purified by column chromatography using EtOAc: MeOH (30:1) to give 11a. (48 mg, 78%). ^{1}H NMR (400 MHz, $CDCl_3$) δ 8.23(s, 3H), 7.83 (s, 2H), 6.67 (s, 2H), 5.95 (s, 2H), 5.64 (s, 1H), 5.24(s,3H), 4.60(m, 6H), 4.33(s, 8H), 4.12 (s, 8H), 3.98 (s, 2H), 3.71 (s, 6H), 3.04 (d, J =33.2Hz, 4H)2.40 (s, 1H), 2.19 (s, 2H), 2.09 (s, 2H), 2.06 (s, 2H), 1.90 (s, 10H), 1.68 (s, 2H), 1.44 (s, 14H), 1.26– 1.36 (m, 42H). HRMS (ESI) Calculated for $C_{80}H_{122}N_{16}O_{25}$: 1706.8767; Found: 1707.8838(M+H).

Compound 11b:

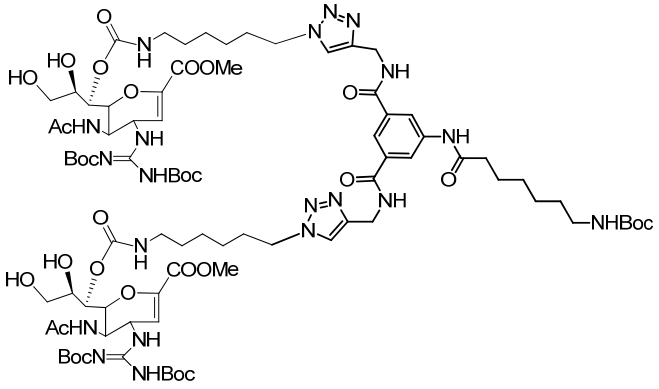

To a solution of **10b** (40 mg, 0.056 mmol) in THF/H_2O (1.0 ml, 1:1), 4 (13 mg, 0.025 mmol) was added. $CuSO_4$ (14 mg, 0.088 mmol) was added with sodium *L*-ascorbate (17 mg, 0.088 mmol). The reaction was stirred at rt for 12 h. Upon completion, solvent was removed in vacuo and the product was purified by column chromatography using EtOAc : MeOH (20:1) to give 9. (38 mg, 80%). ^{1}H NMR (400 MHz, $CDCl_3$) δ 11.38 (s, 1H), 9.74 (s, 1H), 8.19 (m, 5H), 7.28 (s, 2H), 5.89 (s, 2H), 5.31 (s, 6H), 5.21 – 5.05 (m, 2H), 4.78 (s, 2H), 4.52 (s, 5H), 4.17 – 3.90 (m, 4H),4.09-3.85 (m, 4H), 3.80-3.74 (m, 8H), 3.54 (s, 2H), 3.36 (s, 1H), 3.30 – 2.72 (m, 6H), 2.35 (d, *J* = 13.9 Hz, 2H), 2.05 (s, 2H), 1.81 (s, 7H), 1.54 (m, 22H), 1.45 – 1.33 (m, 12H), 1.33 – 0.99 (m, 28H), 0.90-0.84 (m, 10H). HRMS(ESI) Calculated for $C_{86}H_{134}N_{20}O_{29}$: 1910.9626; Found: 1912.0572(M+H)

Compound SC5:

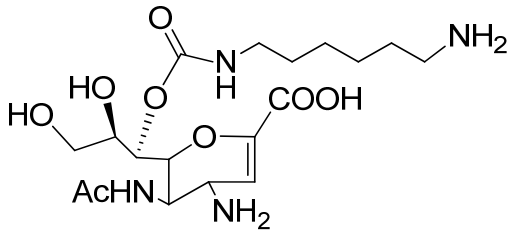

To a solution of compound **10a** (1.8 mg, 0.29 μmol) in MeOH (5.0 ml), NaOH (0.50 M, 1.0 ml) was added. The solution was stirred at rt for 2 h. The progress of the reaction was

monitored by TLC. Upon completion, the reaction mixture was neutralized by H^+ resin, the suspension was filtered. The filtrate was collected and dried in vacuo. The residue was added to DCM/TFA (5.0 ml, 1:1), the mixture was stirred at rt for 1 h. DCM was removed in vacuo, the product was dissolved in EtOH (5.0 ml), Lindlar catalyst (10%) was added. H_2 gas was bubbled to the solution and stirred at rt for 12 h. The suspension was filtered and the filtrate, which contained product SC5, was collected and crude product was purified by Biogel P2 column to give pure SC5 (1.0 mg, 76%). ^{1}H NMR (400 MHz, D_2O) δ 5.73 (s, 1H), 4.34 – 4.23 (m, 2H), 4.16 – 4.04 (m, 2H), 3.71 – 3.57 (m, 1H), 3.39 (dt, *J* = 13.3, 6.8 Hz, 2H), 3.02 (s, 4H), 1.98 (s, 3H), 1.55 – 1.30 (m, 4H), 1.23-1.18 (m, 4H). HRMS (ESI) Calculated for $C_{18}H_{32}N_4O_8$, 432.2220. Found: 433.2292 (M+H).

Compound SC6:

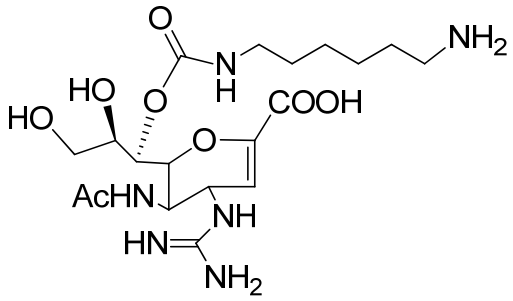

SC6 was synthesized in a manner similar to that of **SC5** using **10b** (1.6 mg, 0.22 μmol) and the crude product was purified by P2 column to give the SC6 (0.75 mg, 72%). ^{1}H NMR (400 MHz, D_2O) δ 5.63 (s, 1H), 4.38 – 4.18 (m, 2H), 4.10-3.87 (m, 2H), 3.74-3.61(m, 2H), 3.38 (t, *J* = 7.2 Hz, 1H), 3.02 (s, 4H), 1.93 (s, 3H), 1.52 – 0.99 (m, 8H). HRMS (ESI) Calculated for $C_{19}H_{34}N_6O_8$: 474.2438; Found: 475.2516 (M+H).

Compound SC7:

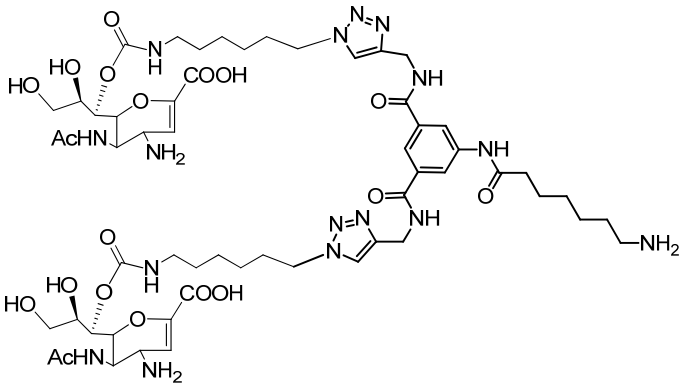

To a solution of compound **11a** (4.5 mg, 0.26 μmol) in MeOH (5.0 ml), NaOH (0.50 M, 1.0 ml) was added. The solution was stirred at rt for 2 h. The progress of the reaction was monitored by TLC. Upon completion, the reaction mixture was neutralized by H^+ resin and the suspension was filtered. The filtrate was dried in vacuo and DCM/TFA (1:1, 5.0 ml) was added to the residue and was stirred at rt for 1 h. After removal of solvent, the crude product was purified by P2 column to give **SC7**. (2.4 mg, 70%). ^{1}H NMR (400 MHz, D_2O) δ 7.89 (s, 2H), 7.80 (s, 3H), 5.91 (s, 2H), 4.84 (d, *J* = 9.4 Hz, 2H), 4.54 (s, 2H), 4.47 (d, *J* = 10.5 Hz, 2H), 4.29 (s, 3H), 4.25 – 4.08 (m, 3H), 3.96 (s, 4H), 3.53 (d, J = 9.8 Hz, 2H), 3.37 (dd, *J* = 11.9, 6.4 Hz, 2H), 2.88 (d, *J* = 7.4 Hz, 4H), 1.90 (s, 6H), 1.76 (s, 2H), 1.57 (s, 2H), 1.30 (s, 6H), 1.13-1.05 (m, 14H), 0.70-0.63 (m, 6H). HRMS (ESI) Calculated for $C_{57}H_{86}N_{16}O_{19}$: 1298.6255; Found: 1299.6329(M+H).

Compound SC8:

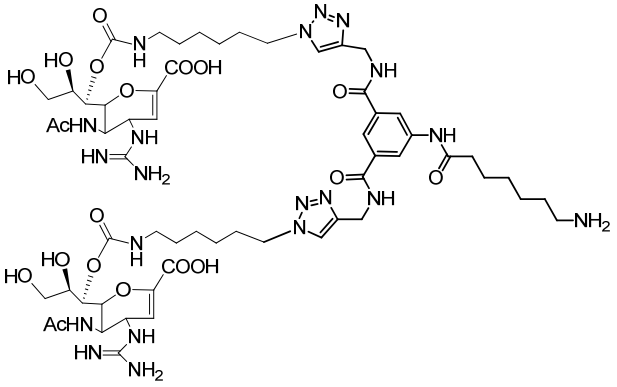

SC8 was synthesized in a manner similar to **SC7** using **11b** (3.5 mg, 0.18 μmol) and the crude product was purified by P2 column to give SC8. (2.0 mg, 79%). ^{1}H NMR (400 MHz, D_2O) δ 7.89 (s, 5H), 5.80 (d, *J* = 17.5 Hz, 2H), 4.44 (d, *J* = 10.1 Hz, 2H), 4.38 (d, *J* = 8.5 Hz, 2H), 4.34 – 4.20 (m, 4H), 4.16 (dd, *J* = 26.4, 10.1 Hz, 2H), 4.01 (dt, *J* = 13.9, 6.9 Hz, 4H), 3.62 (d, *J* = 8.8 Hz, 2H), 3.51 (d, *J* = 11.6 Hz, 1H), 2.99 – 2.79 (m, 5H), 2.29 (d, *J* = 7.5 Hz, 2H), 1.96 (s, 2H), 1.95 – 1.85 (m, 5H), 1.82 (d, *J* = 14.9 Hz, 2H), 1.71 (s, 3H), 1.54 (s, 4H), 1.27 (s, 8H), 1.20 – 1.11 (m, 6H), 1.06 (s, 6H). HRMS (ESI) Calculated for $C_{57}H_{86}N_{16}O_{19}$:1382.6691; Found: 1383.6761(M+H).

1.2.6.4 Immobilization of Glycans

Synthetic glycans were covalently immobilized onto Nexterion® NHS slides using DIGILAB Omnigrid Micro printer in 300 mM phosphate buffer with 0.005% Tween-20 at pH 8.5. Each glycan was printed twenty times in quintuplicate at 200 μM concentration. Following printing, the glycans were allowed to react for 30 min at 60% humidity. After overnight desiccation, the slides were blocked for 60 min with 50 mM ethanolamine in 50 mM boric acid buffer (pH 9.5), washed 3 times with deionized (DI) water, dried and stored at -20°C.

1.2.6.5 Limit of Detection Assay

To determine limit of detection, a serial 10 fold dilution was performed for A/Brisbane/59/2007, A/Solomon Islands/2006 and A/Aichi/2/1968 strains. The concentration of A/Brisbane/59/2007 was tested from 2.4 x 10^6-2.4 x 10^1 PFU (Plaque Forming Units), A/Solomon Islands/3/2006 from 9.0 x 10^6 - 9.0 x 10^1 PFU and A/Aichi/2/1968 from 1.5 x 10^6 - 1.5 x 10^1 PFU. Each concentration of virus was applied to the microarray for 60 min in a buffer consisting of PBS, 2% BSA and 0.05% Tween-20. Post-virus incubation and wash (three times with PBS and 0.05% Tween-20 and two times with PBS), antibodies specific to each virus were diluted and added to the microarray for 60 min. For A/Brisbane/59/2007, ferret hyperimmune sera to influenza A/Brisbane/59/2007 (H1N1), NR-19260 was diluted 5000 fold, for A/Solomon Islands/3/2006 ferret hyperimmune sera to influenza A/Solomon Islands/3/2006 (H1N1), NR-19262 was diluted 1000 fold and for A/Aichi/2/1968 polyclonal anti-influenza virus A/Aichi/2/1968 (H3N2) antiserum chicken, NR-3125 was diluted 5000 fold. Slides were washed as previously described above and incubated for 60 min with the appropriate fluorescently tagged secondary antibodies. For A/Brisbane/59/2007, anti-ferret IgG, IgA, IgM (H+L) rhodamine antibody was diluted 10,000 fold, for A/Solomon Islands/3/2006 anti-ferret IgG, IgA, IgM (H+L) rhodamine antibody was diluted 5000 fold and for A/Aichi/2/1968 Alexa Fluor® 633 goat anti-chicken IgG (H+L) was diluted 20,000 fold. The slides were washed as described above, followed by a DI water rinse. The slides were dried and scanned using the GenePix®4000B scanner. A/Brisbane/59/2007 and A/Solomon Islands/3/2006 were scanned at 532nm and A/Aichi/2/1968 at 635nm. All experiments were performed in triplicate.

1.2.6.6 Drug Susceptibility Assay

To determine drug susceptibility for A/Brisbane/59/2007, A/Solomon Islands/3/2006 and A/Aichi/2/1968, each virus strain, 10^5 PFU, was premixed with 10 ng of antiviral Zanamivir® or Oseltamivir®, for 30 min at rt. The premixed sample was subsequently added to the microarray and allowed incubate for 60 min. Fluorescence intensity was measured as previously described in the limit of detection methods. All experiments were performed in triplicate.

1.3 Electrochemical Assay to Detect Influenza Virus and Measure Drug Susceptibility

This part of the thesis has been published. (Zhang, Xiaohu, et al. "Electrochemical Assay to Detect Influenza Viruses and Measure Drug Susceptibility." *Angewandte Chemie* **127**. *20*. **2015**. 6027-6030).

1.3.1 Abstract

We report a novel electrochemical assay that targets the Neuraminidase (NA) enzyme of the virus. Exposure of a glucose bearing electrochemically inactive substrate specific for NA releases glucose. Glucose was detected using an electrochemical cell. Using this approach, we successfully detected a library of nineteen unique H1N1 and H3N2 influenza strains using disposable screen printed electrode strips and an electrochemical cell in less than 1 hour. We also demonstrated drug susceptibility of two major antivirals, Zanamivir, and Oseltamivir using the assay. The limit and range of detection of this first generation assay is 10^2 and 10^2-10^8 plaque forming units (PFU), respectively. While we have focused on influenza in this report, other enzymes, e.g. beta-lactamase, hydrolases, sulfatases, present in hard to detect pathogens can be identified and drug susceptibility measured rapidly using appropriately designed glucose releasing substrates. Existing, ubiquitous, user friendly glucose meters, used by millions worldwide to determine glucose concentration in the blood, can now be recalibrated to detect enzymes present in pathogens or in the host.

1.3.2 Introduction

As mentioned in Chapter 1, rapid and accurate determination of influenza viruses is important to reduce disease burden.[69] Several tests are available, but none of them can meet the seven different ASSURED criteria. We envisioned a rapid diagnostic test that would be selective, sensitive, user friendly, inexpensive, and can be used in different settings. The blood glucose monitoring test used by millions worldwide satisfies all these needs and can measure glucose within minutes using a battery operated device and disposable strips multiple times in a day.[70] Our innovation is to develop assays that can use existing, widely adopted, off the shelf sensors like the glucose meters to detect influenza viruses. The strategy was to develop and

expose substrates containing glucose to enzymes integral to the lifecycle of influenza virus. (Figure 1.25) Presence of glucose would indicate presence of the enzyme, and by inference, the virus. The virus can be quantified because the amount of glucose released is directly proportional to the enzyme activity. Drug susceptibility can be measured as the two major antivirals, Zanamivir and Oseltamivir, are enzyme inhibitors. We choose to measure glucose concentration after 1 hour of incubation with the virus using disposable test strips, however, a continuous measurement system can also be designed.

1.3.3 Design and Synthesis

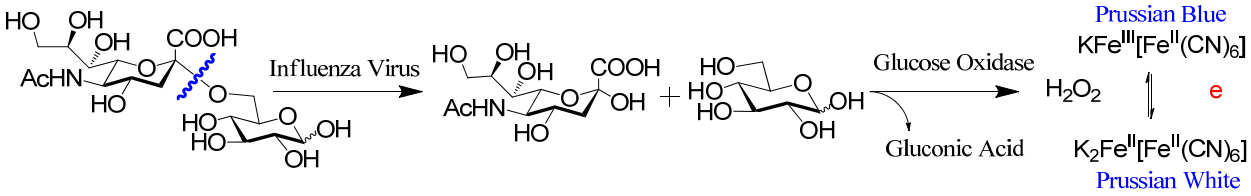

Figure 1.25 Electrochemical assay detect influenza virus

Sialic acid derivative SG1 can be cleaved by influenza virus to release glucose, which can be detected by a glucose meter set up. This process will represent the presence of influenza virus.

As mentioned in Chapter 1, Hemagluttinin (HA) and Neuraminidase (NA) are two important surface proteins on the surface of the virus. HA is implicated in viral entry and NA is the enzyme that cleaves N-acetylneuraminic acid (sialic acid) from the surface of host cells to facilitate release of viral progeny.[5] There are approximately 50-100 copies of NA on the viral surface as determined by immunogold labeling and cryo-electron tomography.[71] Since NA is present as a tetramer with four active sites, there are approximately 200-400 individual units capable of cleaving sialic acids, which makes it a suitable target for biosensing applications. We synthesized a sialic acid derivative, (**SG1**) where sialic acid is attached to the 6 position of D-

glucose. (Figure 1.25) To measure D-glucose, we developed a three electrode electrochemical cell comprising of a reference, working and counter electrode and developed a standard curve.[72] Glucose oxidase was coated onto the working electrode using chitosan as glue. A suitable promoter was used to amplify the current. This electrochemical cell was used to develop a standard curve with different concentrations of glucose. The virus could cleave O linkage between sialic acid and glucose in **SG1**, and three electrode system could detect the concentration of glucose. Therefore, the current can be used as output of this detection assay.

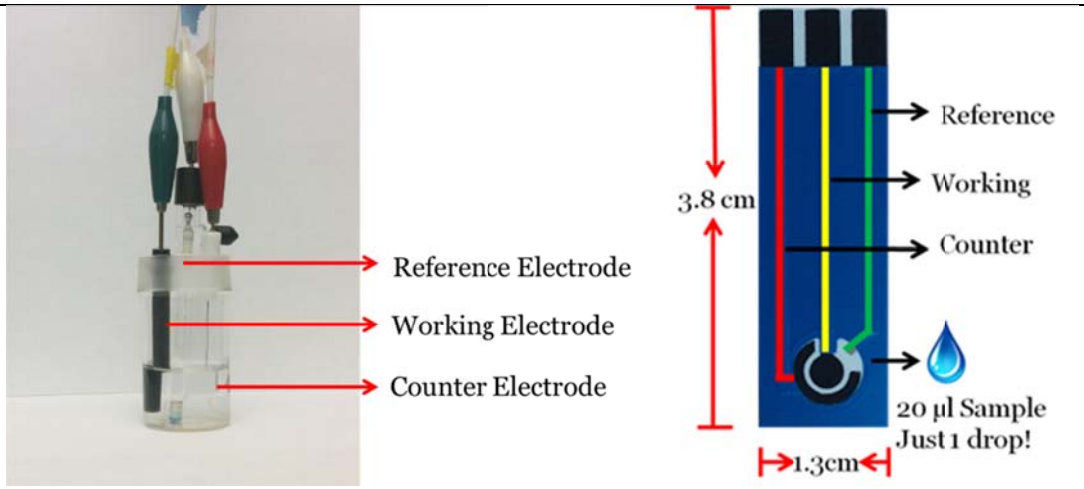

Figure 1.26 Three electrode system and printed electrode system

Lift: three electrode system. Right: disposable test strips. All of the electrode will be connected to the electrode analyzer to obtain the signal.

We synthesized a sialic acid derivative (**SG1**) where sialic acid is attached to glucose at the 6-position. (Scheme 1.3). Briefly, benzyl 2,3,4-tri-O-benzyl-α/β-D-glucopyranoside (**1α,β**) was synthesized using a modified procedure and reacted with the known *N*-acetyl-5-*N*, 4-*O*-carbonyl-protected thiosialoside donor (**2**)[73] to yield **3α,β**. Exclusive α sialoside was obtained, which was confirmed by NMR spectroscopy. [74] Next, a three-step procedure was performed.

First, Zemplén deacetylation conditions were used to remove the acetates and regioselectively open the oxazolidinone ring to obtain the N-acetamido group. This was followed by hydrogenation to remove the benzyl groups and the resulting product was saponified to produce SG1 in excellent yield. To measure glucose, we developed a three-electrode electrochemical cell comprising a reference, working and counter electrode and used this electrochemical cell to develop a standard curve. (Figure 1.28)

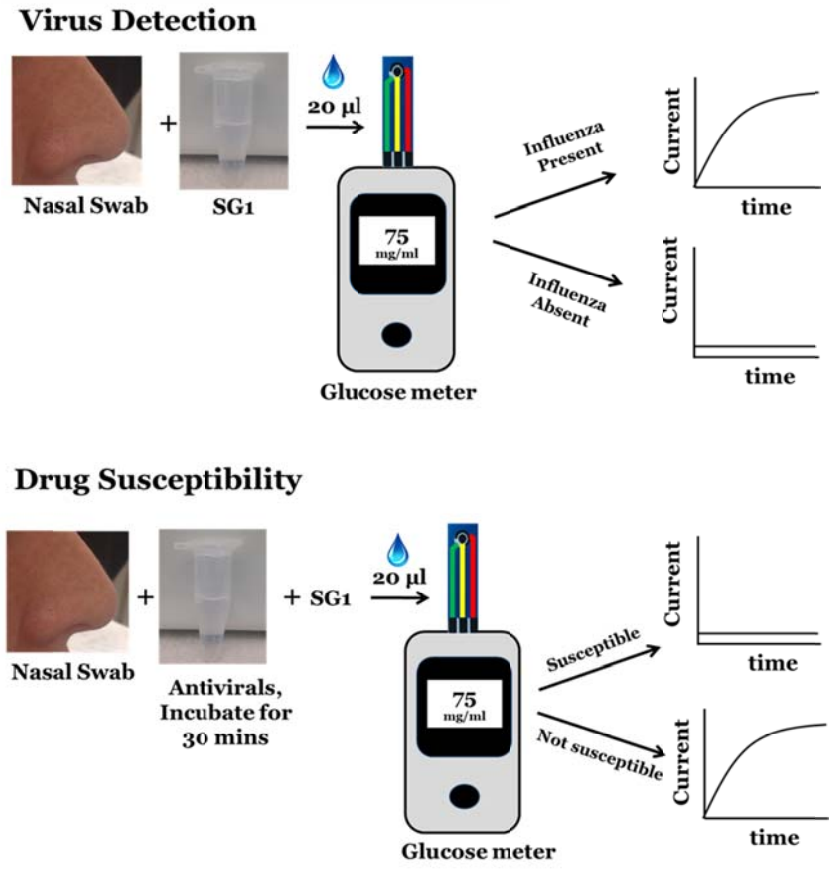

Figure 1.27 Schematic diagram of Electrochemical Assay to Detect Influenza Virus and Measure Drug Susceptibility

Virus detection: the nasal swab of the patient is collected to incubate with SG1 for 1 h. The resulted

solution is detected by glucose meter, positive readout indicates the viruses are present in nasal swab, negative readout indicated the viruses are absent in nasal swab.

Drug susceptibility: the nasal swab of the patient is collected to incubate with antivirals for 30 mins, the resulted solution is incubated with SG1 for 1 h. the solution is eventually detected by glucose meter, positive readout indicates the antiviral is not susceptible, negative readout indicated the antiviral is susceptible.

1.3.4 Result and Discussion

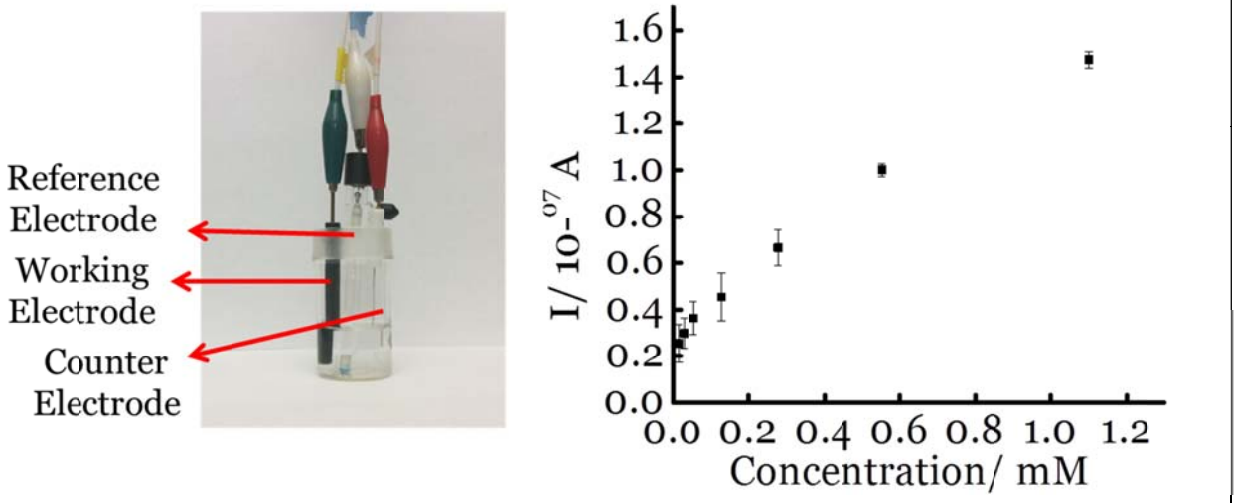

Figure 1.28 Left. Image of the electrochemical cell. Right: Standard curve glucose concentration versus current using the electrochemical cell.

Amperometric i-t curve was recorded using different concentrations of glucose and the current at 100 seconds is reported.

SG1 (0.5 mM) was dissolved in PBS buffer and tested for the presence of glucose. In the absence of enzymes, there is no glucose released. (Figure 1.29, sample N, negative control, no

NA or virus added). Membrane free influenza viral NA from two different strains (N1 from strain H5N1 A/Anhui/1/2005 and N2 from strain A/Babol/36/2005) was incubated for 2 hours at rt in PBS buffer with SG1. The sample was analyzed for the presence of glucose directly without further sample preparation. We determined that glucose was released as determined by the current measured amperometrically, which indicated that complete cleavage of SG1 had occurred. (Figure 1.29, samples A, B). The positive control (Figure 1.29, sample P) was a solution with glucose as the only analyte in PBS buffer. These studies proved that viral NA cleaves SG1 to release glucose, which can be measured using a standard electrochemical setup.

Next, we tested three influenza strains, H1N1 A/Brisbane/59/2007, H3N2 A/Aichi/2/1968, and H3N2 A/HongKong/8/68, which were quantified by plaque assays and rRT-PCR. (Figure 1.35). Introduction of 100 μL of UV inactivated virus to SG1 and incubation for 2 hours, releases glucose. (Figure 1.29, Samples C, D, E). The cleavage was confirmed by mass spectral analysis. The mass spectra of the control where there is no virus or NA revealed a peak at m/z 494.1497 (M+Na, positive ion) corresponding to uncleaved SG1. A new peak emerges at m/z, 181.0711 (M+1, positive ion) corresponding to glucose when virus or NA is added.

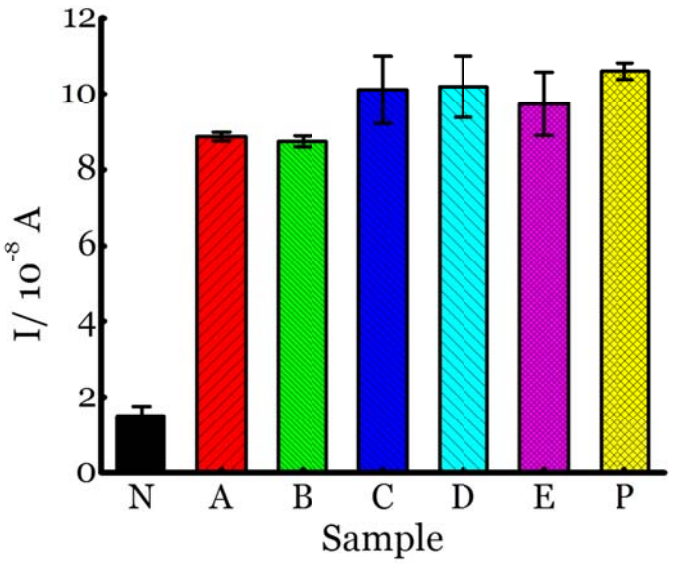

Figure 1.29 Detection of influenza virus or viral NA.

SG1 (0.5 mM) was incubated with membrane-free soluble N1 NA (sample A, strain H5N1 A/Anhui/1/2005) or N2 NA (sample B, strain H3N2A/Babol/36/2005) or three different UV-inactivated influenza strains, H3N2 A/ Aichi/2/1968 (sample C), H1N1A/Brisbane/59/2007 (sample D), or H3N2A/HongKong/8/68 (sample E) for two hours. The negative control where no virus or NA was added (sample N) did not show any noticeable current and the positive control (sample P) was D-glucose at 0.5 mM.

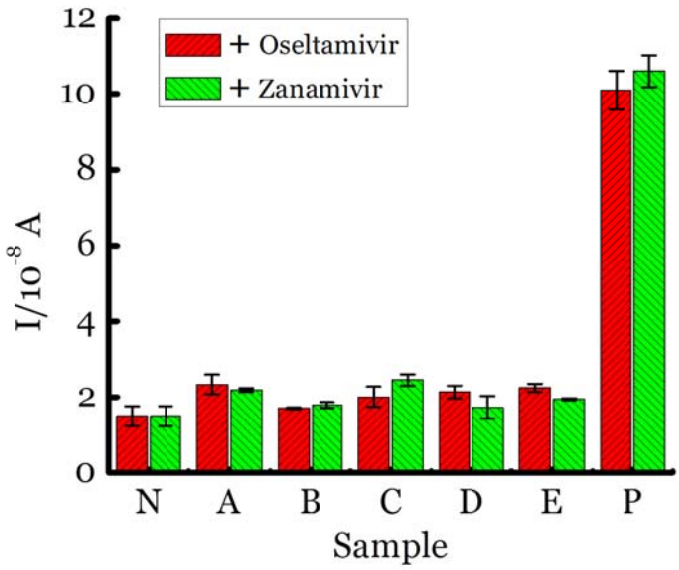

Figure 1.30 Drug susceptibility studies.

10 ng of Zanamivir or Oseltamivir (Carbosynth, USA, San Diego, CA) were premixed with the strains (as detailed in Figure 1.29) for 30 min at RT before addition of SG1.

Next, we premixed FDA approved antivirals, Zanamivir or Oseltamivir to virus or NA for 30 minutes before introducing **SG1** to the solution. These two antivirals are NA inhibitors. Therefore, if the strains are not resistant to the antivirals, they are expected to block the action of NA and a signal for glucose should not be observed. As seen in Figure 1.30, the three strains and NA are completely inhibited by the antivirals. These strains are not resistant to the action of the antivirals. We also used the same assay to distinguish viral NA from bacterial NA. To this end, we introduced bacterial NA (B NA) from Clostridium perfringens (Sigma Aldrich, St. Louis, MO) to SG1. (Figure 1.31, sample B NA). However, when Zanamivir was premixed with bacterial NA, we observed that NA still cleaved **SG1** because the antivirals are specific for viral

NA. (Figure 1.31, sample B NA + Z). Therefore, we can distinguish between BNA and viral NA using the antivirals.

We obtained nasal and throat swabs from healthy volunteers and tested for the presence of glucose. There was no glucose present in any of the samples. Next, we spiked 10^5 PFU of H1N1 A/Brisbane/59/2007 strains and tested the sample for glucose. We found that the matrix does not affect the cleavage of the lead compound **SG1** (Figure 1.32), indicating that this assay can be used in a point of care setting.

Since commercial glucose meters use disposable screen-printed enzyme electrodes for blood glucose measurements, we used disposable printed electrodes (CH instruments, Austin, Texas) for the next set of experiments. (Figure 1.26) We introduced glucose oxidase to the strips after activation and tested a library of twenty H1N1 and H3N2 influenza strains that were quantified using plaque assays and rRT-PCR. Strains were incubated with **SG1** (1 mM) using a specific set of buffers and reagents to release the viral NA from the membranes as described in the supplementary materials for 1 hour before introduction of 20 μL of the solution to the disposable strips. We found that all strains release glucose, most strains release **SG1** with high efficiency in one hour. However, some strains require longer time to completely cleave **SG1**. (Figure 1.34, Table 1.2) We note that, despite variations in printed electrodes from different manufacturer or different batches from the same manufacturer which affects the performance, the assay detects all strains. The advantages of printed electrodes compared to our previous setup is the limited volume of solution needed (20 μL) and the user friendliness of the system. We also determined the analytical sensitivity using one of the strains using this rudimentary setup. (Figure 1.33) This limit of detection and range is 10^2 and 10^2-10^8 PFU, respectively.

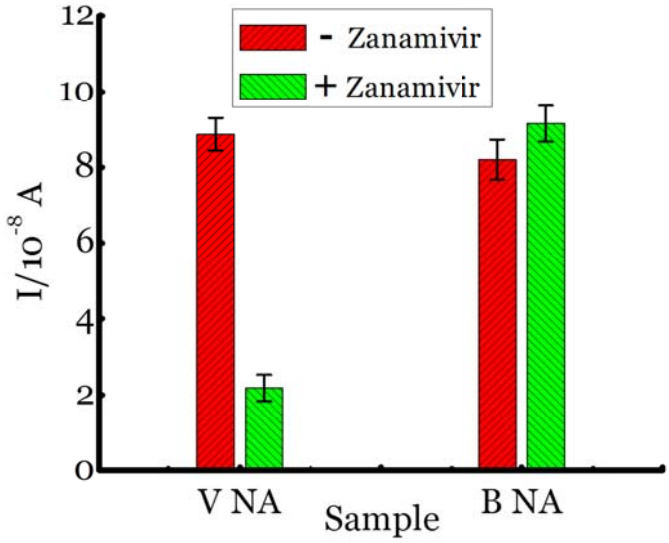

Figure 1.31 Studies with bacterial NA (BNA).

BNA cleaves **SG1** to release glucose, however, Zanamivir does not inhibit BNA and glucose is released when BNA was premixed with Zanamivir and incubated with SG1.

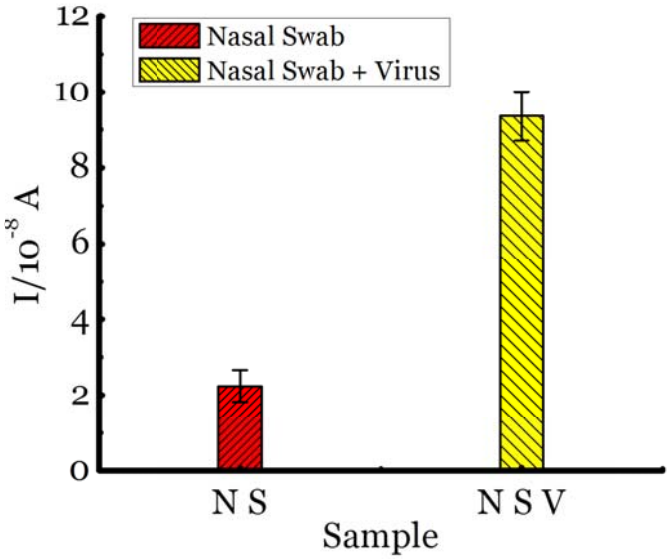

Figure 1.32 Studies with human samples.

NS denotes nasal swab only, and shows that no glucose is present. NSV denotes a nasal swab spiked with 10^5 PFU of H1N1A/Brisbane/59/2007 and added to SG1. The positive signal indicates there are no matrix effects. In (1.19-1.32), they axis shows current (i) in amperes measured after 100 s using an amperometric i–t curve at a working potential of 0.00 V. All experiments were performed in triplicate independently on different days.

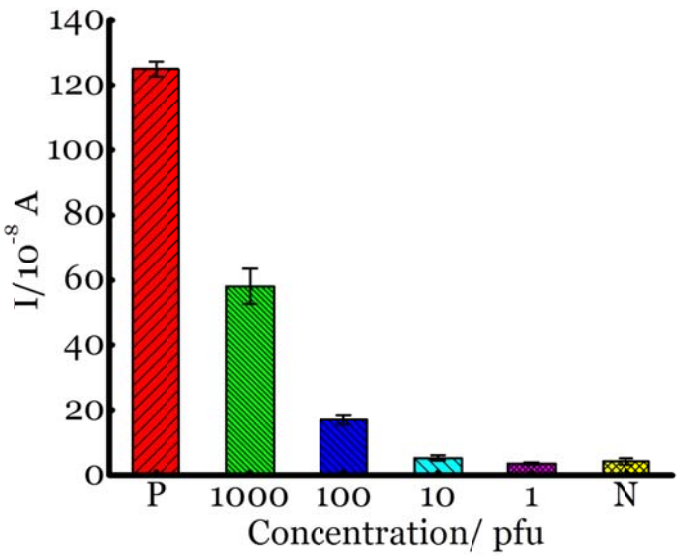

Figure 1.33 Analytical sensitivity studies

A/HongKong/8/1968 (H3N2) strain is used to detect analytical sensitivity. P is positive sample, which is 1 mM glucose, N is negative control (**SG1** but no virus), and the numbers represent the number of viral particles in the sample. 100 µL of virus containing solution was mixed with SG1 (100 µL, $2x10^{-3}$ M) for 1 h. 20 µL of this solution was used to test for the presence of glucose. The y axis represents current, I, in amperes measured after 100 s using an amperometric i-t curve at a working potential of 0.00 V, and the x-axis represents different samples.

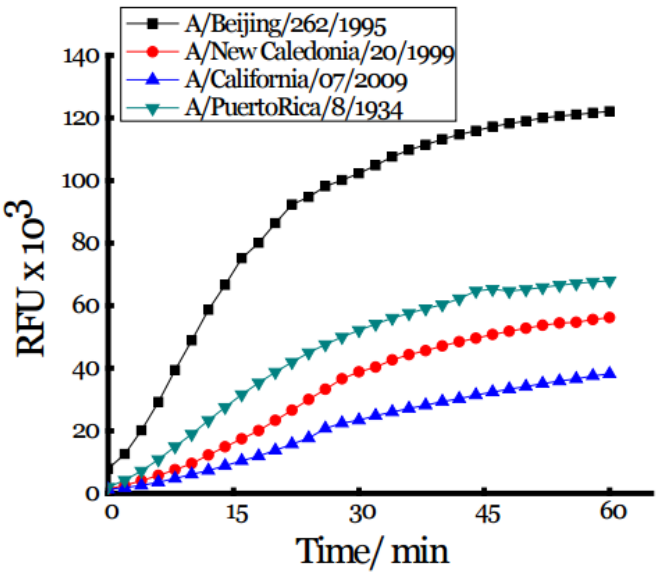

Figure 1.34 Fluorescence experiments to demonstrate relative NA activity of four different strains.

MUNANA (10 µL, 1mM) was added to 100 µL of virus strains. Fluorescent intensity was monitored using a microplate reader (Synergy 2, Biotek, Inc. Winooski, VT) at 2 min intervals for 1 hour at 37 ^{o}C after the addition of the substrate. Fluorescent intensity was read at 460 nm with an excitation at 360 nm.

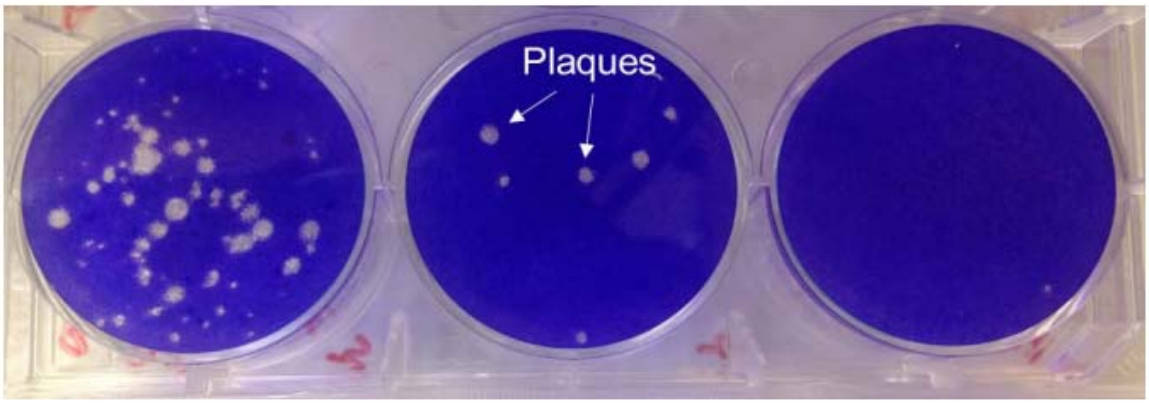

Figure 1.35 Images of plaque assay for one strain.

Confluent MDCK cells were infected with approximately 60, 6 and 0 viral particles (A/Brisbane/59/2007) and incubated for 5 days with a semi-solid media overlay. Plaque forming units (PFU) were counted after fixing and staining the cells.

Influenza strains	**Plaque Assay[a]**	**rRT-PCR (C_T)[b]**	**Electrochemical assay. (x 10^{-8} A)[c]**
No virus + SG1	N/A	N/A	3.6 ± 2.2
No glucose	N/A	N/A	3.4 ± 1.4
β-Galactosidase	N/A	N/A	4.2±1.9
α-Mannosidase	N/A	N/A	4.7±1.6
Glucose (1mM)	N/A	N/A	124.9 ± 2.3
A/Wilson-Smith/1933 (H1N1)	4.2 X10^6	18	99.5 ± 4.4
A/PuertoRico/8/1934 (H1N1)	1.4 X10^4	15	13.4 ± 2.0
A/HongKong/8/1968 (H3N2)	1.5 X 10^5	22	64.4 ± 5.2
A/Aichi/2/1968 (H3N2)	1.0 X 10^5	15	31.3 ± 5.3
A/Beijing/262/1995 (H1N1)	3.5 X 10^5	21	118.1 ± 11.6
A/Nanchang/933/1995 (H3N2)	0.7 X 10^6	18	15.1 ± 2.8
A/Sydney/5/1997 (H3N2)	0.8 X 10^4	29	115.7 ± 4.3
A/NewCaledonia/20/1999 (H1N1)	4.4 X 10^7	12	17.7 ± 2.6
A/SolomonIslands/3/2006 (H1N1)	1.1 X 10^9	11	79.7 ± 5.0
A/Uruguay/716/2007 (H3N2)	1.2 X10^7	20	132.4 ± 6.3

A/Brisbane/59/2007 (H1N1)	2.5×10^7	12	106.2 ± 5.1
A/Brisbane/10/2007 (H3N2)	2.2×10^6	21	78.6 ± 4.9
A/California/07/2009 (H1N1)	3.6×10^6	13	13.4 ± 1.5
A/New York/18/2009 (H1N1)	3.5×10^5	17	74.4 ±5.6
A/San Diego/1/2009 (H1N1)	1.2×10^5	19	108.5 ± 12.0
A/Wisconsin/629-D02452/2009 (H1N1)	0.6×10^5	13	98.9 ± 5.7
A/Wisconsin/15/2009 (H3N2)	0.5×10^4	26	107.8 ± 5.9
A/Brownsville/31H/2009 (H1N1)	0.4×10^4	22	91.7 ± 9.7
A/Victoria/361/2011 (H3N2)	7.0×10^6	26	94.5 ± 2.3

Table 1.2 Electrochemical detection of 19 influenza strains and validation with rRT-PCR and cell-culture plaque assays.

1.3.5 Conclusion

To summarize, we have developed an electrochemical assay that releases glucose upon introduction of influenza viruses. We have successfully detected a library of nineteen influenza strains. The assay can be used to measure drug susceptibility, which is a significant advantage over current genotypic and phenotypic methods that take time, resources, and a laboratory environment with specialized equipment and trained personnel. The assay can be integrated into current glucose meters by calibrating the instruments to test nasal or throat swabs for influenza. Since glucose meters with disposable test strips are user friendly, ubiquitous, and inexpensive, this method has great potential to improve clinical decisions and minimize disease burden due to influenza. Finally, this concept is unique because any enzyme, e.g. beta lactamase[75] or sulfatases

[76] present in drug resistant bacterial strains can be detected by blood glucose meters provided there are sufficient copies of the enzyme and the drugs being tested are enzyme inhibitors.

1.3.6 Experiment Section

1.3.6.1 General Information

Glycosylation reactions were performed under argon with solvents dried using a solvent purification system (Innovative Technology Inc., Amesbury, MA, USA). Other chemical reagents were of analytical grade, used as supplied, without further purification unless indicated. The acidic ion exchange resin used was Amberlite® IR-120 (H^+) resin. Analytical thin layer chromatography (TLC) was performed on silica gel 230-400 mesh (Silicycle, Quebec City, Canada). Plates were visualized under UV light, and/or by staining with acidic $CeH_8Mo_3N_2O_{12}$, followed by heating. ^1H and ^{13}C NMR spectra were recorded on Bruker 400 MHz spectrometer. Chemical shifts are reported in δ (ppm) units using ^{13}C and residual ^1H signals from deuterated solvents as references. Spectra were analyzed with MNova® (Mestrelab Research, Escondido, CA, USA). Electrospray ionization mass spectra were recorded on a Micromass QT 2 (Waters) and data were analyzed with MassLynx® 4.0 (Waters, Milford, MA, USA) software. Reported yields refer to spectroscopically and chromatographically pure compounds that were dried under high vacuum (10–2 mbar) before analytical characterization, unless otherwise specified.

1.3.6.2 Abbreviations

N, *N*-Dimethyl formamide, DMF; Ethyl acetate, EtOAc; Dichloromethane, DCM; Thin layer chromatography, TLC; Methanol, MeOH; Ethanol, EtOH; Sodium hydride, NaH; Benzyl bromide, BnBr; Triethylamine, NEt_3; *tert*-Butyldimethylsilyl chloride, TBSCl; 4-Dimethylaminepyridine, DMAP; Sulphuric acid, H_2SO_4,; Trifluoromethanesulfonic acid, TfOH;

N-Iodosuccinimide, NIS; Sodium methoxide, NaOMe; Palladium hydroxide, $Pd(OH)_2$; Sodium hydroxide, NaOH; Sodium thiosulfate, $Na_2S_2O_3$; Hydrochloric acid, HCl; Glucose oxidase, GOD.

1.3.6.3 Synthesis and Characterization

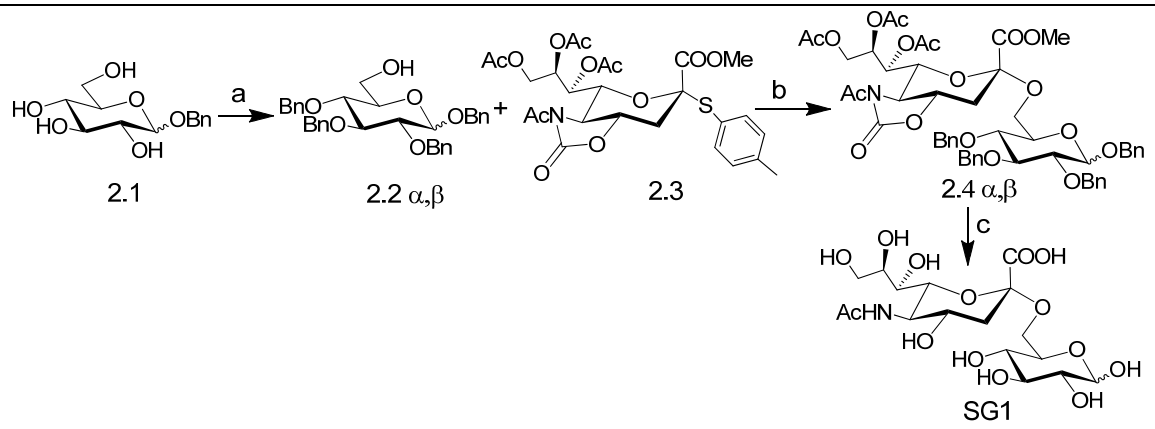

Scheme 1.3 Synthesis route of SG1

Reagents and Conditions: a) i) Pyridine, TBSCl, DMAP, rt, overnight; ii) NaH, BnBr, DMF, 0 ^oC- rt, 3h; iii) 1M H_2SO_4 in MeOH, MeOH, rt, 1h, 27% yield for **2α** and 20% yield for **2β** over three steps; b) TfOH, NIS, DCM, -60 °C, 2h, 75%; c) i) NaOMe, MeOH, rt, 30 min.; ii) $Pd(OH)_2/C/H_2$, EtOH, rt, 12h.; iii) 0.05 M NaOH in H_2O, rt, 4h, 93% over three steps.

Benzyl 2,3,4-tri-O-benzyl-α,β-D-glucopyranoside (2α,β) :

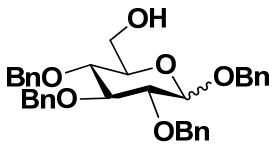

2α,β

To a solution of compound **1** (1.0 g, 3.7 mmol) in pyridine (0.010 L), TBSCl (0.85 g, 5.5 mmol) was added, followed by addition of DMAP (0.04 g, 0.37 mmol). The reaction mixture was stirred overnight at rt. After completion of reaction as monitored by TLC, the solvent was removed using a rotary evaporator and the crude compound was used directly without further

purification. To a stirred suspension of NaH (0.89 g, 18 mmol, prewashed with dry hexane to remove the oil present in 60% suspension of NaH) in anhydrous DMF (0.010 L), the crude TBS compound in DMF (0.010 L) was added at 0 °C. The reaction mixture was stirred under argon atmosphere for 30 min. BnBr (2.2 ml, 18 mmol) was added dropwise via syringe and reaction mixture was stirred for 3 h. The reaction mixture was quenched with 1M HCl (10 mL), diluted with EtOAc (20 mL) and washed with water (2 x 10 mL) and brine (2 x 10 mL). The organic layer was dried over Na_2SO_4 and concentrated under reduced pressure to obtain the tetra benzyl protected compound. The crude compound was used directly without further purification. To a stirred solution of the crude compound in MeOH (0.020 L), H_2SO_4 in MeOH (1M, 0.50 mL) was added. The reaction mixture was stirred at rt and the reaction progress was monitored by TLC using two solvent systems: EtOAc–hexanes (1:9) and EtOAc–hexanes (1:1). After completion of reaction as monitored by TLC, the reaction mixture was diluted with EtOAc (20 mL) and washed with saturated $NaHCO_3$ (2 x 20 mL) and brine (2 x 20 mL). The organic layer was dried over NaSO4, concentrated under reduced pressure and subjected to flash chromatography to give **2 α**(0.55 g, 27% yield over three steps) and **2β** (0.40 g, 20% yield over three steps). Spectral data is in complete agreement with reported value.

Methyl 5-acetamido-7,8,9-*tri*-O-acetyl-5-N,4-O-carbonyl-3,5-dideoxy-D-glycero-α-D-galacto-non-2-ulopyranosylonate-(2,6)-1,2,3,4-*tetra*-O-benzyl-α-D-glucopyranoside (4α) :

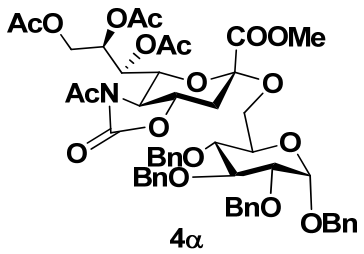

4α

To the stirred solution of acceptor **2α** (0.20 g, 0.35 mmol) and donor **3**[74] (0.24 g, 0.38 mmol) in anhydrous DCM (4.0 ml) under an argon atmosphere at -40 0C, NIS (0.19 g, 0.84 mmol) was added followed by TfOH (0.52 ml, 0.35 mmol, 10% in anhydrous DCM). The reaction mixture was stirred at this temperature for ~2h until complete disappearance of the acceptor as determined by TLC. Et_3N (0.50 mL) was added to quench the reaction and warmed to rt. The reaction mixture was diluted with DCM (20 mL), washed with aqueous solution of $Na_2S_2O_3$ (2 x 10 mL) dried over Na_2SO_4 and concentrated under reduced pressure. The residue was subjected to flash silica gel column chromatography eluting with (hexanes:EtOAc 7:3) to afford the **4α** (0.27 g, 75 % yield) as a white solid. ^{1}H NMR (400 MHz, $CDCl_3$) : δ 7.45 – 7.26 (m, 20H), 5.58 (dd, *J* = 8.9, 1.7 Hz, 1H), 5.45 (ddd, *J* = 8.5, 6.1, 2.5 Hz, 1H), 4.97 (d, *J* = 10.8 Hz, 1H), 4.86 – 4.78 (m, 3H), 4.76 (d, *J* = 6.1 Hz, 1H), 4.73 – 4.65 (m, 2H), 4.56 (dd, *J* = 15.0, 12.2 Hz, 2H), 4.26 (dd, *J* = 12.4, 2.7 Hz, 1H), 4.20 (dd, *J* = 10.8, 4.5 Hz, 1H), 4.14 (d, *J* = 7.2 Hz, 1H), 4.08 – 3.98 (m, 2H), 3.98 – 3.84 (m, 2H), 3.73 (s, 3H), 3.66 (dd, J = 11.2, 9.4 Hz, 1H), 3.60 (d, *J* = 9.4 Hz, 1H), 3.58 – 3.52 (m, 1H), 3.49 (dd, *J* = 10.6, 2.0 Hz, 1H), 2.94 (dd, *J* = 12.1, 3.4 Hz, 1H), 2.49 (s, 3H), 2.15 (s, 3H), 2.12 – 2.06 (m, 1H), 2.04 (s, 3H), 1.81 (s, 3H). ^{13}C NMR (100 MHz, $CDCl_3$) : δ 171.8, 170.6, 169.9, 169.9, 168.4, 153.6, 138.8, 138.4, 138.2, 137.1, 128.4, 128.3, 128.0, 127.9, 127.8, 127.7, 127.5, 99.2, 95.5, 81.9, 79.6, 77.5, 75.7, 75.2, 75.0, 74.9, 73.0, 71.4, 69.9, 69.0, 68.4, 64.7, 62.8, 59.1, 52.9, 36.6, 24.7, 21.1, 20.7, 20.5. HRMS (ESI): Calculated for $C_{53}H_{59}NO_{18}Na$ [M+ Na] 1020.3630; Found 1020.3629.

Methyl 5-acetamido-7,8,9-*tri*-O-acetyl-5-N,4-O-carbonyl-3,5-dideoxy-D-glycero-α-D galacto-non-2-ulopyranosylonate-(2,6)-1,2,3,4-*tetra*-O-benzyl-β -D-glucopyranoside (4β):

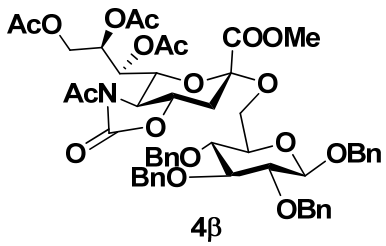

4β

4β was synthesized in a manner from donor **3** (0.24 g, 0.38 mmol) and 2β (0.20 g, 0.35 mmol) similar to that of **4β** and the product was purified using flash silica gel column chromatography eluting with hexanes:Et_2OAc (7:3) to afford the compound **4β** (0.27 g, 75 % yield) as a yellowish solid.^{1}H NMR (400 MHz, $CDCl_3$) : δ 7.46 – 7.24 (m, 20H), 5.65 (d, *J* = 8.6 Hz, 1H), 5.52 (dt, *J* = 8.7, 4.3 Hz, 1H), 4.97 (d, *J* = 11.5 Hz, 2H), 4.91 (d, *J* = 10.9 Hz, 1H), 4.82 (s, 2H), 4.76 (t, *J* = 11.0 Hz, 2H), 4.68 (dd, *J* = 10.8, 5.5 Hz, 2H), 4.51 (d, *J* = 7.9 Hz, 1H), 4.37 (dd, *J* = 12.4, 2.8 Hz, 1H), 4.21 (dd, *J* = 11.2, 4.6 Hz, 1H), 4.11 – 3.95 (m, 2H), 3.76 (s, 3H), 3.75 – 3.60 (m, 4H), 3.56 – 3.44 (m, 2H), 2.99 (dd, *J* = 12.3, 3.2 Hz, 1H), 2.51 (s, 3H), 2.16 (s, 3H), 2.11 (s, 3H), 2.12-2.01 (m, 1H), 1.91 (s, 3H). ^{13}C NMR (100 MHz, $CDCl_3$) : δ 177.5, 171.8, 170.6, 170.0, 168.3, 153.7, 138.6, 138.4, 138.3, 137.3, 128.4, 128.4, 128.4, 128.3, 128.1, 128.1, 127.9, 127.9, 127.8, 127.8, 127.7, 127.7, 127.6, 127.6, 102.3, 99.3, 84.5, 82.0, 75.7, 75.20, 75.1, 74.8, 73.9, 71.5, 71.0, 68.6, 64.6, 62.9, 59.1, 52.9, 36.6, 24.7, 21.2, 20.8, 20.6. HRMS (ESI): Calcd for $C_{53}H_{59}NO_{18}Na$ [M+ Na] 1020.3630; Found 1020.3629.

5-acetamido-3,5-dideoxy-D-glycero-α-D-galacto-non-2-ulopyranosylonate-(2,6)-α,β-D-gluco pyranoside (SG1) :

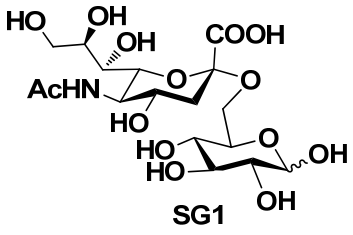

SG1

4α or **4β** (0.060 g, 0.060 mmol) was dissolve in MeOH (0.010 L) and treated with a 30% solution of NaOMe (75 µl) in CH_3OH and stirred at rt for 1 h. The solution was neutralized with Amberlite® IR 120 (H^+) resin, filtered and concentrates to dryness. The dried compound was treated with $Pd(OH)_2/C$ (0.010 g) in absolute EtOH was stirred for 12h at rt under H_2 at 1 atmosphere. After completion of reaction as monitored by TLC, reaction mixture was filtered using celite pad, washed with EtOH and combined solvent was concentrate to dryness. The dried compound was treated with NaOH (0.05 N, 3.0 mL) and reaction was stirred for 4h. After completion of reaction, as monitored by TLC (DCM:MeOH:NH_4OH) (8:2:1), reaction was neutralized using Amberlite® IR 120 (H^+) resin, filter, concentrate and subjected to P-2 gel column to furnish **SG1**. (0.013 g, 93 % yield over three steps) (54:46, ratio determined by ^1H NMR spectroscopy). ^1H NMR (400 MHz, D_2O) δ 5.12 (d, *J* = 3.2 Hz, 1H, H1 α), 4.54 (d, *J* = 7.8 Hz,1H, H1 β), 4.07 – 3.86 (m, 2H), 3.86 – 3.69 (m, 7H), 3.68-3.53 (m, 5H), 3.51 – 3.41 (m, 2H), 3.40 – 3.33 (m, 1H), 3.19-3.14 (m, 1H), 2.63 (dd, *J* = 12.5, 4.2 Hz, 1H), 1.95 (s, 3H), 1.74-1.68 (m, 1H) ^{13}C NMR (101 MHz, D_2O) δ 177.7, 176.8, 174.7, 95.9, 92.1, 75.6, 74.4, 73.9, 72.3, 72.8, 71.4, 71.8, 69.5, 69.45, 6.2, 68.2, 67.9, 63.1, 62.9, 62.7, 51.8, 39.7, 22.0. HRMS (ESI): Calcd for $C_{17}H_{29}NO_{14}Na$ [M+ Na]+ 494.1486, found 494.1497.

1.3.6.4 Cells and Viruses

MDCK (Madin-Darby canine kidney) cells were purchased from ATCC® (CCL-34™, Manassas, VA) and maintained in Dulbecco's Modified Eagle Medium (DMEM, Gibco, Grand Island NY) supplemented with 10% Fetal Bovine Serum (FBS Gibco, Grand Island NY). Influenza A virus strains used in this study were obtained from BEI Resources (Manassas, VA).

1.3.6.5 Nasal and Throat Sample Collection

Nasal and throat samples were collected from four healthy volunteers. Dry sterile cotton tipped swab was used for each sample collection. Samples were stored in phosphate buffered saline (PBS) at 4 °C until subsequent use.

1.3.6.6 Plaque Assays

Virus titers of different influenza strains were determined using standard plaque assays in MDCK cells to quantify the amount of virus. MDCK cells were grown to confluency in 6-well plates. Once confluent, media was removed from the cells and were washed three times with plain DMEM to remove residual FBS. Virus suspension was serially diluted 10-fold and added to duplicate wells at 400 µL/ well. Virus was adsorbed for 1 h at 37 °C in a 5.0% CO_2 incubator. One-hour post-adsorption, virus suspension was removed and Avicel (1.2%, 2.0 mL, FMC Biopolymer) supplemented with 2 µg/mL TPCK-trypsin (Sigma-Aldrich, St. Louis, MO) was added to each well. Avicel was prepared as described previously.[77] Plates were incubated for 5 days to allow for plaque formation. On day 5, the Avicel overlay was removed carefully from each well and the wells were washed two times with 1X PBS followed by methanol (100%) fixation. Fixed wells were stained with 0.2% crystal violet and plaques were counted to determine virus titers.

1.3.6.7 Real-time RT-PCR

Viral RNA was extracted according to manufacturer's instructions using MagMAX viral isolation kit (Life Technologies, Grand Island NY). cDNA was synthesized from the viral RNA using High Capacity cDNA Reverse Transcription Kit purchased from Applied Biosystems (Grand Island, NY). Real time PCR was performed using primers and probe for matrix gene, as described previously.[78] The oligonucleotide probe sequence is 5`CTCAGTTATTCTGCTGGTGCACTTGCCA consisting of 5` reporter dye 6-carboxyfluorescein (FAM) and 3` quencher dye 6-carboxytetramethylrhodamine (TAMRA). The forward primer sequence (5` GGACTGCAGCGTAGACGCTT) and two reverse primers sequences (5` CATCCTGTTGTATATGAGGCCCAT and 5` CATTCTGTTGTATATGAGGCCCAT) were used to facilitate amplification of all the strains. PCR mix of 30 µL was prepared using 15 µL TaqMan Universal PCR mix (Applied Biosystems, Grand Island NY), 1µM primers, 0.5 µM probe, and 5 µL of cDNA. Real time PCR amplification and detection was conducted using Applied Biosystems 7500 Fast Real-Time PCR System.

1.3.6.8 Electrochemical Assay using the 3 electrode system

The initial proof of principle studies were performed using three-electrode system.[72] (Figure 1.26) Briefly, a glassy carbon working electrode (GCE, 3.0 mm in diameter), a saturated calomel reference electrode, and a platinum counter electrode. Fabrication of the electrode was performed by polishing the surface of the glassy carbon electrode on the alumina slurries to form a clear mirror followed by washing with distilled water and drying with N_2. The electrode was coated with coating solution achieved by mixing 1ml of solution A (2 mM Bi (NO_3). $5H_2O$ and 3mM SeO_2 in 1:20 diluted nitric acid) and 2 ml of solution B (2mM $K_3Fe(CN)_6$, 2mM $FeCl_3$,

0.1M KCl and 10mM HCl) followed by cyclic voltammetry scanning from +0.60 V to -0.20 V at 20 mVs^{-1} for 30 cycles. After the coating, the electrode was activated by cycling from 0.35 V to -0.05 V at 50 mVs^{-1} for 30 times in solution C (0.1M KCl and 10mM HCl). 5 mg of Glucose oxidase (GOD) was dissolved in 1 mL of 0.5% chitosan solution (prepared in 2% acetic acid) and the resulting GOD (10 µL) solution was dropped on the surface of the electrode to form a GOD layer. The GOD layer was air dried to form a firm coated layer on the working electrode. To detect the neuraminidase activity of influenza virus, 100-200 µL of virus stock (PFU determined by plaque assays) was incubated with SG1 (500 µL, $1x10^{-3}$ M) for 1 h. To detect the Amperometric response, final solution volume was adjusted to 1 mL. Virus was inactivated using UV light or 1% Triton X-100 (Sigma Aldrich, St. Louis MO). The amount of glucose released by NA cleavage of SG1 was detected by glassy carbon electrode using electrochemical analyzer (CH Instruments Ltd, China) at rt. An amperometric i-t curve at a working potential of 0.00 V was recorded and the current at 100 seconds (when stable) is reported. Increase in peak current correlates with increased glucose concentration, which in turn, reflects the activity of influenza virus neuraminidase.

1.3.6.9 Drug susceptibility studies

10 ng of Zanamivir or Oseltamivir carboxylate was premixed with the virus for 30 min. Next, the solution was incubated with **SG1** for 1 h at rt. and glucose released was measured as described in the previous section.

1.3.6.10 Electrochemical assay using printed electrodes

Printed electrodes were purchased from CH instruments, Austin, Texas, USA, coated and activated the surface using the solutions as described above. GOD was coated on the surface using chitosan as previously described. Next, 100 µL of virus containing solution was mixed

with SG1 (100 μL, 2 x10^{-3} M) for 1 h at 37^{o}C. 20 μL of this solution was dropped onto the surface of the test area of printed electrode to test for the presence of glucose as described previously.

2 Glycan Based Norovirus Detection

2.1 Norovirus Introduction

Norovirus is a non-enveloped, single-stranded RNA virus. [79] It is a highly contagious virus that causes patient stomachs and/or intestines to get inflamed. Typically patients have nausea, diarrhea, and vomiting if they get infected by norovirus. It can affect people of all ages, especially young children and older adults. In some cases, norovirus infection leads to death, although this virus does not have a significant death rate. The virus affects approximately 267 million people and is responsible for an estimated 2 hundred thousand deaths annually in the entire world. [80] There are no vaccines or antivirals available for this disease.

Norovirus was previously known as Norwalk virus, which was first identified in Norwalk, OH in 1972.[81] The Norwalk virus was originally visualized by immune electron microscopy as 27nm in size. Cultivating the pathogen in cell culture and in animal model is essential to further discover and develop the virology and treatment for norovirus infection, however, all attempts have failed thus far. [82]. However, recent reports suggest that this virus can indeed be grown in culture using B cells, but the results are still under investigation. [74]

Norovirus belongs to the family Caliciviridae which is a group of small, non-enveloped, positive stranded RNA virus. There are five genera in Caliciviridae family including Norovirus, Sapovirus, Lagovirus, Nebovirus, and Vesivirus.[83] Due to unsuccessful attempts of virus cultivation, most of the literature has been focused on the virus protein and nucleic acid composition. The human norovirus genome is a linear, positive sense RNA which is approximately 7.6kb length.[84] The genome is attached to the viral protein genome (VPg) covalently. The genome is shown in Figure 2.1. It is comprised of three open reading frames including ORF-1, ORF-2, and ORF-3 and encodes eight viral proteins.

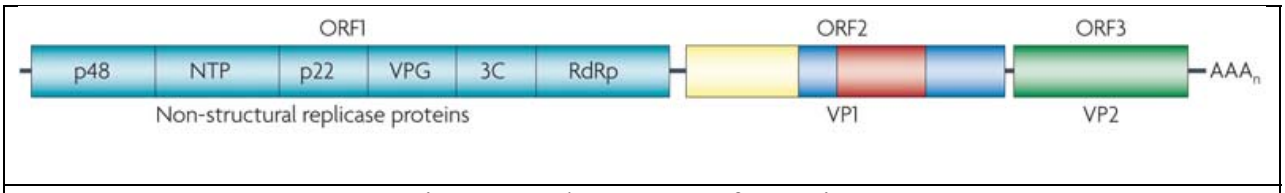

Figure 2.1 The genome of norovirus.

Different box represent different domain, which used to translate different proteins.

Figure is taken from publisher with permission. [80]

Norovirus mutate rapidly and can be descripted as a "shape-shifter". [80] This description was determined by the VP1 amino acid sequence which refers to the virus protein encoding. Six genogroups (GI- GVI) and more than 40 genotypes have been identified due to the rapid mutation.[85] The genetic diversity of the human noroviruses is apparent from the VP1 amino acid sequence. For example, the VP1 amino acid sequence of GII.4 strains differs by about 40% from the GI.1 norwalk strain and 5%-7% for the GII genotype.[86] This variability represents the diversity of the norovirus. With the continued evolution, the sequence cutoff of different strains is no longer sufficient to classify each other; new approach such as addition of a phylogenetic tree would provide more accurate details for the classification of norovirus.[87]

2.1.1 Structure of Norovirus

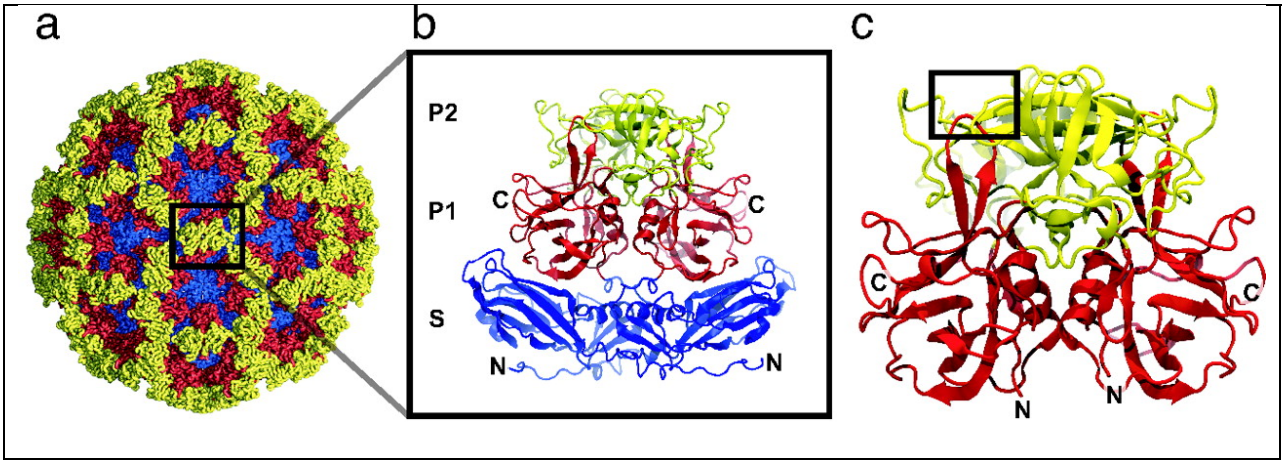

Figure 2.2 The x-ray crystallographic structure of the recombinant Norwalk virus capsid and P domain.

a: The T=3 capsid structure of norovirus. [88] b: Representation of the VP1 dimer shows S domain (blue), P1 domain (read) and P2 domain (gold). c: The structure of P domain.

Figure is taken from publisher with permission. [89]

The X-Ray crystallographic structure of the recombinant Norwalk virus capsid was shown in Figure 2.2 which clearly represents the structure of the norovirus. [88] The diameter of the virus is approximately 390 Å and the capsid exhibits a T=3 icosahedral organization. The capsid is formed by 90 dimers of the capsid protein which is composed of two distinct domains including the shell (S) domain and protruding (P) domain. The S domain contributed to the icosahedral shell formation and the P domain is involved in the dimeric contacts. Because the P domain decorates the surface of the virus, it is hypothesized that the P domain would be contributed to several biological functions such as causing strain diversity, binding to the host cell, and involving in immunogenicity.

Figure 2.3 shows the norovirus structure from electron microscope. In this figure, P dimer was enlarged from a single virus like particle to represent the HBGA-binding site filling model. A tri-saccharide is shown in a stick model binding to the amino acid residues in the P dimer binding site.

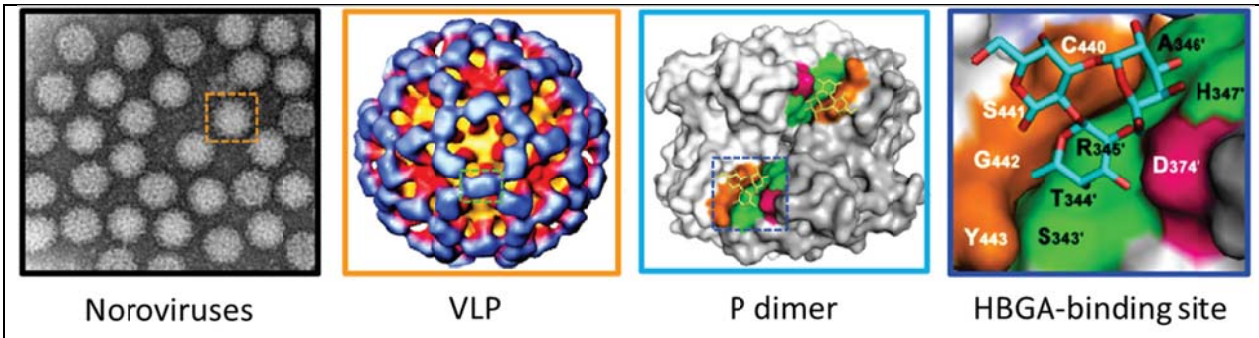

Figure 2.3 The structure of noroviruses at different levels

From left to right, Noroviruses electron microscopy, a single virus like particle, the P dimer with HBGAs binding site, the crystal structure of the HBGA binding interface. Figure is taken from publisher with permission. [90]

The norovirus genome is a single strain, positive sense RNA molecule which ranging in the size from 7.3 to 7.5kb. It is organized into three conserved ORFs as shown in figure 2.2. In all norovirus, ORF 1 will be translated to a large polyprotein, which is co- and post-translationally cleaved to release at least six mature nonstructural proteins. ORF 2 and ORF 3 are translated to the major capsid protein. This genome is packaged by capsid protein to form the major structure of norovirus.

2.1.2 Life Cycle of Norovirus

A number of steps are involved in norovirus life cycle. The different steps are described below.

1). Norovirus attach to the specific carbohydrate which located on the host cell surface to "anchor" itself on the host cell surface.

2). Norovirus entry to the hose cell and release the genomic material.

3). The viral genome is translated through interactions with VPg at the 5' end of the genome.

4). The ORF1 polyprotein is cleaved and the replication complex is generated.

5). Genome replication was achieved by RNA replication.

6). The replicated genomes are translated and finally packaged into the virus capsid.

7). Virion assembly and virus exit from the host cell.

2.1.3 Norovirus binding and entry to the host cell

The initial stage of norovirus life cycle is the virus binds with the host cell. This process is known to involve carbohydrates which are located on the host cell surface. HBGAs have been shown to bind with norovirus via capsid protein - carbohydrate intersection.[91] Protruding (P) domain of the capsid protein is responsible for the recognition in the norovirus and host cell binding process. Structure of the P domain complexed with A type HBGA and H type HBGA is shown in figure 2.4.

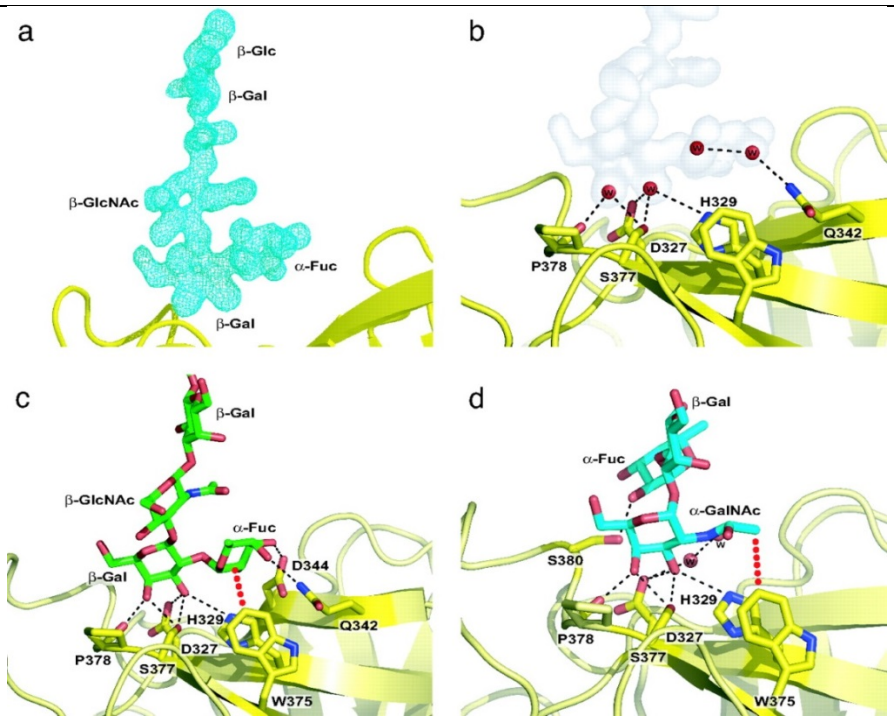

Figure 2.4 Norovirus P domain- HBGAs interactions.

a) The electron density of the bound penta-saccharide. b) The binding site of P domain. c) and d). The hydrogen bond interactions in the P domain binding site. Figure is taken from publisher[89] with permission.

The HBGA binding site in GI strains is very different from that in GII strains (Figure 2.5). Although the genotype sequence of GI and GII is different, the P dimer are similar organized, the carbohydrate binding site in GII and GI is distinctly different, not only different in its location, but also in its structural characteristics. Although some studies have been performed to elucidate the binding preferences of some VLPs, several questions are still unanswered. For example, most of the binding studies have used glycopolymers, which were not chemically well defined. Second, most of the studies were performed using VLPs and not intact viruses. Thus, the binding preferences are not very clear. We have attempted to study the binding preferences using glycan

microarrays and SPR in an attempt to develop glycan based tests for norovirus. These studies are described below.

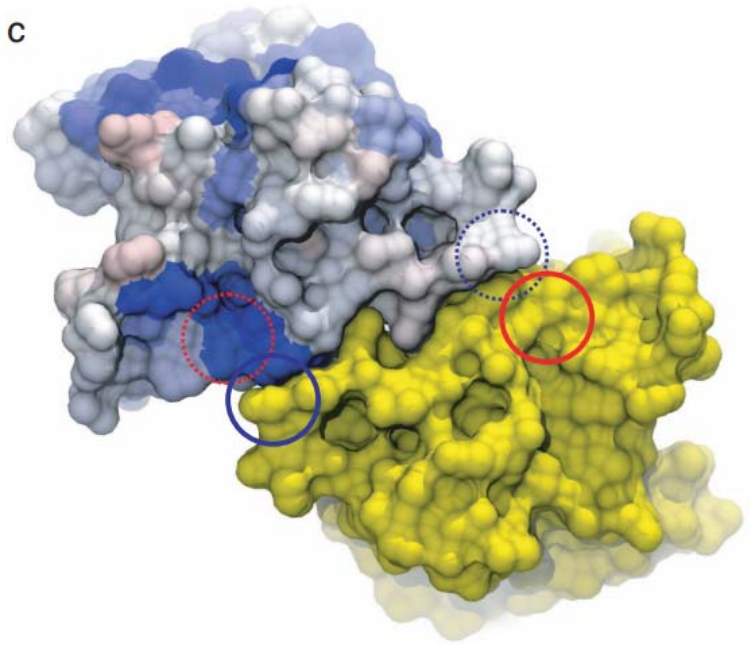

Figure 2.5 Different locations of the HBGAs binding sites in GI (red circle) and GII (blue circle). Relative locations of the HBGA biding sites in GI (red circle) and GII (blue circle) in P dimer. Figure is taken from publisher with permission. [89]

2.2 Microarray Detection for Norovirus

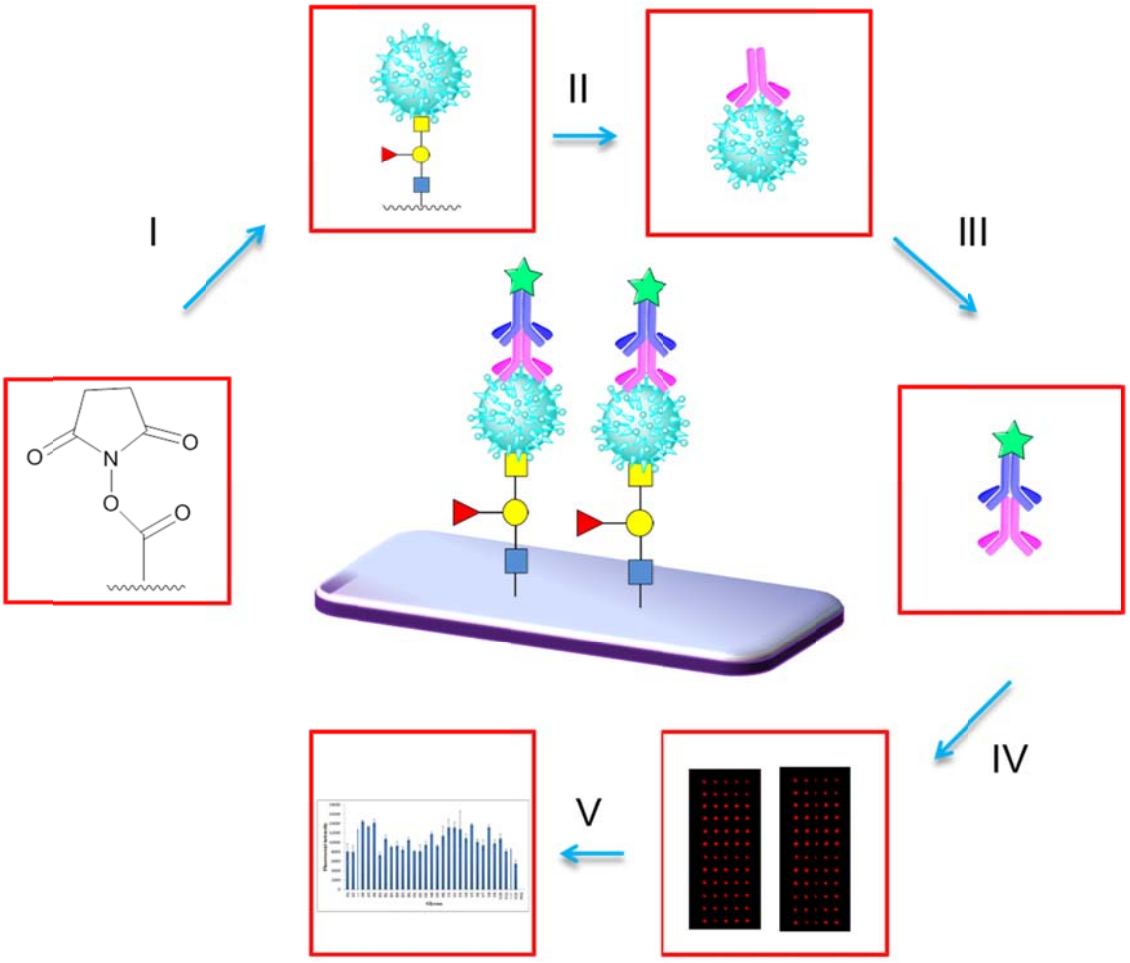

Figure 2.6 Glycan microarray to detect norovirus

Glycan microarray technology is used to detect the binding pattern of norovirus with HBGAs. This technology has been discussed in chapter 1. Here, the NHS modified array slide is used to immobilize the HBGAs on the array surface. The different steps are described below. (Figure 2.6)

1. A library of Histo blood group antigens and Lewis antigens have been synthesized and attached on BSA via the amine groups of the lysine side chain. Approximately 30 units of glycan units have been attached to a single molecule of BSA.
2. A focused glycan array of 31 HBGAs and LAs were printed on the surface of array slide which modified with NHS active ester, after incubation, glycans could be anchored on the surface by forming covalent bond between NHS active ester and amine of BSA.
3. Ethanol amine is used to cover the unprinted area to block unreacted NHS esters.
4. The array slide is incubated with different strains of norovirus or VLP. Nonspecific binding is washed away by DI water and PBS buffer.
5. The array slide is incubated with primary antibody, followed by extensive washing using DI water and PBS buffer to remove unbound antibody
6. The array slide is incubated with secondary antibody bearing fluorescent tag, followed by extensive washing using DI water and PBS buffer to removed unbound secondary antibody.
7. The slide is scanned by microarray scanner to generate the binding image.
8. The image is analyzed by image analyzer software, and the binding pattern is given as a graph format.

In this chapter, a panel of Histo Blood Group Antigens (HBGAs) and Lewis antigens (LA) has been used to capture norovirus. The HBGAs were developed and tested with different strains of norovirus and VLP using glycan microarrays. A glycan array of 31 glycans with different HBGA/LA glycans were printed onto a surface modified slide to generate a small focused microarray. The binding of different virus like particles (VLPs) including GI1, GII4 and

SMV and their corresponding intact viruses obtained from human challenge studies were evaluated using the glycan microarrays. We found that unique binding patterns for the different VLPs were obtained suggesting that a "fingerprint" pattern of recognition could be obtained for each strain. However, the binding patterns of the intact viruses did not match the binding patterns for the corresponding VLPs, indicating that matrix issues or antibodies may be affecting the binding when intact viruses were used. Since the virus cannot be grown in a laboratory environment, the antibodies are generated using VLPs, therefore, the antibodies for the VLPs may be different than that observed for the intact virus. To understand these differences, we developed biotinylated H type glycans and these glycans were tested using SPR (Surface Plasmon Resonance). We found that the different H type glycans give rise to differential binding, suggesting that the matrix may be interfering with the binding of intact viruses. These results are presented in this chapter.

The chemical structures of the 31 glcyans are given in figure 2.7 and the Symbols represent the structures are given in figure 2.8. These glycans were synthesized by members of Professor Todd Lowary's group, Alberta, Canada. The synthesis of the glycans has been published. [92]

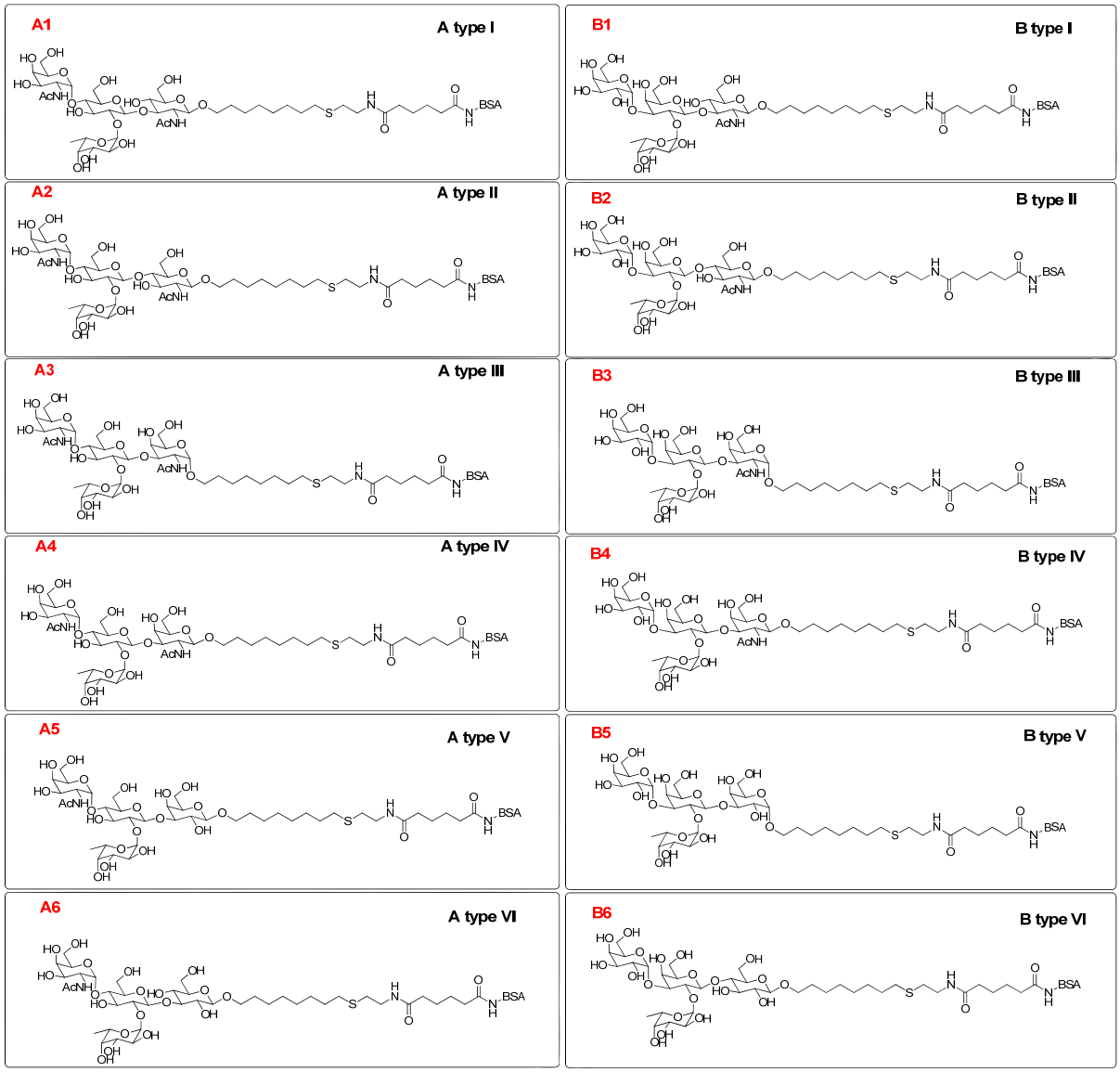
A1
A type I
B1
B type I
A2
A type II
B2
B type II
A3
A type III
B3
B type III
A4
A type IV
B4
B type IV
A5
A type V
B5
B type V
A6
A type VI
B6
B type VI

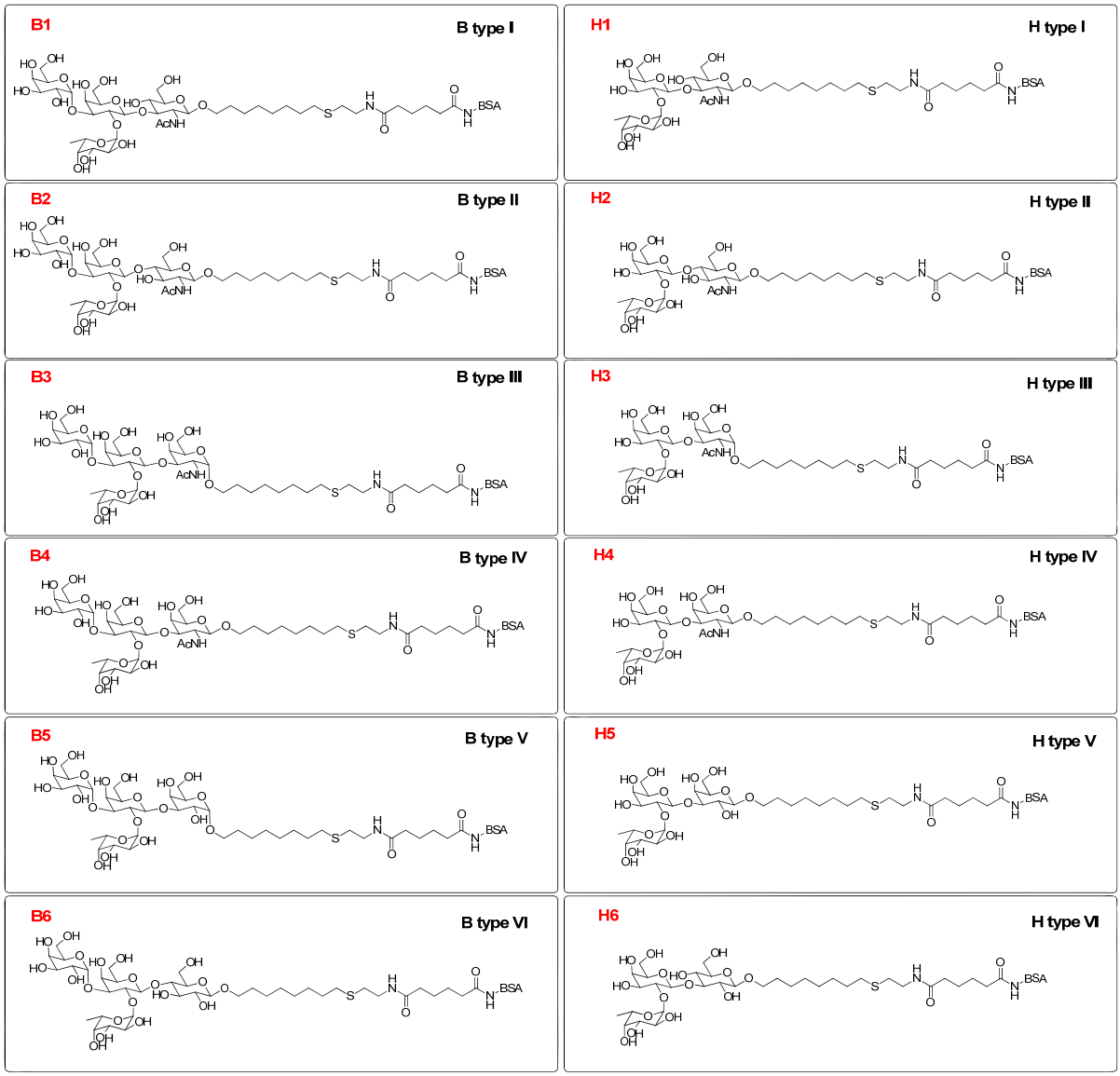
B1
B type I
H1
H type I
B2
B type II
H2
H type II
B3
B type III
H3
H type III
B4
B type IV
H4
H type IV
B5
B type V
H5
H type V
B6
B type VI
H6
H type VI

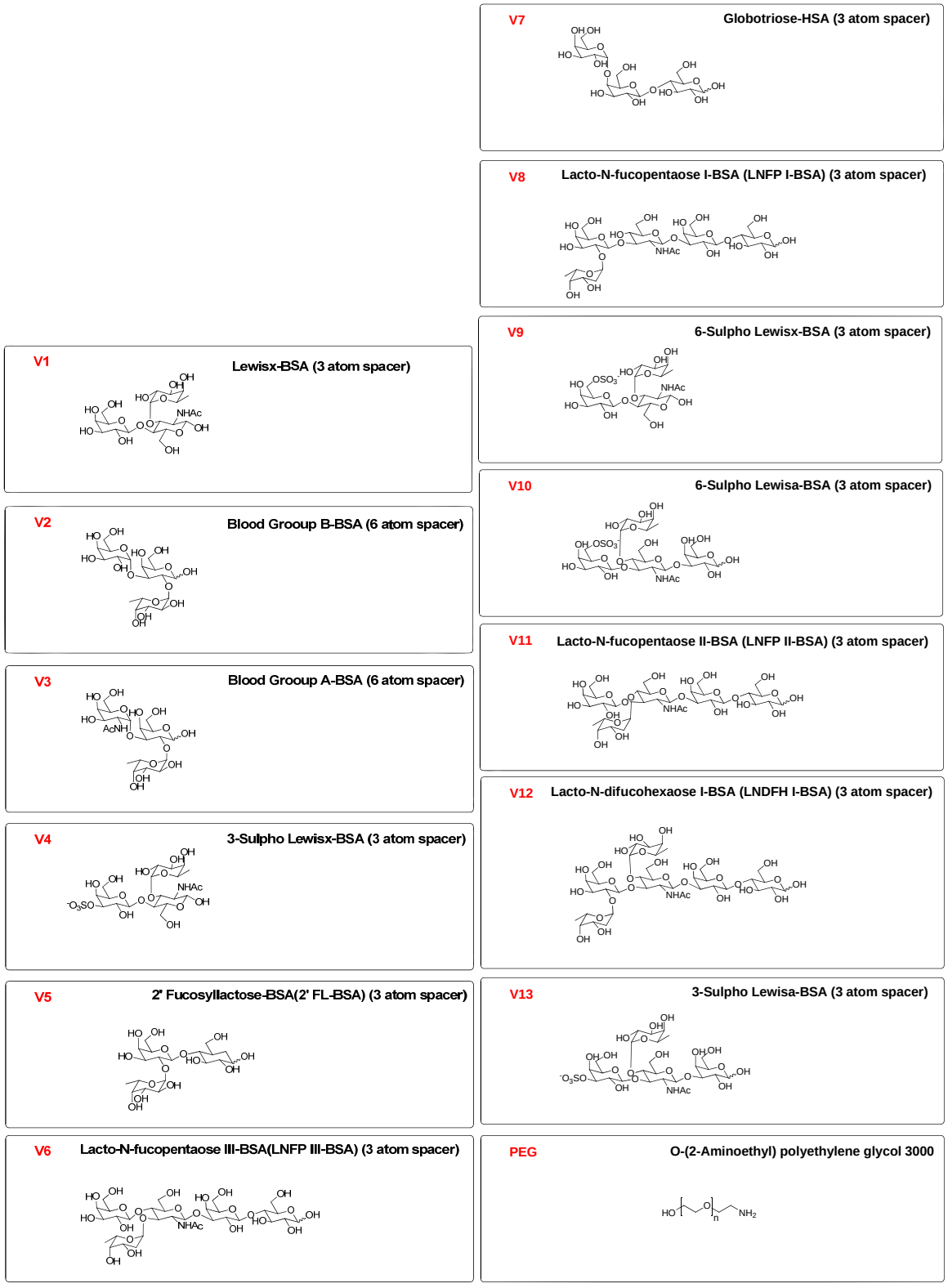

Figure 2.7 Structures of 31 unique histoblood group antigens

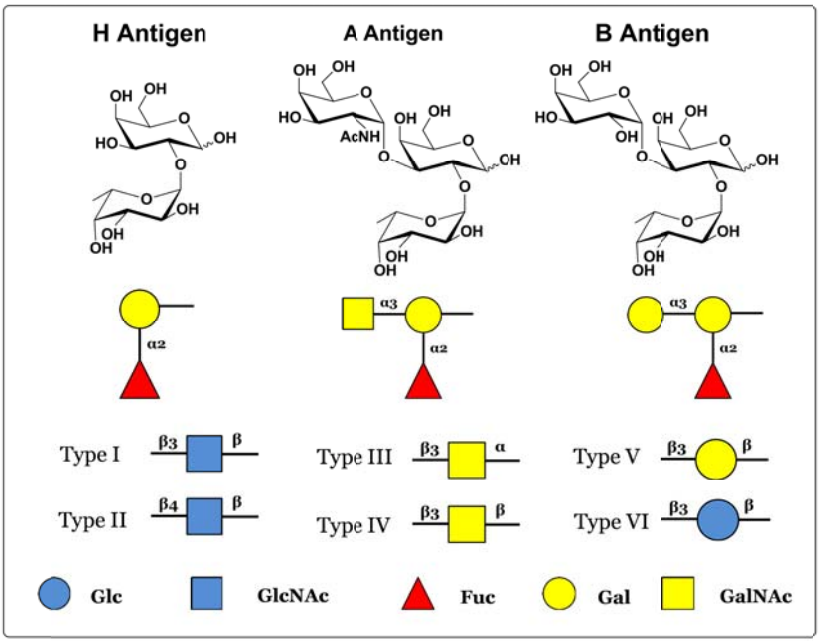
H Antigen
A Antigen
B Antigen
Type I
Type II
Type III
Type IV
Type V
Type VI
Glc
GlcNAc
Fuc
Gal
GalNAc

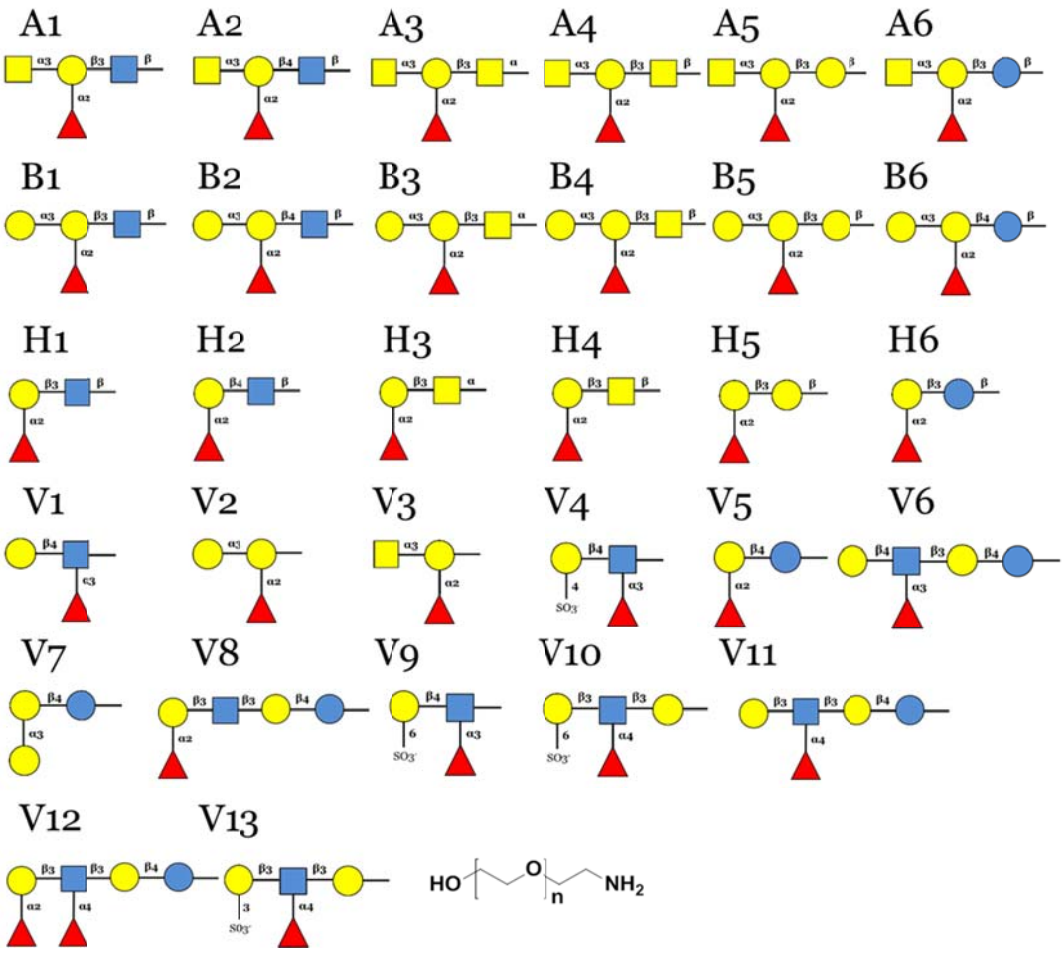
A1
A2
A3
A4
A5
A6
B1
B2
B3
B4
B5
B6
H1
H2
H3
H4
H5
H6
V1
V2
V3
V4
V5
V6
V7
V8
V9
V10
V11
V12
V13
HO
O
n
NH2

Figure 2.8 Symbols of 31 unique histo blood group antigens

2.2.1 Microarray Results with VLPs

For our initial studies, we tested the microarrays using VLPs (virus like particles) before testing with the actual virus samples. . The results with the VLPs are shown in Figure 2.9-2.11. As one can see, the binding pattern for the VLPs generated using three different types of strains, namely, GI.1. Norwalk, GII.2 Snow Mountain (SMV) and GII.4 New Orleans (NO) strains are very different and unique. This indicates that a pattern of recognition could be used to type each strain. We also performed a concentration study using different concentrations of the VLP for Snow Mountain virus strain and we can detect 2.5 µg/ml of VLPs. This is the current limit of detection. All studies were performed in duplicate.

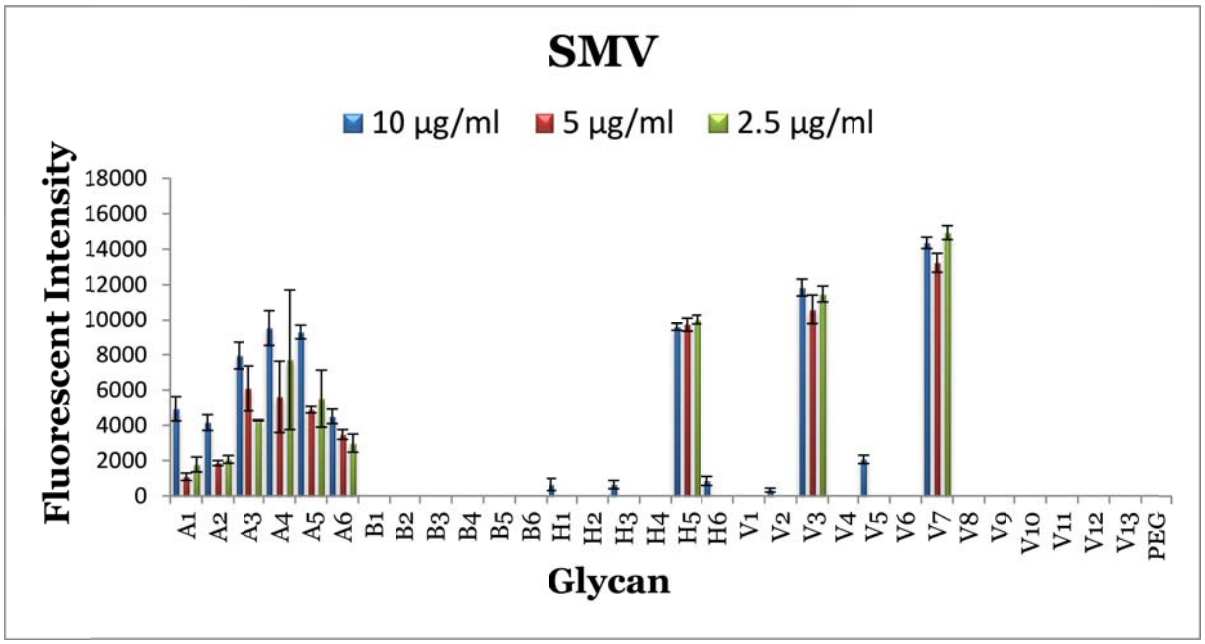

Figure 2.9 Different concentrations of SMV VLPs binding pattern with HBGAs

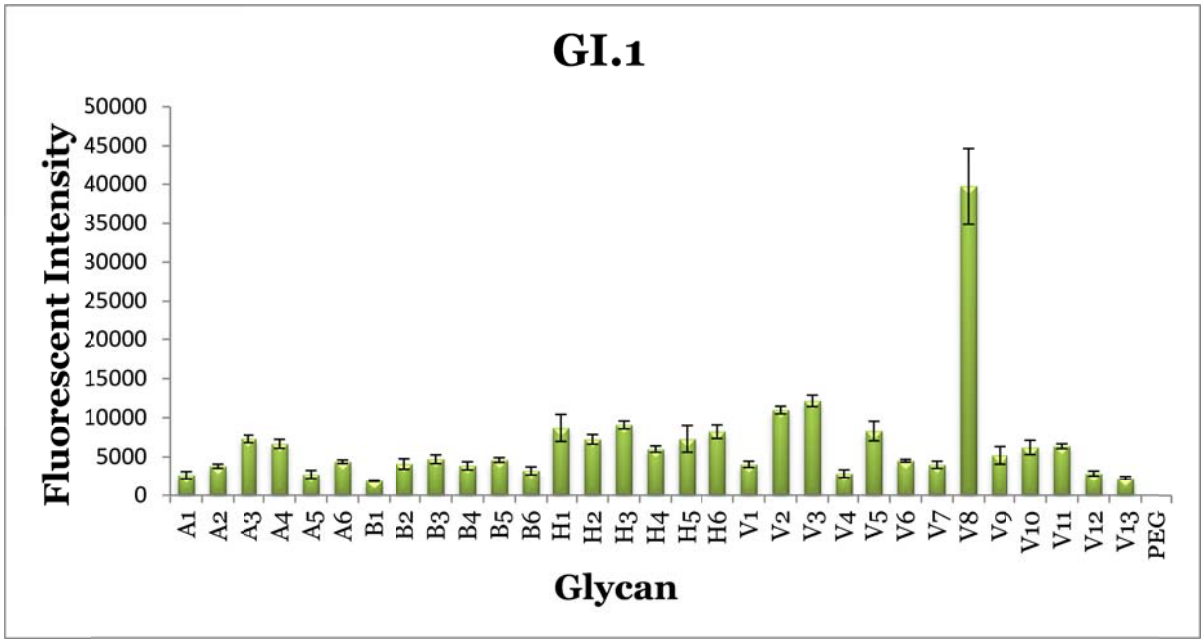

Figure 2.10 GI.1 VLPs binding pattern with HBGAs

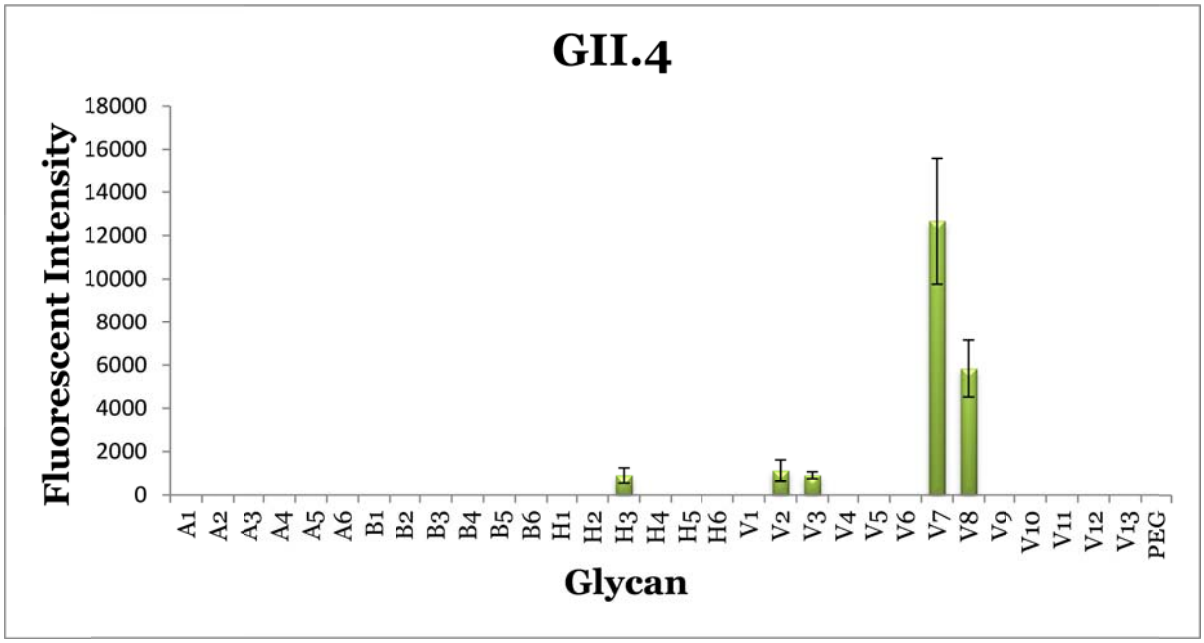

Figure 2.11 GII.4 VLPs binding pattern with HBGAs

Fluorescence detection of SMV, GI.1 and GII.4 New Orleans strains using synthetic glycans. Glycans and PEG (negative control) were printed at 200μM. VLP concentration was 10 ug/mL. Fluorescence intensity

was measured by the Genepix scanner using mouse (or rabbit) sera to the respective strain and anti-mouse or anti rabbit rhodamine labeled antibody was scanned at 532nm. The experiments were performed in duplicate.

The SMV VLP shows high binding affinity with H5, V3, and V7 glycans in three different concentrations. The fluorescent intensity was not decreased when the VLP concentration was reduced. This indicates that SMV VLP have strong binding affinity with H5, V3 and V7. All of Blood Group Antigens A types shows binding with SMV VLP. But the fluorescent intensity was decreased when the concentration was reduced. This indicates that the A type antigen can bind with SMV VLP, but the binding affinity is weak, once the VLP concentration decreased, the glycan cannot capture enough VLP to represent the fluorescent signal.

GI.1 shows the binding affinity with the entire glycan library except the negative control, however, the binding is weak except V8. GII.4 shows strong binding with V7 and weak binding with V8.

2.2.2 Microarray results with virus from stool suspensions

We performed the same assays with the actual viruses, namely GI.1. Norwalk, GII.2 Snow Mountain (SMV) and GII.4 New Orleans strains obtained from human challenge studies The results are shown in Figure 2.12-2.14. Our first studies were with SMV viruses and it was gratifying to observe that the binding pattern for the virus mirrors that of the SMV VLPs. We tested at different concentrations and found that glycans capture the virus at very low titers. We also found that stool samples without SMV virus did not bind to any of the glycans, which was as expected.

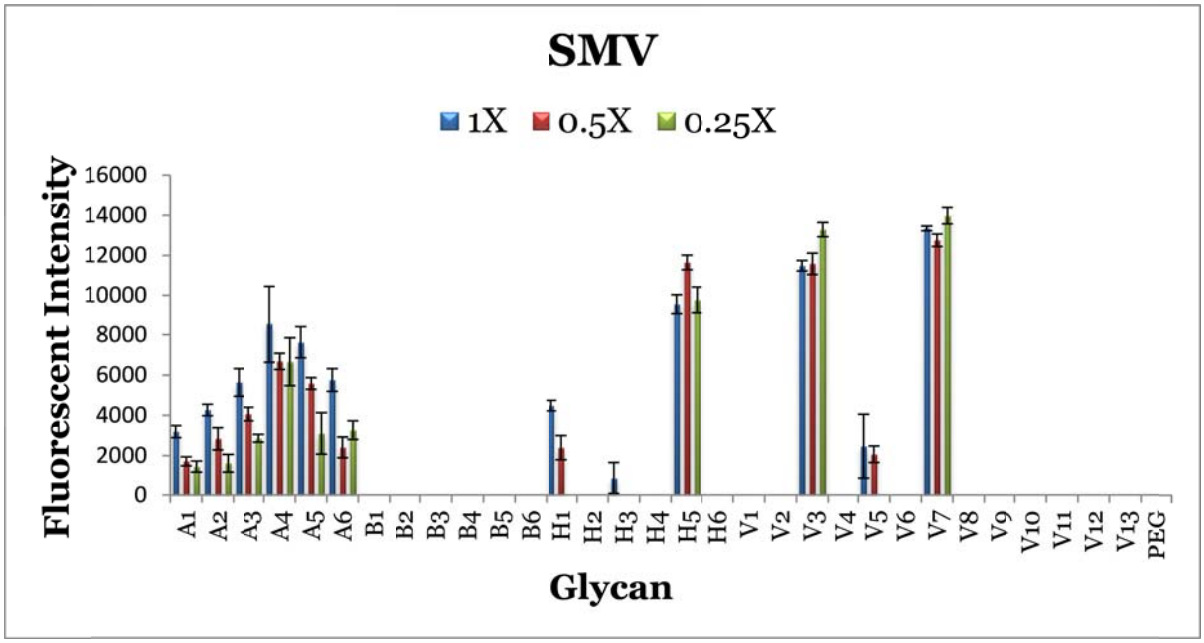

Figure 2.12 SMV stool sample binding pattern with HBGAs

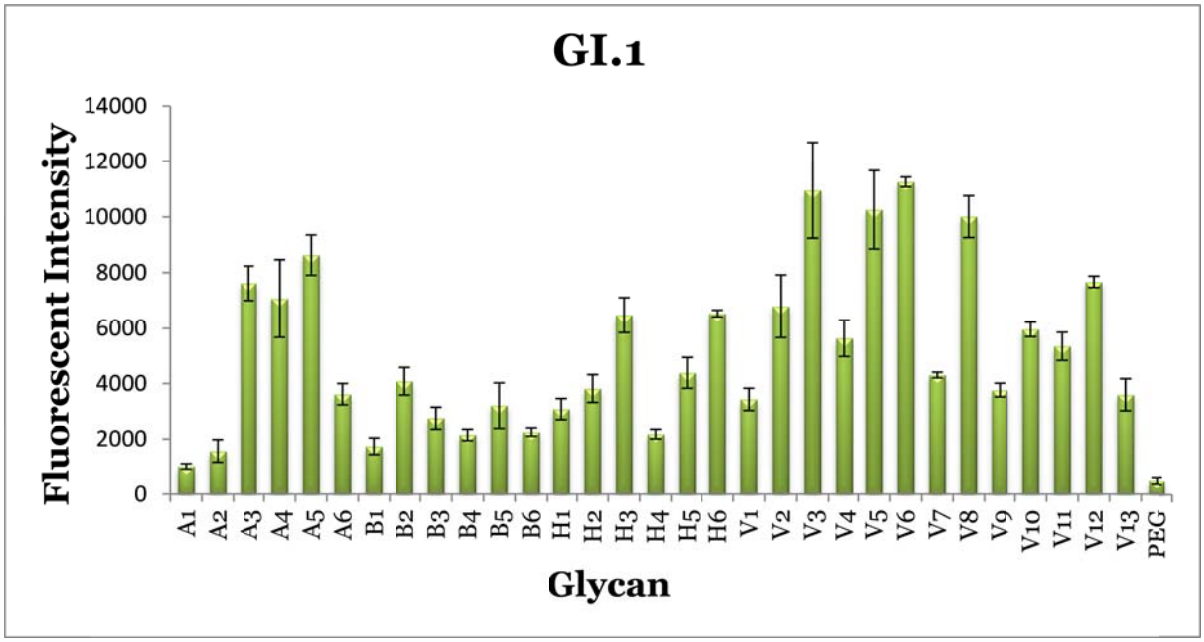

Figure 2.13 GI.1 stool sample binding pattern with HBGAs

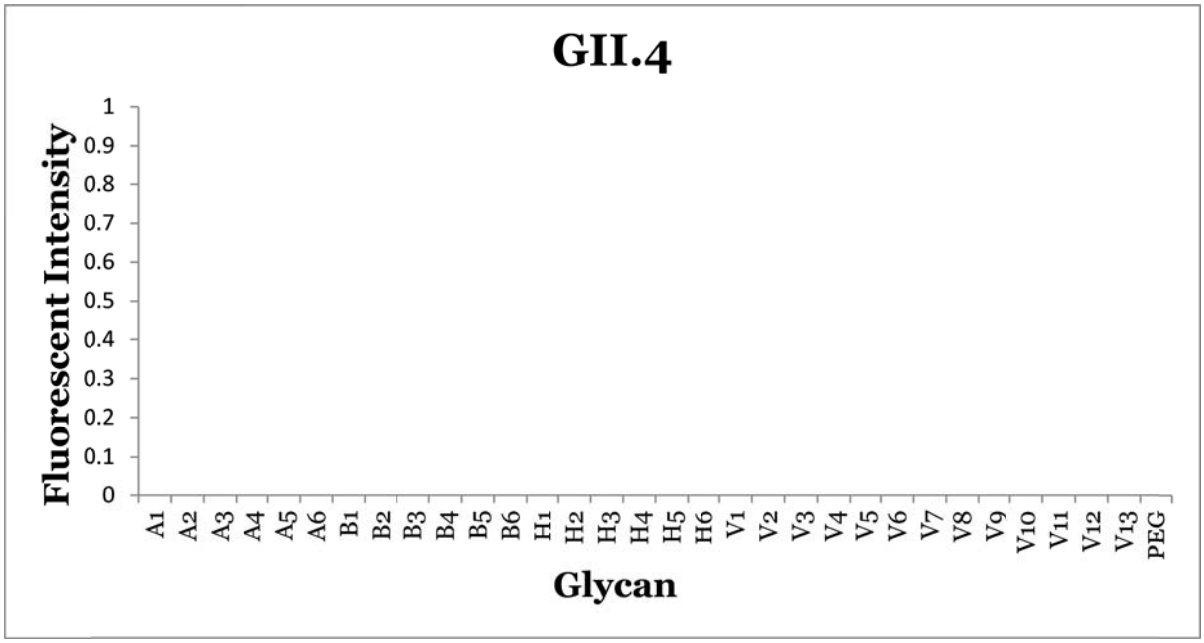

Figure 2.14 GII.4 stool sample binding pattern with HBGAs

Fluorescence detection of SMV, GI.1 and GII.4 New Orleans strains using synthetic glycans. Glycans and PEG (negative control) were printed at 200μM. Fluorescence intensity was measured by the Genepix scanner using mouse (or rabbit) sera to the respective strain, and anti-mouse or anti rabbit rhodamine labeled antibody was scanned at 532nm. The experiments were performed in duplicate.

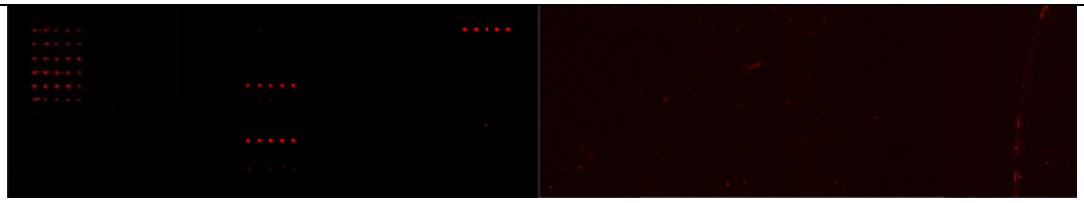

Figure 2.15 Microarray scanner picture of SMV virus with HBGAs

Left: Fluorescence image of microarray containing 32 glycans with 5 spots each, after exposure to SMV strain, followed by mouse primary and anti-anti- mouse rhodamine labeled secondary antibody scanned

by Genepix scanner at 532 nm. Rignt: Fluorescence image of Stool supernatant with no virus. As expected, there was no nonspecific binding.

Testing with Norwalk virus and the NO strains was also performed. Unlike the SMV strain, the Norwalk and NO virus strains did not behave like their respective VLPs, the patterns were very different. We tested these strains with antibodies from different sources and the results varied depending on the source of the VLPs used to generate the antibodies.

2.2.3 Summary of the glycan microarray results

A library of synthetic analogs of Histo Blood Group Antigens conjugated to BSA was printed onto commercial glass slides. VLPs and intact virus samples were screened for binding using the focused microarrays. The binding patterns for the VLP's (GI.1 Norwalk, GII.2 Snow Mountain and GII.4 New Orleans) are very different and unique. This indicates that a pattern of recognition could be used to type each strain. We also performed the same assays with intact virus. The SMV virus shows same binding pattern with SMV VLP. The stool sample without SMV shows no binding with any glycans. The binding of GI.1 and GII.4 shows very different pattern with VLPs. We tested these strains with antibodies from different sources and the results varied depending on the source of the VLPs used to generate the antibodies. Antibodies generated against VLPs may not recognize the actual virus, which could be one of the reasons why antibody based lateral flow assays are not highly sensitive and/or selective. Our approach to overcome this problem is using synthetic glycans as reporters because noroviruses have multiple protein receptors that bind to HBGA glycans and therefore, one can envision capture and report with glycans. While we obtained excellent results for one strain, the binding pattern for two other strains did not match the binding pattern of the respective VLPs. There could be a number of

reasons for these differences. First, antibodies generated using VLPs may not recognize the intact virus. Second, soluble glycans may be present in stool samples that inhibit the binding of the virus to the glycan microarray. Third, the sample preparation process may result in result in virus destruction. In the next section, we used a non-labeling technique i.e. SPR (Surface Plasmon Resonance) to ascertain if antibodies were the issue or matrix issues contributed to the differences between VLPs and viruses.

2.3 SPR Detection for Norovirus

2.3.1 SPR Introduction

Surface plasmon resonance (SPR) has been widely used to detect biological and chemical analytes. [93] In our case, the glycan is immobilized on a sensor surface and another analyte flows pass the surface. The SPR angle is monitored when the analyte flows pass by, the change of the SPR angle is detected to determine the interaction of the analyte. The concentration of glycan and analyte can be controlled and the results can be monitored in real time as it is a flow technique. Since SPR technology is a label free technique, it is a great tool to avoid the analyte labeling issue. Here, we used SPR to detect Histo Blood Groups Antigens binding affinity with norovirus VLPs and one strain of norovirus

Three biotinylated glycans were synthesized for SPR studies. The syntheses of these glycans will be published elsewhere. The structures of these glycans are shown in Figure 2.16. The biotin allows for facile conjugation to streptavidin coated sensor chips.

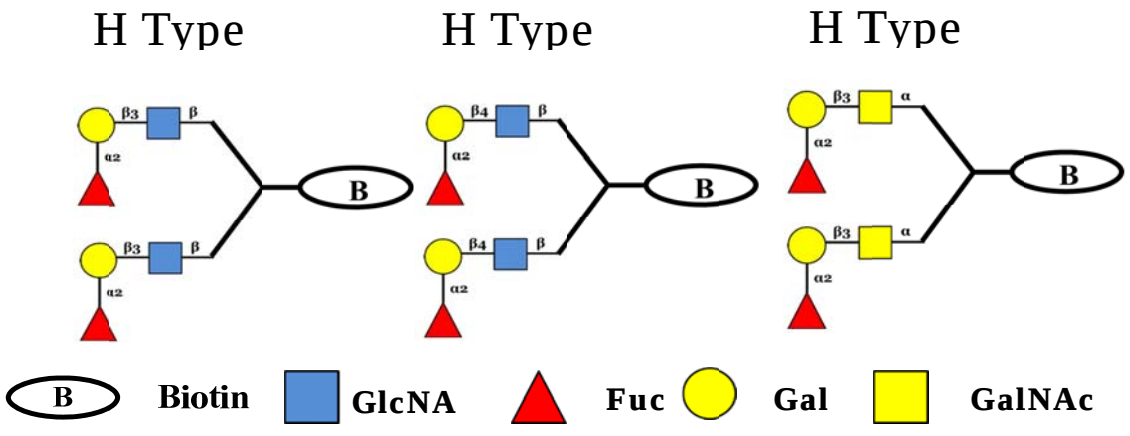

Figure 2.16 Structures of the synthetic biotinylated glycans for reporter molecules

2.3.2 Results and Discussion

The streptavidin coated Biacore microfluidics sensor chip SA was prepared following manufacturer protocols. Briefly,four biotinylated ligands (H type I, II, III and the biotinylated PEG) were coated onto four channels of a streptavidin coated biosensor chip as different ligand densities. Next, VLPs from different strains were introduced onto the sensor to determine the relative binding affinities.

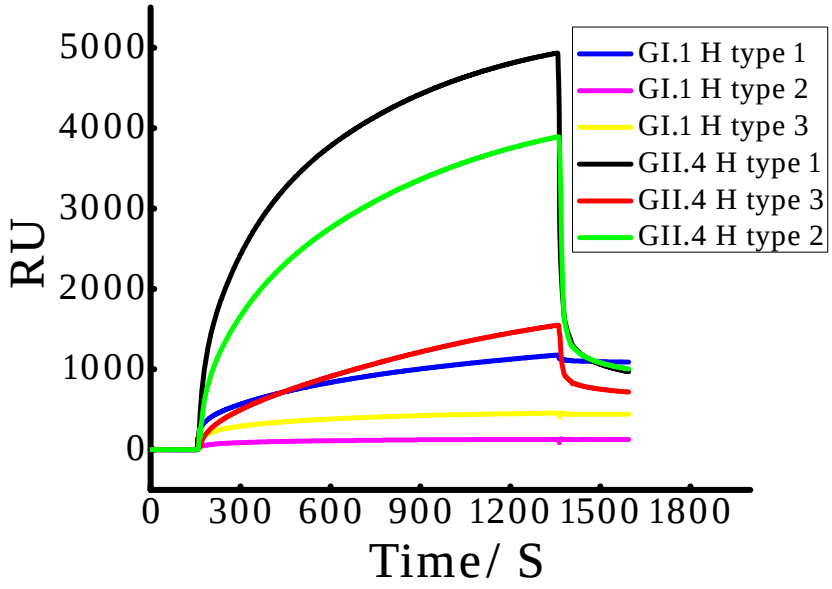

Figure 2.17 Example of a sensogram to determine relative binding affinities of the glycans**.** Two different VLPs, G1.1 and GII.4 were used in these sets of experiments and the sensor surface had a high density of ligands. SPR binding is expressed in response unit (RU). The chemical structures of HBGAs immobilized on the SPR surfaces are indicated.

For the initial test, we immobilized H type I, H type II and H type III at 10ug/ml for 7 mins with the flow rate of 10 µl/min. The glycans have been successfully immobilized on the sensor chip SA, and gives an increase in relative refraction units (RU) of 800.3 (H type I), 759.9 (H type II), and 630.8(H type III), respectively. Surface performance test indicates that the glycan is stable and couldn't be removed by the PBS buffer flow. 10µg/ml of GI.1 VLPs or GII.4 VLPs was injected over the sensor chip SA at the flow rate of 5 µl/min for 20 min. The binding was monitored as increasing relative RU. The result shows that GI.1 VLPs has strong binding affinity with H type I which gives the increased RU of 1177.1. H type II and H type III shows weak binding affinity and gives the increased RU of 128.5 and 455.9, respectively. This indicated that H type I could be used to capture GI.1 VLPs. The GII.4 shows higher binding affinity compare to GI.1 VLPs with those glycans as shown in figure 2.19. H type I shows the highest binding and gives the increased RU as 4935.4, H type II and H type III gives the increased RU of 1548.8 and 3891.1 respectively. Taken together, H type I is a suitable glycan to capture GI.1 and GII.4 VLPs. It is also clear from the sensograms that GII.4 binds with a higher affinity to the glycans than G1.1. We tried to regenerate the sensor chipsusing a variety of conditions to obtain binding affinity constants. Unfortunately, we were unsuccessful in removing the VLPs without destroying the glycan coated surface, which indicates that the binding is very strong.

Therefore, we decided to reduce the glycan density (Figure 2.20). When the ligand densities are high, the VLPs bound extremely tightly. In contrast, when the ligand density is reduced, the VLPs do not bind tightly and therefore we can regenerate the surface. To successfully regenerate the glycan surface of sensor chips, we decreased the contact time of immobilization process. 10µg/ml glycans is immobilized for 30s with the flow rate of 10 µl/min

on the sensor chip SA, and gives an increase in relative refraction units (RU) of 160.3 (H type I), 163.4 (H type II), and 168.9 (H type III), respectively. The low intensive immobilization gives lower RU change as shown in Figure 2.18. We were able to obtain apparent K_D's for the GI.1 (Figure 2.19) using low densities of the ligands. The apparent K_D for GII.4 cannot be accurately determined as we have reached the highest concentration of VLPs before it precipitates out of solution, but it is > 27 nM.

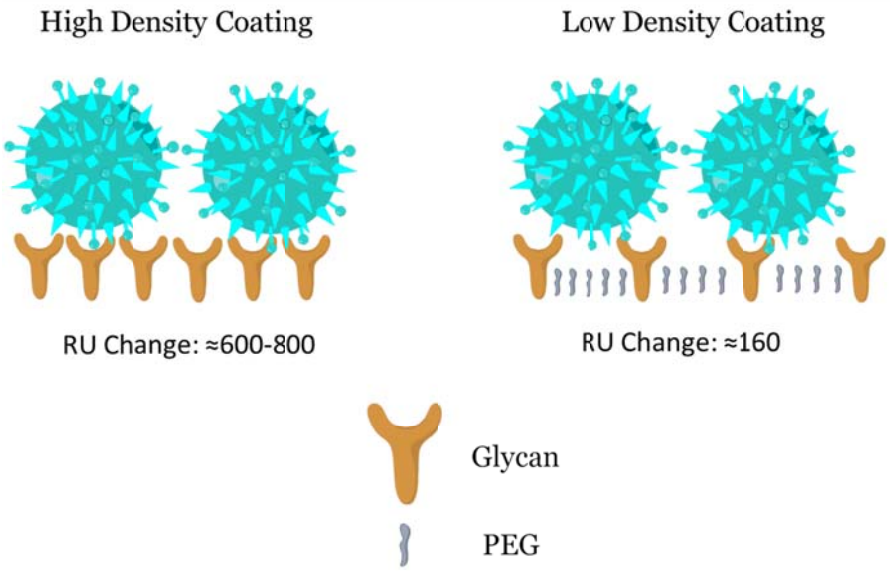

Figure 2.18 Demonstration of high density coating VS low density coating

Left: high density coating. Right: low density coating.

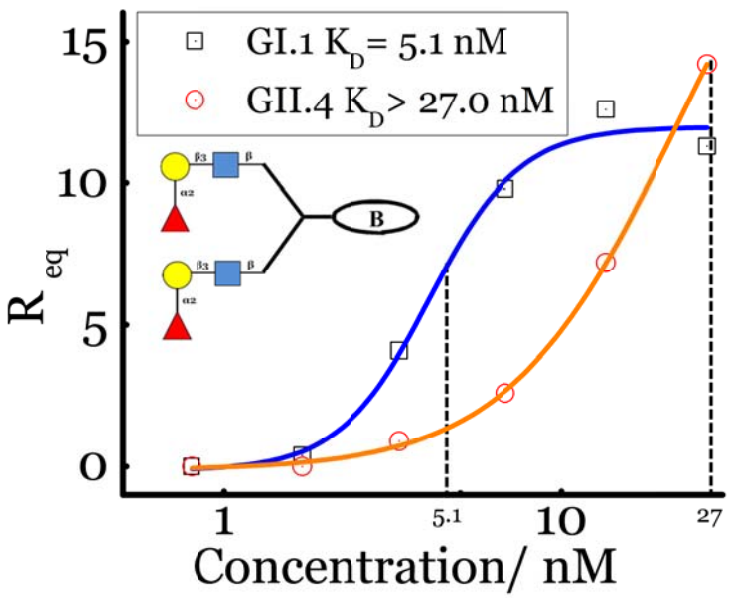

Figure 2.19 Plot of the R_{eq} versus concentration of VLPs for H type I glycan and two different VLPs at low ligand densities.

The apparent K_D for GII.4 cannot be accurately determined as we have reached the highest concentration of VLPs before it precipitates out of solution, but it is > 27 nM.

Next, we tested intact virus for binding with the immobilized glycans. When we used G1.1 virus, we found no response change (data not shown), indicating that there is no binding. Since this result is similar to that of the microarray, this indicates that the antibodies may not be a problem but that matrix issues abrogate binding. However, we cannot exclude that the filtration of the stool sample to remove particulate matter did not remove the virus and we are currently testing the filtrate and the residue for presence of the pathogen. These studies are ongoing.

2.3.3 Summary and Future Work

In this chapter, we developed a focused microarray for the detection of norovirus strains. We envisioned a "fingerprint" pattern for each strain. This strategy works well when VLPs are tested. However, when viruses are tested, matrix effects play a major role. Unfortunately, the virus cannot be cultivated in vitro, which poses problems for the study of this virus as we have to rely on human challenge studies for obtaining the virus, which is obtained as a stool suspension. We are currently exploring other methods to detect this virus.

2.3.4 Experiment section

2.3.4.1 Immobilization of Glycans

Synthetic glycans were covalently immobilized onto Nexterion® NHS slides using DIGILAB Omnigrid Micro printer in 300 mM phosphate buffer with 0.005% Tween-20 at pH 8.5. Each glycan was printed twenty times in quintuplicate at 200 μM concentration. Following printing, the glycans were allowed to react for 30 min at 60% humidity. After overnight desiccation, the slides were blocked for 60 min with 50 mM ethanolamine in 50 mM boric acid buffer (pH 9.5), washed 3 times with deionized (DI) water, dried and stored at -20°C.

2.3.4.2 Virus Binding Assay

To determine binding pattern of detection, a serial double fold dilution was performed for SMV VLP. GI.1 and GII.4 were tested with a constant concentration (10μg/ml). The concentration of SMV VLP was tested from 10μg/ml. Each concentration of virus was applied to the microarray for 60 min in a buffer consisting of PBS and 0.05% Tween-20. Post-virus incubation and wash (three times with PBS and 0.05% Tween-20 and two times with PBS), antibodies specific to each virus were diluted and added to the microarray for 60 min. Slides

were washed as previously described above and incubated for 60 min with the appropriate fluorescently tagged secondary antibodies. The slides were washed as described above, followed by a DI water rinse. The slides were dried and scanned using the GenePix®4000B scanner. All experiments were performed in triplicate.

2.3.4.3 SPR studies

Binding of VLPs to biotinylated glcyans was measured using a BIACORE T200 instrument (GE Healthcare). Biotinylated glycoconjugates were injected over streptavidin-coated SA sensor chips (GE Healthcare) at 10 μL min^{-1}. A reference flow cell was used to record the background response, and background was subtracted from each sample. Biotinylated PEG was used as the reference. The running buffer used in all experiments was PBS buffer (pH 7.4). All SPR experiments were performed at room temperature. VLPs were injected over the chip at 5 μL min^{-1} for 20 min. Binding was detected as a change in the refractive index at the surface of the chip as measured by response units (RU). Data analysis was carried out using BIA evaluation 3.0 software.

REFERENCES

1. Fiore, A. E.; Shay, D. K.; Broder, K.; Iskander, J. K.; Uyeki, T. M.; Mootrey, G.; Bresee, J. S.; Cox, N. J., Prevention and control of seasonal influenza with vaccines: recommendations of the Advisory Committee on Immunization Practices *MMWR Recomm. Rep.* **2009,** *58* (8), 1-52.

2. Yuen, K. Y.; Wong, S. S., Human infection by avian influenza A H5N1. *Hong Kong Med. J.* **2005,** *11* (3), 189-99.

3. Jamieson, D. J.; Honein, M. A.; Rasmussen, S. A.; Williams, J. L.; Swerdlow, D. L.; Biggerstaff, M. S.; Lindstrom, S.; Louie, J. K.; Christ, C. M.; Bohm, S. R.; Fonseca, V. P.; Ritger, K. A.; Kuhles, D. J.; Eggers, P.; Bruce, H.; Davidson, H. A.; Lutterloh, E.; Harris, M. L.; Burke, C.; Cocoros, N.; Finelli, L.; MacFarlane, K. F.; Shu, B.; Olsen, S. J.; Novel Influenza, A. P. W. G., H1N1 2009 influenza virus infection during pregnancy in the USA. *Lancet* **2009,** *374* (9688), 451-8.

4. Hara, K., Report on Options for the Control of Influenza Virus IV. *Uirusu* **2000,** *50* (2), 331-6.

5. Von Itzstein, M., The war against influenza: discovery and development of sialidase inhibitors. *Nat. Rev. Drug Discovery* **2007,** *6* (12), 967-74.

6. Noah, D. L.; Krug, R. M., Influenza virus virulence and its molecular determinants. *Adv. Virus. Res.* **2005,** *65*, 121-45.

7. Couceiro, J. N.; Paulson, J. C.; Baum, L. G., Influenza virus strains selectively recognize sialyloligosaccharides on human respiratory epithelium; the role of the host cell in selection of hemagglutinin receptor specificity. *Virus Res.* **1993,** *29* (2), 155-65.

8. Matrosovich, M.; Klenk, H. D., Natural and synthetic sialic acid-containing inhibitors of influenza virus receptor binding. *Rev. Med. Virol.* **2003,** *13* (2), 85-97.

9. Huang, Q.; Sivaramakrishna, R. P.; Ludwig, K.; Korte, T.; Bottcher, C.; Herrmann, A., Early steps of the conformational change of influenza virus hemagglutinin to a fusion active state: stability and energetics of the hemagglutinin. *Biochim. Biophys. Acta* **2003,** *1614* (1), 3-13.

10. Skehel, J. J.; Wiley, D. C., Receptor binding and membrane fusion in virus entry: the influenza hemagglutinin. *Annu. Rev. Biochem.* **2000,** *69*, 531-69.

11. Buchy, P.; Mardy, S.; Vong, S.; Toyoda, T.; Aubin, J. T.; Miller, M.; Touch, S.; Sovann, L.; Dufourcq, J. B.; Richner, B.; Tu, P. V.; Tien, N. T.; Lim, W.; Peiris, J. S.; Van der Werf, S., Influenza A/H5N1 virus infection in humans in Cambodia. *J. Clin. Virol.* **2007,** *39* (3), 164-8.

12. Gambaryan, A.; Tuzikov, A.; Pazynina, G.; Bovin, N.; Balish, A.; Klimov, A., Evolution of the receptor binding phenotype of influenza A (H5) viruses. *Virology* **2006,** *344* (2), 432-8.

13. Samji, T., Influenza A: understanding the viral life cycle. *Yale J. Biol. Med.* **2009,** *82* (4), 153-9.

14. Pinto, L. H.; Lamb, R. A., The M2 proton channels of influenza A and B viruses. *J. Biol. Chem.* **2006,** *281* (14), 8997-9000.

15. Colman, P. M.; Ward, C. W., Structure and diversity of influenza virus neuraminidase. *Curr. Top. Microbiol. Immunol.* **1985,** *114*, 177-255.

16. Harris, A.; Cardone, G.; Winkler, D. C.; Heymann, J. B.; Brecher, M.; White, J. M.; Steven, A. C., Influenza virus pleiomorphy characterized by cryoelectron tomography. *PNAS* **2006,** *103* (50), 19123-19127.

17. Air, G. M.; Laver, W. G., The neuraminidase of influenza virus. *Proteins* **1989,** *6* (4), 341-56.

18. Shidmoossavee, F. S.; Watson, J. N.; Bennet, A. J., Chemical Insight into the Emergence of Influenza Virus Strains That Are Resistant to Relenza. *J. Am. Chem. Soc.* **2013,** *135* (36), 13254-13257.

19. Schnell, J. R.; Chou, J. J., Structure and mechanism of the M2 proton channel of influenza A virus. *Nature* **2008,** *451* (7178), 591-5.

20. Sugrue, R. J.; Hay, A. J., Structural characteristics of the M2 protein of influenza A viruses: evidence that it forms a tetrameric channel. *Virology* **1991,** *180* (2), 617-24.

21. (a) Pinto, L. H.; Holsinger, L. J.; Lamb, R. A., Influenza-Virus M2 Protein Has Ion Channel Activity. *Cell* **1992,** *69* (3), 517-528; (b) Tang, Y.; Zaitseva, F.; Lamb, R. A.; Pinto, L. H., The gate of the influenza virus M2 proton channel is formed by a single tryptophan residue. *J. Biol. Chem.* **2002,** *277* (42), 39880-6.

22. (a) Pinto, L. H.; Dieckmann, G. R.; Gandhi, C. S.; Papworth, C. G.; Braman, J.; Shaughnessy, M. A.; Lear, J. D.; Lamb, R. A.; DeGrado, W. F., A functionally defined model for the M2 proton channel of influenza A virus suggests a mechanism for its ion selectivity. *P Natl Acad Sci USA* **1997,** *94* (21), 11301-6; (b) Wang, J.; Kim, S.; Kovacs, F.; Cross, T. A., Structure of the transmembrane region of the M2 protein H(+) channel. *Protein Sci.* **2001,** *10* (11), 2241-50.

23. Boivin, S.; Cusack, S.; Ruigrok, R. W.; Hart, D. J., Influenza A virus polymerase: structural insights into replication and host adaptation mechanisms. *J. Biol. Chem.* **2010,** *285* (37), 28411-7.

24. Zurcher, T.; de la Luna, S.; Sanz-Ezquerro, J. J.; Nieto, A.; Ortin, J., Mutational analysis of the influenza virus A/Victoria/3/75 PA protein: studies of interaction with PB1 protein and identification of a dominant negative mutant. *J. Gen. Virol.* **1996,** *77 (Pt 8)*, 1745-9.

25. Drake, J. W., Rates of spontaneous mutation among RNA viruses. *P Natl Acad Sci USA* **1993,** *90* (9), 4171-5.

26. Miotto, O.; Heiny, A. T.; Albrecht, R.; Garcia-Sastre, A.; Tan, T. W.; August, J. T.; Brusic, V., Complete-proteome mapping of human influenza A adaptive mutations: implications for human transmissibility of zoonotic strains. *PloS one* **2010,** *5* (2), e9025.

27. (a) Obayashi, E.; Yoshida, H.; Kawai, F.; Shibayama, N.; Kawaguchi, A.; Nagata, K.; Tame, J. R. H.; Park, S. Y., The structural basis for an essential subunit interaction in influenza virus RNA polymerase. *Nature* **2008,** *454* (7208), 1127-U57; (b) Sugiyama, K.; Obayashi, E.; Kawaguchi, A.; Suzuki, Y.; Tame, J. R. H.; Nagata, K.; Park, S. Y., Structural insight into the essential PB1-PB2 subunit contact of the influenza virus RNA polymerase. *EMBO J.* **2009,** *28* (12), 1803-1811.

28. Resa-Infante, P.; Jorba, N.; Coloma, R.; Ortin, J., The influenza virus RNA synthesis machine: advances in its structure and function. *RNA Biol.* **2011,** *8* (2), 207-15.

29. Neumann, G.; Brownlee, G. G.; Fodor, E.; Kawaoka, Y., Orthomyxovirus replication, transcription, and polyadenylation. *Curr. Top. Microbiol. Immunol.* **2004,** *283*, 121-43.

30. (a) Rodriguez, A.; Perez-Gonzalez, A.; Nieto, A., Influenza virus infection causes specific degradation of the largest subunit of cellular RNA polymerase II. *J. Virol.* **2007,** *81* (10), 5315-24; (b) Fodor, E.; Crow, M.; Mingay, L. J.; Deng, T.; Sharps, J.; Fechter, P.; Brownlee, G. G., A single amino acid mutation in the PA subunit of the influenza virus RNA polymerase inhibits endonucleolytic cleavage of capped RNAs. *J. Virol.* **2002,** *76* (18), 8989-9001.

31. (a) Dias, A.; Bouvier, D.; Crepin, T.; McCarthy, A. A.; Hart, D. J.; Baudin, F.; Cusack, S.; Ruigrok, R. W., The cap-snatching endonuclease of influenza virus polymerase resides in the PA subunit. *Nature* **2009,** *458* (7240), 914-8; (b) Yuan, P.; Bartlam, M.; Lou, Z.; Chen, S.; Zhou,

J.; He, X.; Lv, Z.; Ge, R.; Li, X.; Deng, T.; Fodor, E.; Rao, Z.; Liu, Y., Crystal structure of an avian influenza polymerase PA(N) reveals an endonuclease active site. *Nature* **2009,** *458* (7240), 909-13.

32. Datta, K.; Wolkerstorfer, A.; Szolar, O. H.; Cusack, S.; Klumpp, K., Characterization of PA-N terminal domain of Influenza A polymerase reveals sequence specific RNA cleavage. *Nucleic Acids Res.* **2013,** *41* (17), 8289-99.

33. Poole, E. L.; Medcalf, L.; Elton, D.; Digard, P., Evidence that the C-terminal PB2-binding region of the influenza A virus PB1 protein is a discrete alpha-helical domain. *FEBS Lett.* **2007,** *581* (27), 5300-5306.

34. Chu, C.; Fan, S.; Li, C.; Macken, C.; Kim, J. H.; Hatta, M.; Neumann, G.; Kawaoka, Y., Functional analysis of conserved motifs in influenza virus PB1 protein. *PloS one* **2012,** *7* (5), e36113.

35. Graef, K. M.; Vreede, F. T.; Lau, Y. F.; McCall, A. W.; Carr, S. M.; Subbarao, K.; Fodor, E., The PB2 subunit of the influenza virus RNA polymerase affects virulence by interacting with the mitochondrial antiviral signaling protein and inhibiting expression of beta interferon. *J. Virol.* **2010,** *84* (17), 8433-45.

36. Almond, J. W., A single gene determines the host range of influenza virus. *Nature* **1977,** *270* (5638), 617-8.

37. (a) Engelhardt, O. G.; Fodor, E., Functional association between viral and cellular transcription during influenza virus infection. *Rev. Med. Virol.* **2006,** *16* (5), 329-345; (b) Guilligay, D.; Tarendeau, F.; Resa-Infante, P.; Coloma, R.; Crepin, T.; Sehr, P.; Lewis, J.; Ruigrok, R. W.; Ortin, J.; Hart, D. J.; Cusack, S., The structural basis for cap binding by influenza virus polymerase subunit PB2. *Nat. Struct. Mol. Biol.* **2008,** *15* (5), 500-6.

38. Carr, S. M.; Carnero, E.; Garcia-Sastre, A.; Brownlee, G. G.; Fodor, E., Characterization of a mitochondrial-targeting signal in the PB2 protein of influenza viruses. *Virology* **2006,** *344* (2), 492-508.

39. (a) Kilby, J. M.; Eron, J. J., Novel therapies based on mechanisms of HIV-1 cell entry. *N. Engl. J. Med.* **2003,** *348* (22), 2228-38; (b) Hattori, T.; Zhang, X.; Weiss, C.; Xu, Y.; Kubo, T.; Sato, Y.; Nishikawa, S.; Sakaida, H.; Uchiyama, T., Triazine dyes inhibit HIV-1 entry by binding to envelope glycoproteins. *Microbiol. Immunol.* **1997,** *41* (9), 717-24; (c) Didigu, C. A.; Doms, R. W., Novel approaches to inhibit HIV entry. *Viruses* **2012,** *4* (2), 309-24.

40. Quarles, J. M.; Couch, R. B.; Cate, T. R.; Goswick, C. B., Comparison of amantadine and rimantadine for prevention of type A (Russian) influenza. *Antiviral Res.* **1981,** *1* (3), 149-55.

41. Kaiser, L.; Crump, C. E.; Hayden, F. G., In vitro activity of pleconaril and AG7088 against selected serotypes and clinical isolates of human rhinoviruses. *Antiviral Res.* **2000,** *47* (3), 215-20.

42. Bodian, D. L.; Yamasaki, R. B.; Buswell, R. L.; Stearns, J. F.; White, J. M.; Kuntz, I. D., Inhibition of the Fusion-Inducing Conformational Change of Influenza Hemagglutinin by Benzoquinones and Hydroquinones. *Biochemistry* **1993,** *32* (12), 2967-2978.

43. (a) Boulter, E. A.; Thornton, B.; Bauer, D. J.; Bye, A., Successful treatment of experimental B virus (Herpesvirus simiae) infection with acyclovir. *Br. Med. J.* **1980,** *280* (6215), 681-3; (b) Bean, B., Acyclovir in the treatment of herpesvirus infections. *Postgrad. Med.* **1983,** *73* (3), 297-303.

44. (a) Navarrete, M. S.; Castelo, A., Zidovudine (ZDV) and Lamivudine (3TC) Combination Therapy for HIV Infection - A Review. *Braz. J. Infect. Dis.* **1998,** *2* (1), 1-9; (b)

Bhana, N.; Ormrod, D.; Perry, C. M.; Figgitt, D. P., Zidovudine: a review of its use in the management of vertically-acquired pediatric HIV infection. *Paediatr Drugs.* **2002,** *4* (8), 515-53.

45. (a) Bai, J.; Rossi, J.; Akkina, R., Multivalent anti-CCR ribozymes for stem cell-based HIV type 1 gene therapy. *AIDS Res. Hum. Retroviruses* **2001,** *17* (5), 385-99; (b) McCaffrey, A. P.; Meuse, L.; Karimi, M.; Contag, C. H.; Kay, M. A., A potent and specific morpholino antisense inhibitor of hepatitis C translation in mice. *Hepatology* **2003,** *38* (2), 503-8; (c) Deas, T. S.; Binduga-Gajewska, I.; Tilgner, M.; Ren, P.; Stein, D. A.; Moulton, H. M.; Iversen, P. L.; Kauffman, E. B.; Kramer, L. D.; Shi, P. Y., Inhibition of flavivirus infections by antisense oligomers specifically suppressing viral translation and RNA replication. *J. Virol.* **2005,** *79* (8), 4599-609.

46. Pielak, R. M.; Schnell, J. R.; Chou, J. J., Mechanism of drug inhibition and drug resistance of influenza A M2 channel. *P Natl Acad Sci USA* **2009,** *106* (18), 7379-84.

47. Davies, W. L.; Grunert, R. R.; Haff, R. F.; McGahen, J. W.; Neumayer, E. M.; Paulshock, M.; Watts, J. C.; Wood, T. R.; Hermann, E. C.; Hoffmann, C. E., Antiviral Activity of 1-Adamantanamine (Amantadine). *Science* **1964,** *144* (3620), 862-3.

48. Edmond, J. D.; Johnston, R. G.; Kidd, D.; Rylance, H. J.; Sommerville, R. G., The inhibition of neuraminidase and antiviral action. *Br. J. Pharmacol. Chemother.* **1966,** *27* (2), 415-26.

49. Babu, Y. S.; Chand, P.; Bantia, S.; Kotian, P.; Dehghani, A.; El-Kattan, Y.; Lin, T. H.; Hutchison, T. L.; Elliott, A. J.; Parker, C. D.; Ananth, S. L.; Horn, L. L.; Laver, G. W.; Montgomery, J. A., BCX-1812 (RWJ-270201): Discovery of a novel, highly potent, orally active, and selective influenza neuraminidase inhibitor through structure-based drug design. *J Med Chem* **2000,** *43* (19), 3482-3486.

50. Burnham, A. J.; Baranovich, T.; Govorkova, E. A., Neuraminidase inhibitors for influenza B virus infection: efficacy and resistance. *Antiviral Res.* **2013,** *100* (2), 520-34.

51. Okomo-Adhiambo, M.; Sheu, T. G.; Gubareva, L. V., Assays for monitoring susceptibility of influenza viruses to neuraminidase inhibitors. *Influenza and other respiratory viruses* **2013,** *7 Suppl 1*, 44-9.

52. Nayak, D. P.; Reichl, U., Neuraminidase activity assays for monitoring MDCK cell culture derived influenza virus. *J. Virol. Methods* **2004,** *122* (1), 9-15.

53. Balish, A.; Warnes, C. M.; Wu, K.; Barnes, N.; Emery, S.; Berman, L.; Shu, B.; Lindstrom, S.; Xu, X.; Uyeki, T.; Shaw, M.; Klimov, A.; Villanueva, J., Evaluation of Rapid Influenza Diagnostic Tests for Detection of Novel Influenza A (H1N1) Virus-United States. *Jama-J Am Med Assoc* **2009,** *302* (11), 1163-1164.

54. Beck, E.; Fan, J.; Hendrickson, K.; Kumar, S.; Shively, R.; Kramp, W.; Villanueva, J.; Jernigan, D.; Klimov, A.; Chen, L.-M.; Donis, R.; Williams, T.; Pirkle, J.; Barr, J., Evaluation of 11 commercially available rapid influenza diagnostic tests--United States, 2011-2012. *MMWR Morb Mortal Wkly Rep, Centers for Disease Control and Prevention,* **2012,** *61* (43), 873-6.

55. (a) Fukui, S.; Feizi, T.; Galustian, C.; Lawson, A. M.; Chai, W., Oligosaccharide microarrays for high-throughput detection and specificity assignments of carbohydrate-protein interactions. *Nat. Biotechnol.* **2002,** *20* (10), 1011-7; (b) Wang, D.; Liu, S.; Trummer, B. J.; Deng, C.; Wang, A., Carbohydrate microarrays for the recognition of cross-reactive molecular markers of microbes and host cells. *Nat. Biotechnol.* **2002,** *20* (3), 275-81; (c) Willats, W. G.; Rasmussen, S. E.; Kristensen, T.; Mikkelsen, J. D.; Knox, J. P., Sugar-coated microarrays: a novel slide surface for the high-throughput analysis of glycans. *Proteomics* **2002,** *2* (12), 1666-71.

56. Schena, M.; Shalon, D.; Davis, R. W.; Brown, P. O., Quantitative monitoring of gene expression patterns with a complementary DNA microarray. *Science* **1995,** *270* (5235), 467-70.

57. Shin, I.; Park, S.; Lee, M. R., Carbohydrate microarrays: an advanced technology for functional studies of glycans. *Chemistry* **2005,** *11* (10), 2894-901.

58. Smoot, J. T.; Demchenko, A. V., Oligosaccharide synthesis: from conventional methods to modern expeditious strategies. *Adv. Carbohydr. Chem. Biochem.* **2009,** *62*, 161-250.

59. Rillahan, C. D.; Paulson, J. C., Glycan Microarrays for Decoding the Glycome. *Annu. Rev. Biochem.* **2011,** *80*, 797-823.

60. Song, X.; Xia, B.; Stowell, S. R.; Lasanajak, Y.; Smith, D. F.; Cummings, R. D., Novel fluorescent glycan microarray strategy reveals ligands for galectins. *Chem. Biol.* **2009,** *16* (1), 36-47.

61. Song, X.; Lasanajak, Y.; Xia, B.; Smith, D. F.; Cummings, R. D., Fluorescent glycosylamides produced by microscale derivatization of free glycans for natural glycan microarrays. *ACS Chem. Biol.* **2009,** *4* (9), 741-50.

62. Lee, M. R.; Shin, I., Facile preparation of carbohydrate microarrays by site-specific, covalent immobilization of unmodified carbohydrates on hydrazide-coated glass slides. *Org. Lett.* **2005,** *7* (19), 4269-72.

63. Bohorov, O.; Andersson-Sand, H.; Hoffmann, J.; Blixt, O., Arraying glycomics: a novel bi-functional spacer for one-step microscale derivatization of free reducing glycans. *Glycobiology* **2006,** *16* (12), 21C-27C.

64. Von Itzstein, M.; Wu, W. Y.; Kok, G. B.; Pegg, M. S.; Dyason, J. C.; Jin, B.; Van Phan, T.; Smythe, M. L.; White, H. F.; Oliver, S. W.; Colman, P. M.; Varghese, J. N.; Ryan, D. M.;

Wood, J. M.; Bethell, R. C.; Hotham, V. J.; Cameron, J. M.; Penn, C. R., Rational design of potent sialidase-based inhibitors of influenza virus replication. *Nature* **1993,** *363* (6428), 418-23.

65. (a) McKimm-Breschkin, J. L.; Colman, P. M.; Jin, B.; Krippner, G. Y.; McDonald, M.; Reece, P. A.; Tucker, S. P.; Waddington, L.; Watson, K. G.; Wu, W. Y., Tethered neuraminidase inhibitors that bind an influenza virus: a first step towards a diagnostic method for influenza. *Angew. Chem., Int. Ed. Engl.* **2003,** *42* (27), 3118-21; (b) Ying, L.; Gervay-Hague, J., One-bead-one-inhibitor-one-substrate screening of neuraminidase activity. *Chembiochem : a European journal of chemical biology* **2005,** *6* (10), 1857-65; (c) Lu, Y.; Gervay-Hague, J., Synthesis of C-4 and C-7 triazole analogs of zanamivir as multivalent sialic acid containing scaffolds. *Carbohyd Res* **2007,** *342* (12-13), 1636-50.

66. Yang, Y.; He, Y.; Li, X.; Dinh, H.; Iyer, S. S., Bifunctional thiosialosides inhibit influenza virus. *Bioorg. Med. Chem. Lett.* **2014,** *24* (2), 636-43.

67. Disney, M. D.; Zheng, J.; Swager, T. M.; Seeberger, P. H., Detection of bacteria with carbohydrate-functionalized fluorescent polymers. *J. Am. Chem. Soc.* **2004,** *126* (41), 13343-6.

68. Russell, R. J.; Haire, L. F.; Stevens, D. J.; Collins, P. J.; Lin, Y. P.; Blackburn, G. M.; Hay, A. J.; Gamblin, S. J.; Skehel, J. J., The structure of H5N1 avian influenza neuraminidase suggests new opportunities for drug design. *Nature* **2006,** *443* (7107), 45-9.

69. (a) Bilcke, J.; Coenen, S.; Beutels, P., Influenza-like-illness and clinically diagnosed flu: disease burden, costs and quality of life for patients seeking ambulatory care or no professional care at all. *PloS one* **2014,** *9* (7), e102634; (b) Kumar, S.; Henrickson, K. J., Update on influenza diagnostics: lessons from the novel H1N1 influenza A pandemic. *Clin. Microbiol. Rev.* **2012,** *25* (2), 344-61.

70. Vashist, S. K.; Zheng, D.; Al-Rubeaan, K.; Luong, J. H.; Sheu, F. S., Technology behind commercial devices for blood glucose monitoring in diabetes management: a review. *Anal. Chim. Acta* **2011,** *703* (2), 124-36.

71. (a) Harris, A.; Cardone, G.; Winkler, D. C.; Heymann, J. B.; Brecher, M.; White, J. M.; Steven, A. C., Influenza virus pleiomorphy characterized by cryoelectron tomography. *P Natl Acad Sci USA* **2006,** *103* (50), 19123-7; (b) Wasilewski, S.; Calder, L. J.; Grant, T.; Rosenthal, P. B., Distribution of surface glycoproteins on influenza A virus determined by electron cryotomography. *Vaccine* **2012,** *30* (51), 7368-73.

72. Wu, S.; Liu, G.; Li, P.; Liu, H.; Xu, H., A high-sensitive and fast-fabricated glucose biosensor based on Prussian blue/topological insulator Bi2Se3 hybrid film. *Biosens. Bioelectron.* **2012,** *38* (1), 289-94.

73. Crich, D.; Li, W., O-sialylation with N-acetyl-5-n,4-o-carbonyl-protected thiosialoside donors in dichloromethane: facile and selective cleavage of the oxazolidinone ring. *The Journal of organic chemistry* **2007,** *72* (7), 2387-91.

74. Zhang, X. T.; Gu, Z. Y.; Xing, G. W., Comparative studies on the O-sialylation with four different alpha/beta-oriented (N-acetyl)-5-N,4-O-carbonyl-protected p-toluenethiosialosides as donors. *Carbohyd Res* **2014,** *388*, 1-7.

75. Xie, H.; Mire, J.; Kong, Y.; Chang, M.; Hassounah, H. A.; Thornton, C. N.; Sacchettini, J. C.; Cirillo, J. D.; Rao, J., Rapid point-of-care detection of the tuberculosis pathogen using a BlaC-specific fluorogenic probe. *Nat. Chem.* **2012,** *4* (10), 802-9.

76. Beatty, K. E.; Williams, M.; Carlson, B. L.; Swarts, B. M.; Warren, R. M.; van Helden, P. D.; Bertozzi, C. R., Sulfatase-activated fluorophores for rapid discrimination of mycobacterial species and strains. *P Natl Acad Sci USA* **2013,** *110* (32), 12911-6.

77. Matrosovich, M.; Matrosovich, T.; Garten, W.; Klenk, H. D., New low-viscosity overlay medium for viral plaque assays. *Virol. J.* **2006,** *3*, 63.

78. van Elden, L. J.; Nijhuis, M.; Schipper, P.; Schuurman, R.; van Loon, A. M., Simultaneous detection of influenza viruses A and B using real-time quantitative PCR. *J. Clin. Microbiol.* **2001,** *39* (1), 196-200.

79. Estes, M. K.; Prasad, B. V. V.; Atmar, R. L., Noroviruses everywhere: has something changed? *Curr Opin Infect Dis* **2006,** *19* (5), 467-474.

80. Donaldson, E. F.; Lindesmith, L. C.; Lobue, A. D.; Baric, R. S., Viral shape-shifting: norovirus evasion of the human immune system. *Nat. Rev. Microbiol.* **2010,** *8* (3), 231-41.

81. Kapikian, A. Z.; Wyatt, R. G.; Dolin, R.; Thornhill, T. S.; Kalica, A. R.; Chanock, R. M., Visualization by immune electron microscopy of a 27-nm particle associated with acute infectious nonbacterial gastroenteritis. *J. Virol.* **1972,** *10* (5), 1075-81.

82. Kapikian, A. Z., The discovery of the 27-nm Norwalk virus: an historic perspective. *J. Infect. Dis.* **2000,** *181 Suppl 2*, S295-302.

83. Neill, J. D., The Complete Genome Sequence of the San Miguel Sea Lion Virus-8 Reveals that It Is Not a Member of the Vesicular Exanthema of Swine Virus/San Miguel Sea Lion Virus Species of the Caliciviridae. *Genome Announc.* **2014,** *2* (6).

84. Jiang, X.; Wang, M.; Wang, K.; Estes, M. K., Sequence and genomic organization of Norwalk virus. *Virology* **1993,** *195* (1), 51-61.

85. Zheng, D. P.; Ando, T.; Fankhauser, R. L.; Beard, R. S.; Glass, R. I.; Monroe, S. S., Norovirus classification and proposed strain nomenclature. *Virology* **2006,** *346* (2), 312-23.

86. Bok, K.; Abente, E. J.; Realpe-Quintero, M.; Mitra, T.; Sosnovtsev, S. V.; Kapikian, A. Z.; Green, K. Y., Evolutionary dynamics of GII.4 noroviruses over a 34-year period. *J. Virol.* **2009,** *83* (22), 11890-901.

87. Kroneman, A.; Vega, E.; Vennema, H.; Vinje, J.; White, P. A.; Hansman, G.; Green, K.; Martella, V.; Katayama, K.; Koopmans, M., Proposal for a unified norovirus nomenclature and genotyping. *Arch. Virol.* **2013,** *158* (10), 2059-68.

88. Prasad, B. V.; Hardy, M. E.; Dokland, T.; Bella, J.; Rossmann, M. G.; Estes, M. K., X-ray crystallographic structure of the Norwalk virus capsid. *Science* **1999,** *286* (5438), 287-90.

89. Choi, J. M.; Hutson, A. M.; Estes, M. K.; Prasad, B. V. V., Atomic resolution structural characterization of recognition of histo-blood group antigens by Norwalk virus. *P Natl Acad Sci USA* **2008,** *105* (27), 9175-9180.

90. Tan, M.; Jiang, X., Norovirus Gastroenteritis, Carbohydrate Receptors, and Animal Models. *PLoS Pathog.* **2010,** *6* (8).

91. Huang, P. W.; Farkas, T.; Zhong, W. M.; Thornton, S.; Morrow, A. L.; Xi, J., Norovirus and histo-blood group antigens: Demonstration of a wide spectrum of strain specificities and classification of two major binding groups among multiple binding patterns. *J. Virol.* **2005,** *79* (11), 6714-6722.

92. (a) Meloncelli, P. J.; Lowary, T. L., Synthesis of ABO histo-blood group type I and II antigens. *Carbohyd. Res.* **2010,** *345* (16), 2305-22; (b) Meloncelli, P. J.; West, L. J.; Lowary, T. L., Synthesis and NMR studies on the ABO histo-blood group antigens: synthesis of type III and IV structures and NMR characterization of type I-VI antigens. *Carbohyd. Res.* **2011,** *346* (12), 1406-1426.

93. Owen, V., Real-time optical immunosensors - A commercial reality. *Biosens. Bioelectron.* **1997,** *12* (1), R1-R2.